LOCKHEED MARTIN ENERGY RESEARCH LIBRARIES

3 4456 0509863 0

ORNL/TM-6029

cy. 1

Survey of Available Creep and Tensile Data for Alloy 800H

M. K. Booker
V. B. Baylor
B. L. P. Booker

[redacted]

OAK RIDGE NATIONAL LABORATORY
CENTRAL RESEARCH LIBRARY
DOCUMENT COLLECTION
LIBRARY LOAN COPY
DO NOT TRANSFER TO ANOTHER PERSON
If you wish someone else to see this
document, send in name with document
and the library will arrange a loan.

UCN-7969
(3 3-67)

OAK RIDGE NATIONAL LABORATORY
OPERATED BY UNION CARBIDE CORPORATION · FOR THE DEPARTMENT OF ENERGY

Printed in the United States of America. Available from
the Department of Energy,
Technical Information Center
P.O. Box 62, Oak Ridge, Tennessee 37830
Price: Printed Copy $9.00; Microfiche $3.00

This report was prepared as an account of work sponsored by an agency of the United States Government. Neither the United States Government nor any agency thereof, nor any of their employees, contractors, subcontractors, or their employees, makes any warranty, express or implied, nor assumes any legal liability or responsibility for any third party's use or the results of such use of any information, apparatus, product or process disclosed in this report, nor represents that its use by such third party would not infringe privately owned rights.

ORNL/TM-6029
Distribution
Category
UC-79b, -h, -k

Contract No. W-7405-eng-26

METALS AND CERAMICS DIVISION

SURVEY OF AVAILABLE CREEP AND TENSILE DATA FOR ALLOY 800H

M. K. Booker, V. B. Baylor, and B.L.P. Booker

Date Published: January 1978

OAK RIDGE NATIONAL LABORATORY
Oak Ridge, Tennessee 37830
operated by
UNION CARBIDE CORPORATION
for the
DEPARTMENT OF ENERGY

LOCKHEED MARTIN ENERGY RESEARCH LIBRARIES

3 4456 0509863 0

CONTENTS

ABSTRACT 1
INTRODUCTION 1
BACKGROUND INFORMATION 2
DATA USED 4
TENSILE PROPERTIES 4
STRENGTH PROPERTIES 5
DUCTILITY PROPERTIES 8
ENGINEERING STRESS-STRAIN RELATIONSHIP 11
METALLURGICAL CONSIDERATIONS 15
CREEP PROPERTIES 17
RUPTURE LIFE 19
TIME TO TERTIARY CREEP 34
STRAIN TO RUPTURE 39
CREEP STRAIN TO TERTIARY CREEP 44
CREEP STRAIN-TIME BEHAVIOR 55
Limitations 68
Calculation of Allowable Stress Values 68
SUMMARY 71
REFERENCES 73
APPENDIX A 81
APPENDIX B 135

SURVEY OF AVAILABLE CREEP AND TENSILE DATA FOR ALLOY 800H*

M. K. Booker, V. B. Baylor, and B.L.P. Booker

ABSTRACT

Most of the transition joints in the Clinch River Breeder Reactor Plant (CRBRP) will consist of trimetallic joints employing a spool piece (about 0.3 m long) of alloy 800H between 2 1/4 Cr-1 Mo steel and austenitic stainless steel. It is therefore important that the mechanical properties of alloy 800H be well characterized and understood. This report presents a summary of the available creep and tensile data for this material, including analytical representations of behavior.

INTRODUCTION

The high-nickel austenitic alloy 800H is an important structural material for elevated-temperature nuclear vessels and components. In fact, it is one of only four materials currently approved under ASME Code Case 1592[1] for nuclear service above 427°C (800°F). Many of the austenitic-to-ferritic transition weld joints[2] in the Clinch River Breeder Reactor Plant (CRBRP) will consist of trimetallic joints employing a spool piece (about 0.3 m long) of alloy 800H between 2 1/4 Cr-1 Mo steel and austenitic stainless steel.[3] Thus, the transition joints will essentially consist of two welds: 2 1/4 Cr-1 Mo steel to alloy 800H via ERNiCr-3 (Inconel 82) filler metal, and alloy 800H to stainless steel via 16-8-2 filler metal. The potentially serious consequences of a failure in these transition joints makes necessary a detailed understanding of their behavior. Such an understanding requires, among other things, a thorough knowledge of the mechanical properties of the materials involved. Toward this end, a

---

*Work performed under 189a OH103, Piping and Fitting Development.

survey of available creep and tensile data for alloy 800H has been completed. Many such data are available, but it is necessary to compile them and to present them in formats that are useful to designers. Therefore, the data have been analyzed to yield mathematical descriptions of the behavior of this important material.

BACKGROUND INFORMATION

The high-nickel austenitic alloys 800 and 800H have been used in a variety of applications such as in furnace equipment and as reformer and cracker tubes in the petrochemical industry.[4] The relatively wide use of this material can be attributed to its excellent elevated-temperature strength and to its resistance to oxidation and carburization at high temperatures. Table 1 shows the specifications on chemical composition currently used for alloys 800 and 800H. In terms of chemistry, the only difference between the two is that alloy 800H must have a minimum carbon content of 0.05 wt %. Also, alloy 800H is required to have a grain size of ASTM No. 5 or coarser. Finally, alloy 800H is solution annealed at about 1150°C (2100°F), whereas alloy 800 is mill-annealed at about 980°C (1800°F). (Before the advent of alloy 800H, the material existed as a solution-annealed "grade 2" material and a mill-annealed "grade 1" material.) The alloy is currently manufactured under a variety of trade names, including Incoloy 800, Escalloy 800, Carlson 800, Pyromet 800, Udimet 800, Sanicro 30 and 31, Croloy 20-30, Crucible 800, Camvac 800, and Hoskins Alloy 800.[5]

Alloy 800H is essentially a solid solution alloy, but its behavior can be strongly influenced by the precipitation of several phases within the material. These phases include γ' [$Ni_3(Al,Ti)$], chromium carbides ($Cr_{23}C_6$), and titanium carbonitrides [$Ti(C,N)$].[6] Thus, it is to be expected that the concentrations of nickel, carbon, aluminum, titanium, and nitrogen may have significant influences upon the behavior of the material.

Much of the long-term elevated-temperature strength of alloy 800H can in fact be attributed to the strengthening effects of precipitated phases. Unfortunately, these phases (particularly γ') may also cause

Table 1. Composition Specifications for Alloys 800 and 800H

Element	Content, wt %	
	Alloy 800[a] (Annealed at about 980°C)	Alloy 800H[b] (Annealed at about 1150°C)
C	0.10 max	0.05–0.10
Ti	0.15–0.60	0.15–0.60
Al	0.15–0.60	0.15–0.60
N		
Ni	30–35	30–35
Cr	19–23	19–23
Si	1.0 max	1.0 max
Mn	1.5 max	1.5 max
Cu	0.75 max	0.75 max
Co		
P		
S	0.015 max	0.015 max
Fe	Balance	Balance
Grain size		ASTM No. 5 or coarser

[a]ASTM B 163.

[b]ASME Code Case 1592.

decreases in long-term ductility. Thus, it is important to examine trends in the creep ductility of the material.

Finally, the effects of precipitated phases can cause complications in the data analysis in two respects. First, the strengthening effects may be lost after long times due to overaging. Second, there is some evidence[7] that the effects of γ' precipitation on mechanical properties are small at about 700°C (1292°F) or above, but large in the range 500–650°C (932–1202°F). Unfortunately, most available American creep data for alloy 800H were obtained at temperatures of 649°C (1200°F) or above, but most CRBRP service will be at 593°C (1100°F) or below. The problem of extrapolation of results from high to low temperatures is thus complicated by the metallurgy of the material.

DATA USED

All data used in this report were derived from tests on file in the ORNL Mechanical Properties Data Storage and Retrieval System (DSRS).[8] The primary original source of both creep and tensile data was the package[9] prepared by Huntington Alloys. For comparison purposes, some tensile data from other sources[10–12] for grade 2 material were examined. Actual tensile stress-strain curves from tests conducted by Huntington were obtained privately from D. I. Roberts of General Atomic Company. Creep strain-time curves from tests conducted by Huntington were obtained privately from C. E. Sessions and J. M. Duke of Westinghouse Tampa Division. Finally, due to the shortage of creep data, especially at low temperatures, data for Sanicro 31 from Sandvik Alloys[13] were examined. (Sanicro 31 is the Swedish solution-annealed version of alloy 800.) Due to possible differences in alloy specifications and in testing techniques, the Sandvik data were not used in the final equation development. They are useful, however, in that they represent long-time data for many heats of material. Moreover, many data were obtained at temperatures of 550 and 600°C.

All data used in equation development or for comparison are tabulated in Appendix A. (In some cases, alloy 800 grade 2 material that was slightly outside the specifications for alloy 800H was used due to shortages of data. The cases will be noted.)

TENSILE PROPERTIES

Short-term monotonic tensile data are directly applicable in setting design stress intensity limits, and they also lend insight into the general flow and failure characteristics of a material. In the current study, available data for ultimate tensile strength, yield strength (0.2% offset), proportional limit, total elongation, and reduction of area have been expressed as functions of temperature. In addition, an analytical model relating stress to plastic strain in the low strain region has been developed as a function of temperature and yield strength. No data were available on the effects of varying strain rates. As far

as could be determined, all tensile tests were conducted according to ASTM, which specifies a strain rate of 8.3×10^{-5}/s up to the determination of the yield strength, and a rate of 8.3×10^{-4}/s thereafter.

STRENGTH PROPERTIES

The 0.2% offset yield strength (σ_y) and ultimate tensile strength (σ_u) were assumed to be describable by polynomials in temperature. Then, the orders of the polynomials were chosen to provide the best balance of fit to the data and simplicity. The results of these analyses are shown in Figs. 1 and 2, including data and curves of expected values and upper and lower central tolerance limits. These limits specify with a confidence level of 0.95 the bounds within which 90% of the observed values are expected to fall. Each limit may be interpreted to mean that at this confidence level 95% of the observations are expected to fall above the lower limit, while 95% are also expected to fall below the upper limit. These tolerance limits are simultaneous in all levels of the independent variable (temperature); that is, they may be simultaneously calculated for different values of the independent variables without affecting the level of confidence. Tolerance limits are discussed in greater detail by Leiberman and Miller.[14] It should be noted that there are indications in Figs. 1 and 2 that the current tolerance limits may be overconservative in an engineering sense.

The expected values of each of the above quantities [for stresses in MPa and temperatures (T) in °C] are given by

$$\sigma_y = 220.2 - 0.389T + 5.33 \times 10^{-4}T^2 - 2.58 \times 10^{-7}T^3 , \qquad (1)$$

$$\sigma_u = 571.6 - 0.882T + 2.98 \times 10^{-3}T^2 - 3.09 \times 10^{-6}T^3 . \qquad (2)$$

For comparison, Figs. 3 and 4 display information similar to Figs. 1 and 2, except that data for both alloy 800H and former alloy 800 grade 2 material are included. Alloy 800 grade 2 meets the same specifications as alloy 800H except with no minimum carbon or grain size levels. No

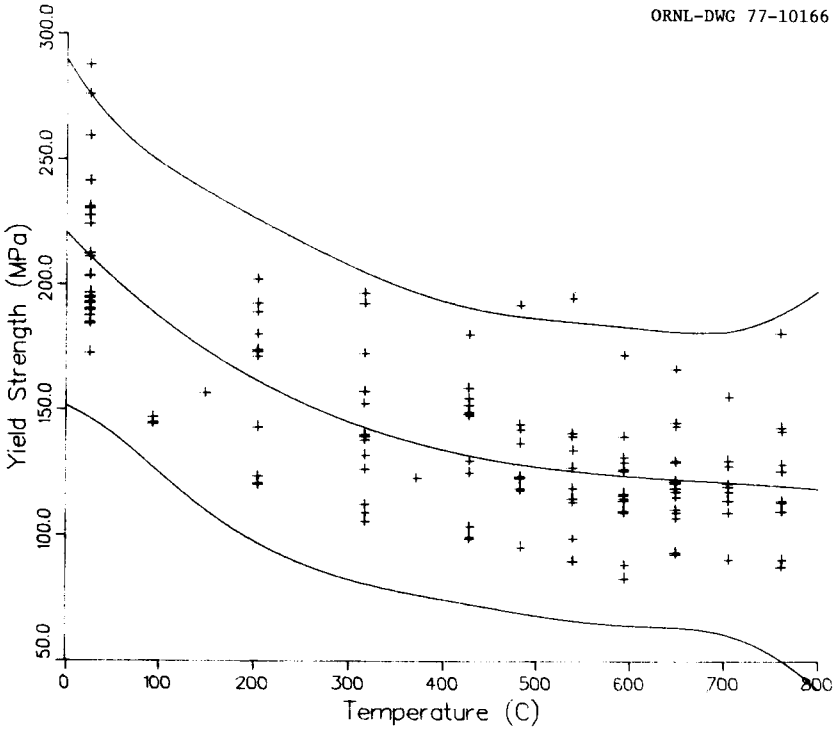

Fig. 1. Relationship Between Yield Strength and Temperature for Alloy 800H. Central lines represent best fit average curves; upper and lower lines represent upper and lower central tolerance limits (P = 0.90, λ = 0.95).

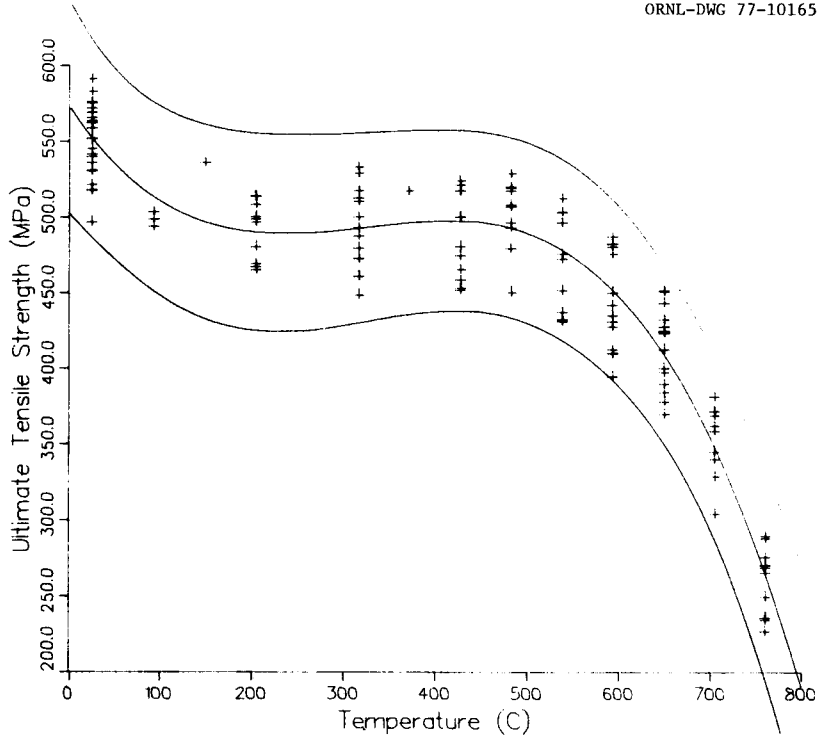

Fig. 2. Relationship Between Ultimate Tensile Strength and Temperature for Alloy 800H. Central lines represent best fit average curves; upper and lower lines represent upper and lower central tolerance limits (P = 0.90, λ= 0.95).

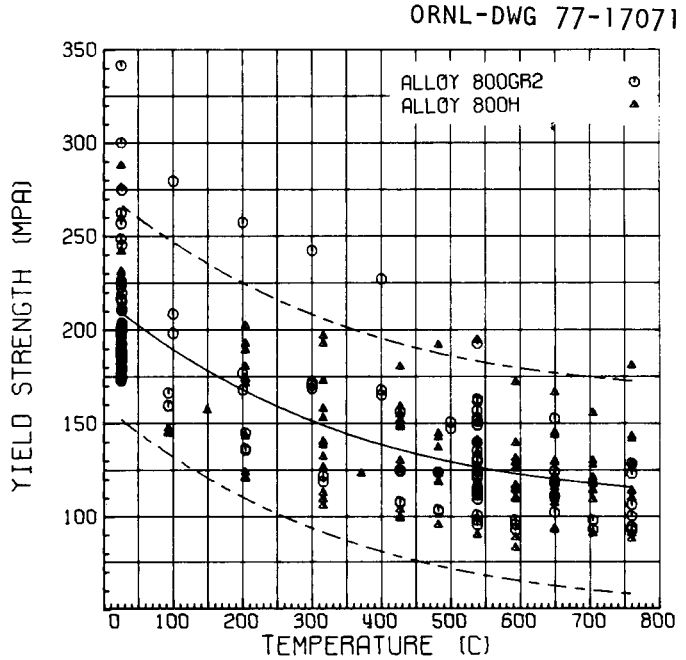

Fig. 3. Relationship Between 0.2% Offset Yield Strength and Temperature for Alloy 800H and Alloy 800 Grade 2. Solid line represents a best-fit average curve; dashed lines represent best-fit ± two standard errors of estimate.

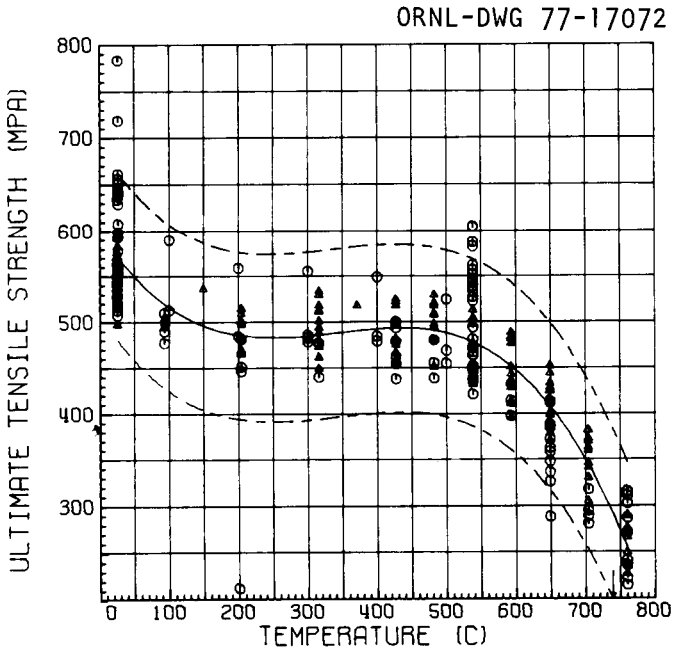

Fig. 4. Relationship Between Ultimate Tensile Strength and Temperature for Alloy 800H and Alloy 800 Grade 2. Solid line represents a best-fit average curve; dashed lines represent best-fit ± two standard errors of estimate.

major differences appear between the trends displayed by the two grades of material. The mean values in Figs. 3 and 4 are given by

$$\sigma_y = 215.6 - 0.368T + 5.26 \times 10^{-4}T^2 - 2.90 \times 10^{-7}T^3 \ , \qquad (3)$$

$$\sigma_u = 559.8 - 0.734T + 2.48 \times 10^{-3}T^2 - 2.67 \times 10^{-6}T^3 \ . \qquad (4)$$

Here, minimum values are given by expected values minus twice the standard of error of estimate.

The plots in Figs. 1–4 show a considerable amount of scatter, presumably due primarily to heat-to-heat variations in strength due to chemistry and microstructure. Smith[15] has presented a method for normalizing such data by taking the ratio of an elevated-temperature strength property to the corresponding strength measured at room temperature for each lot of material. A "trend" curve of strength ratio as a function of temperature is then derived, preferably by least-squares methods.

However, a major goal of the current program was to perform a statistical analysis of property variations, and the number of available data made direct statistical treatment possible. Recent results[16] have shown that the ratio technique can be an oversimplification in that different processes may be operative at different temperatures. Therefore, for the current application, the direct statistical approach has been found to be the preferable method for treating the data. This technique is similar to that used previously for 2 1/4 Cr-1 Mo steel.[17]

DUCTILITY PROPERTIES

The total elongation (ET) and reduction of area (RA) at fracture in tensile tests have also been expressed as functions of temperature, as shown in Figs. 5 and 6. These data have been treated in a manner analogous to that used above for strength properties. The expected values shown by the solid lines in Figs. 5 and 6 are given by

$$\mathrm{ET} = 52.46 - 0.0312T + 8.36 \times 10^{-5}T^2 - 7.66 \times 10^{-8}T^3 \ , \qquad (5)$$

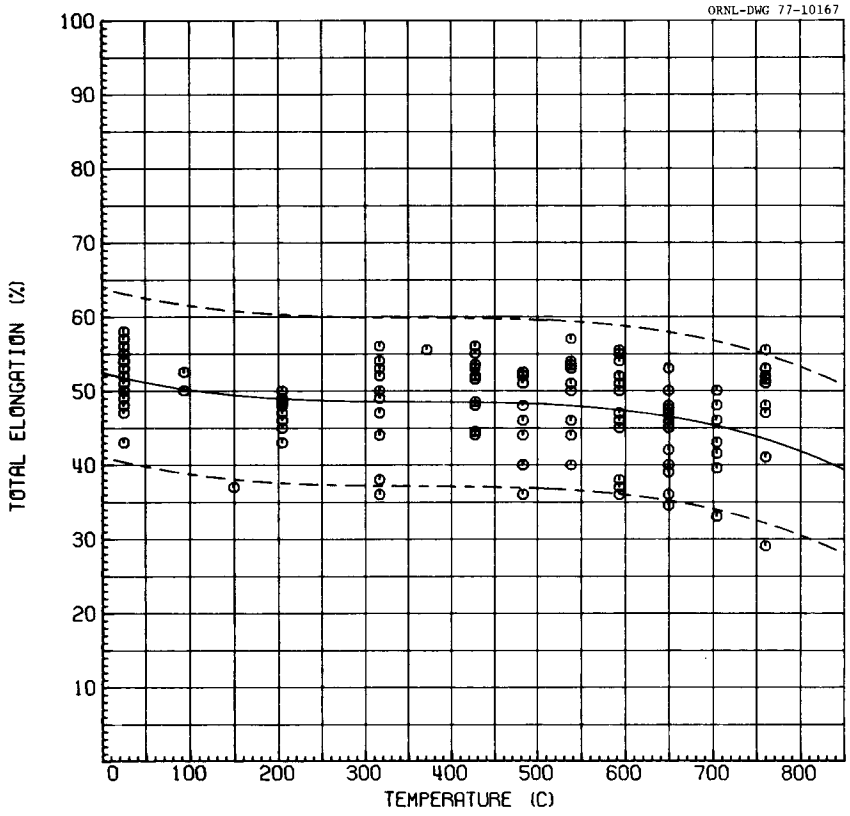

Fig. 5. Relationship Between Total Elongation and Temperature for Alloy 800H. Solid line represents a best-fit average curve; dashed lines represent best-fit ± two standard errors of estimate.

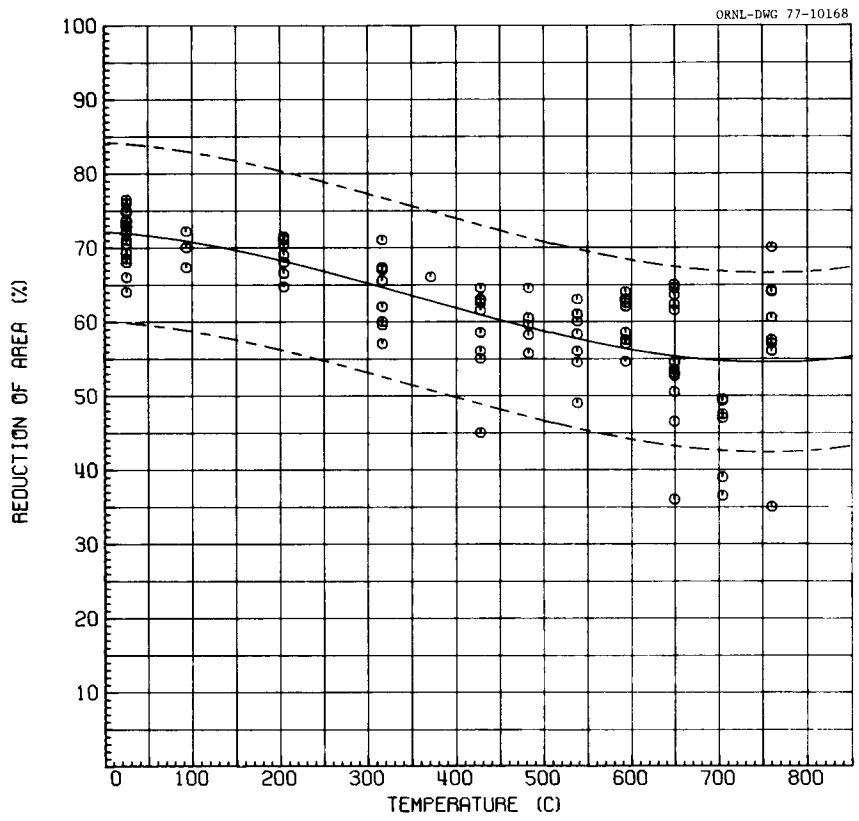

Fig. 6. Relationship Between Reduction of Area of Temperature for Alloy 800H. Solid line represents a best-fit average curve; dashed lines represent best-fit ± two standard errors of estimate.

$$RA = 72.14 - 0.00729T - 7.45 \times 10^{-5}T^2 + 7.03 \times 10^{-8}T^3 \ . \qquad (6)$$

Minimum values are given by expected values minus twice the standard error of estimate.

Figures 7 and 8 again show total elongation and reduction of area as functions of temperature, but include data both for alloy 800H and alloy 800 grade 2. In general, no specific information about specimen geometry was available.

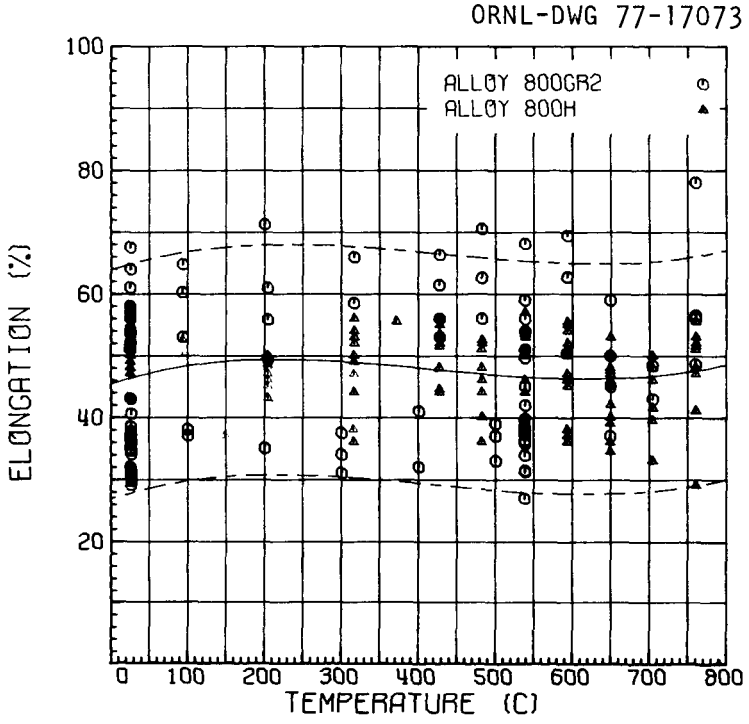

Fig. 7. Relationship Between Total Elongation and Temperature for Alloy 800H and Alloy 800 Grade 2. Solid line represents a best-fit average curve; dashed lines represent best-fit ± two standard errors of estimate.

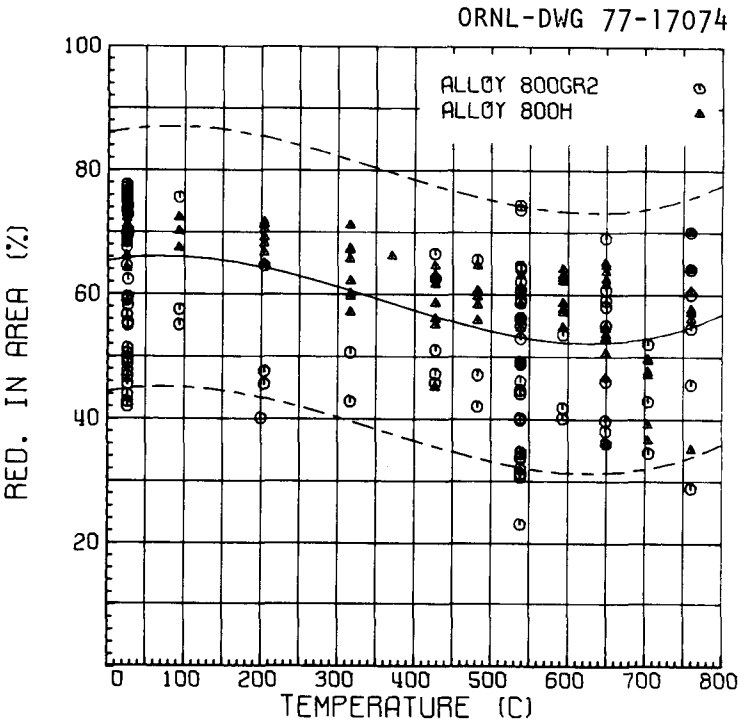

Fig. 8. Relationship Between Reduction of Area and Temperature for Alloy 800H and Alloy 800 Grade 2. Solid line represents a best-fit average curve; dashed lines represent best-fit ± two standard errors of estimate.

ENGINEERING STRESS-STRAIN RELATIONSHIP

Successful inelastic design analyses require, among other things, a knowledge of the shape of the tensile stress-strain curve. For CRBRP transition joint analyses, this relationship is required[18] only up to a strain of 0.4%. Most experimental stress-strain curves were also available only up to strains of about this order. Therefore, the analysis was limited to strains from 0 to 0.4%.

Many different equation forms relating stress to strain (or plastic strain) have been developed for a number of materials. Some of the more common ones are reviewed by Klueh and Hebble.[19] In the current investigation, a total of 64 engineering stress-strain curves were available in the temperature range from 93 to 760°C (200–1400°F). These curves could be adequately represented by a simple rational polynomial equation of the form

$$\sigma - \sigma_0 = \frac{abe_p}{1 + be_p} + \dot{h}_m e_p \ , \tag{7}$$

where σ is the stress (MPa), e_p is the engineering plastic strain (%), and σ_0 corresponds to the proportional limit. The parameters a, b, and $\dot{h}_m$ describe the shape of an individual stress-strain curve. This same equation form has been used to model the stress-strain behavior of type 304 stainless steel[20,21] and of type 316 stainless steel.[21] This same form has also been used to describe the creep strain-time behavior of several materials.[17,20,22—24] The properties of the rational polynomial equation form are summarized by Hobson and Booker.[25]

Variations in the values of a, b, and $\dot{h}_m$ in the current data stem primarily from the effects of temperature and heat-to-heat variability in strength. The effects of these factors were mathematically modeled as follows.

First, the values of a, b, and $\dot{h}_m$ were determined for each available experimental stress-strain curve using the same method used earlier[20,23] for creep data. Details of the technique are given in ref. 23; it essentially consists of picking three points on the experimental curve, which then determine the three constants in the equation. Here, the points used were values of $\sigma - \sigma_0$ corresponding to 0.02%, 0.2%, and 0.4% plastic strain. Note that the form of Eq. (7) guarantees that $\sigma - \sigma_0$ for $e_p = 0$.

The values of a, b, and $\dot{h}_m$ obtained by this method showed a great deal of scatter. However, it was found that $\dot{h}_m$ could be expressed as a function of temperature by

$$\dot{h}_m = 186e^{-0.00261T} \ , \tag{8}$$

where T is the temperature (°C), for $T \geqslant 427$°C. At lower temperatures, $\dot{h}_m$ appears to exhibit a constant value of 61.08. Figure 9 illustrates the relationship between $\dot{h}_m$ and T. No trends in $\dot{h}_m$ with strength level (as measured by σ_y) were noted.

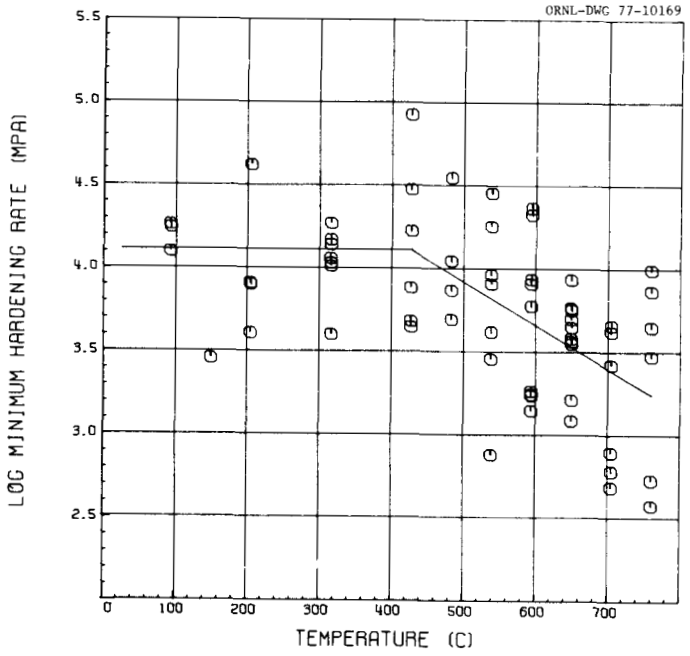

Fig. 9. Relationship Between the Minimum Rate of Work Hardening, h_m, from the Rational Polynomial Tensile Model and Temperature for Alloy 800H.

Values of b varied from 8.8 to 171.4, but no trends with the values of T or σ_y were noted. The value of b tended to decrease as a increased, but the correlation was not strong. Therefore, it was decided to represent b by a constant value of 40.

Next, we chose a value of a such that σ would equal σ_y for $e_p = 0.2$. At this point, Eq. (7) becomes

$$\frac{a(40)(0.2)}{1 + 40(0.2)} + 0.2h_m = \sigma_y - \sigma_0 \ , \tag{9}$$

or

$$a = (9/8)(\sigma_y - \sigma_0 - 0.2\dot{h}_m) \ . \tag{10}$$

Thus, the only quantity that still needs to be estimated is σ_0. Again, variations in σ_0 were found to be large. As shown in Fig. 10, the best estimate obtained for σ_0 was as $0.7\sigma_y$. Thus, a knowledge of T and σ_y allows one to estimate the entire stress-plastic strain curve

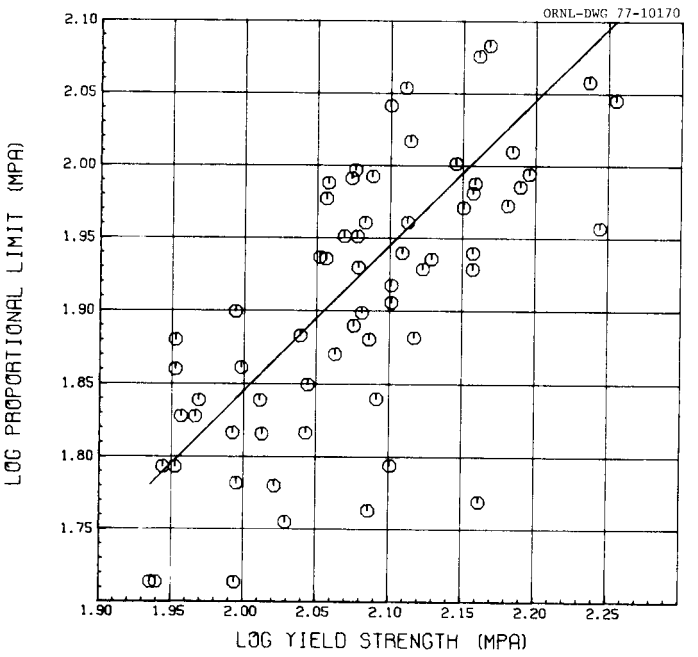

Fig. 10. Relationship Between the Proportional Limit and 0.2% Offset Yield Strength for Alloy 800H.

at low strains. Adding an elastic strain of $100\sigma/E$ (where E is Young's modulus) yields the stress vs total strain curve.

It should be noted that the above stress-strain equation used data only up to e_p = 0.4% and in the range 93 to 760°C. No data were available at lower temperatures or higher strains. However, the results can be extended downward to room temperature and upward to 1% plastic strain with good results. In using the above equation, one can insert σ_y for a given heat, if known, to maximize the precision in predictions. Or, a value of σ_y from Eq. (1) should yield a predicted average stress-strain curve. Likewise, maximum and minimum strength curves can be predicted. Note in Fig. 10 that σ_0/σ_y can vary from about 0.5 to 0.9. Thus, minimum strength predictions can be made by using a minimum yield strength (Fig. 1) and using $\sigma_0 = 0.5\sigma_y$. Maximum strength predictions can be made by using a maximum yield strength and $\sigma_0 = 0.9\sigma_y$. Figure 11 illustrates predictions made this way, including comparisons with the experimental stresses at 0, 0.02%, 0.2%, and 0.4% plastic strain. The predictions appear to describe the data excellently.

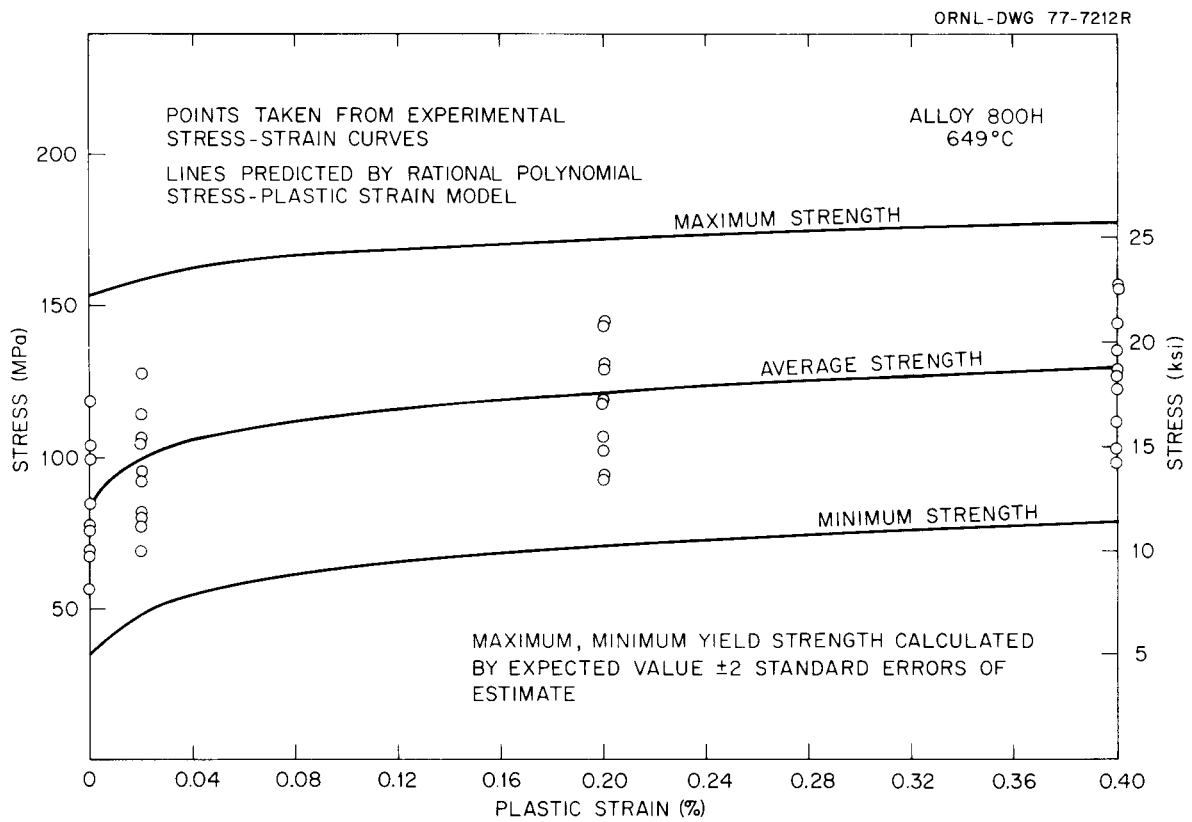

Fig. 11. Comparison Between Experimental Data and Predicted Stress-Strain Curves for Material of Minimum, Average, and Maximum Yield Strength.

METALLURGICAL CONSIDERATIONS

A detailed investigation of the fundamental aspects of the behavior of this material is beyond the scope of this report. However, several features can be noted. For instance, the yield strength appears to go through a "plateau" with temperature in the range from about 500 to 750°C. The ultimate tensile strength even shows a slight peak in this region. Finally, many of the experimental stress-strain curves exhibit serrated yielding at these temperatures. All of these phenomena tend to indicate a possible existence of dynamic strain aging effects, although the temperatures are rather high for classical interstitial-dislocation interactions. The data do not contain enough information to assess the possibilities of strain aging effects involving substitutional atoms, such as have been postulated for some ferritic steels.[26,27]

The total elongation and reduction of area both show minima with temperature in the above region, which is again possibly contributed to by dynamic strain aging effects. However, such ductility minima are common in ductile metals and alloys. Rhines and Wray[28] have explained such minima as follows. Low-temperature fracture is transgranular and ductility is high. Then, the effects of grain boundary shear cause a drop in ductility with temperature. Finally, at still higher temperatures, recrystallization occurs simultaneously with intergranular void formation. The intergranular fracture path is continuously broken up and ductility again increases.

Table 2 shows the chemical compositions of the heats for which tensile data were available. No correlations have been attempted between chemistry and tensile properties. Previous work on mill-annealed alloy 800 (ref. 29) has shown a tendency for the yield and ultimate strengths at 538°C to increase with both carbon and titanium. No trends in room temperature properties with chemistry were observed in that work, however. The current data do appear to indicate an increased tendency toward serrated yielding as carbon level increases.

Table 2. Heats of Material Used in Analysis of the Tensile Properties of Alloy 800H

Heat	Chemical Composition, wt %									
	C	Mn	Fe	S	Si	Cu	Ni	Cr	Al	Ti
HH1022A	0.07	0.87	44.32	0.007	0.35	0.24	31.13	22.16	0.37	0.46
HH1026A	0.07	0.93	44.67	0.007	0.40	0.29	31.42	21.63	0.22	0.34
HH3603A	0.06	1.03	46.42	0.007	0.41	0.30	31.33	20.42	0.39	0.46
HH4391A										
HH5171A										
HH5342A										
HH5356A	0.10	0.91	45.63	0.007	0.33	0.37	33.13	19.50	0.55	0.55
HH5432A										
HH5853A										
HH6279A	0.06	0.89	45.43	0.007	0.44	0.25	31.89	21.01	0.49	0.45
HH6738A										
HH7262A	0.05	0.78	45.35	0.007	0.31	0.44	32.38	20.66	0.45	0.46
HH7534A	0.06	0.98	45.70	0.007	0.42	0.33	31.35	21.13	0.43	0.52
HH7686A	0.07	0.97	45.88	0.007	0.47	0.38	30.94	21.26	0.39	0.49
HH8285A	0.08	0.80	45.55	0.007	0.37	0.40	32.20	20.75	0.50	0.41
HH8416A	0.10	0.88	45.31	0.007	0.29	0.44	31.99	20.96	0.48	0.37
HH8646A										
HH8808A	0.05	0.83	45.15	0.009	0.42		31.06	21.46	0.51	0.51

CREEP PROPERTIES

For CRBRP transition joint design,[18] it is necessary to be able to predict the creep behavior of alloy 800H from about 454 to 721°C (850–1350°F). To encompass the complete range of needed predictions, an analysis of data up to 760°C (1400°F) has been completed. Few alloy 800H data below 649°C (1200°F) and none below 538°C (1000°F) were available, but the results have been extrapolated to 427°C (800°F). Properties examined include time to rupture, time and creep strain to tertiary creep, minimum creep rate, and creep strain-time behavior. Figure 12 defines the properties used, while Fig. 13 defines the conditions of available creep tests.

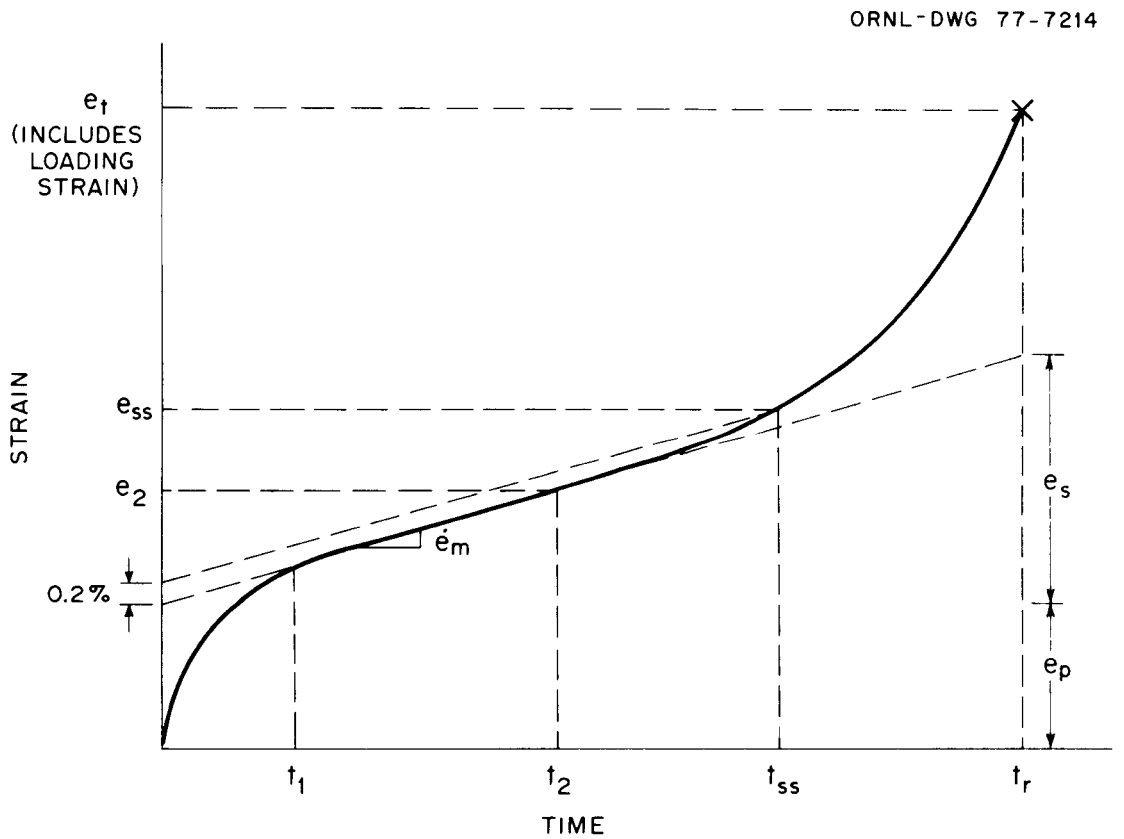

Fig. 12. Schematic Definition of Various Creep Quantities Examined.

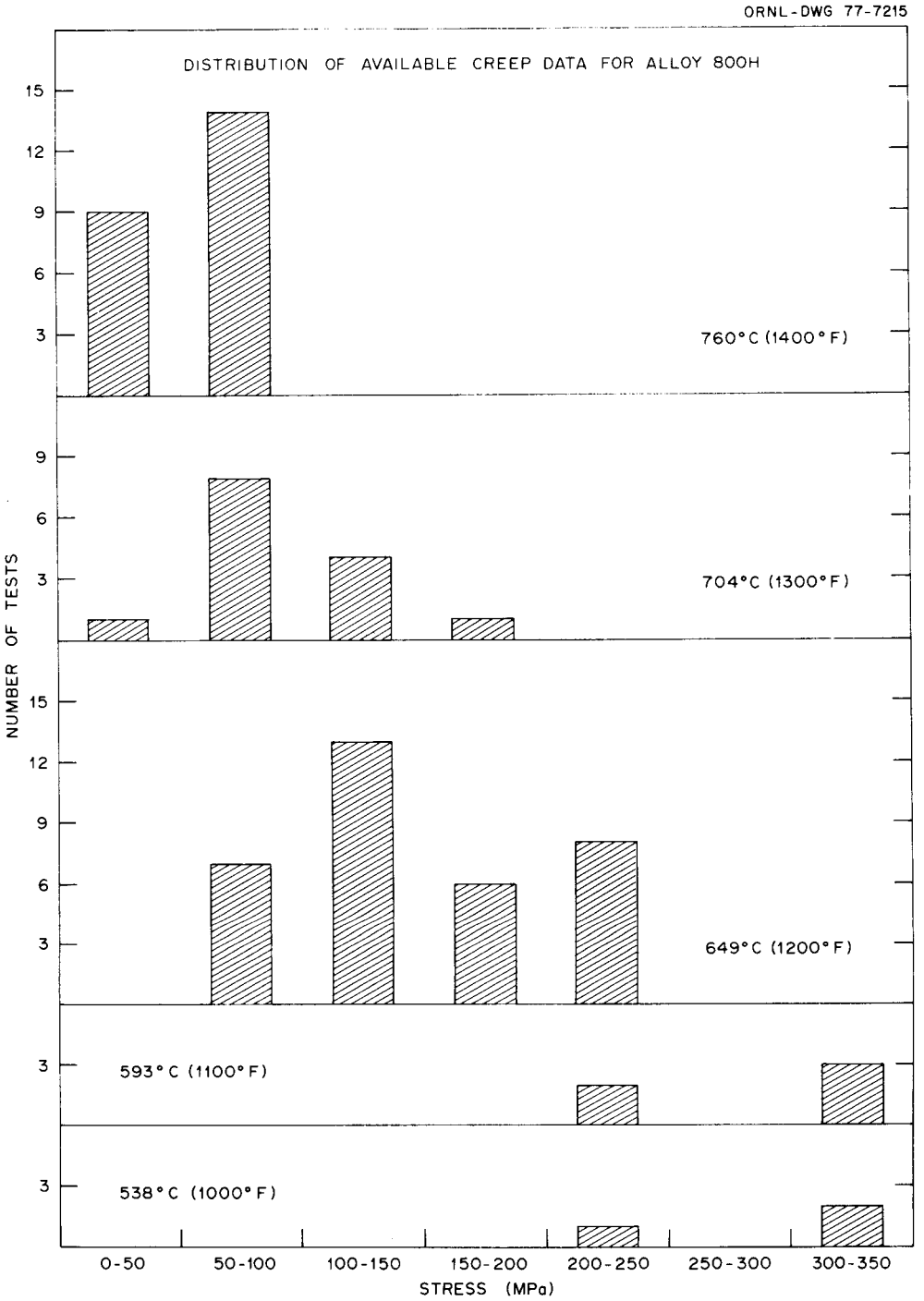

Fig. 13. Distribution of Available Creep Data for Alloy 800H.

RUPTURE LIFE

The creep property that has received the most attention in the literature and for which the most data are available is the rupture life. In particular, we sought to obtain an equation expressing rupture life as a function of stress and temperature.

The available data for rupture life (and for other creep properties examined below) are tabulated in Appendix A. In the initial analyses, data at temperatures up to 871°C (1600°F) were examined, but the results appeared biased toward the higher temperature data. In view of the complex precipitation phenomena prevalent in this material, we decided to use only data up to 760°C since these encompassed the desired temperature range and subsequent fits appeared more consistent with the lower temperature ($T \leqslant 649$°C) data.

The mathematical analysis of rupture data for a material such as alloy 800H consists of two aspects. First, we have to identify the effects of stress and temperature on the rupture life. Second, we want an expression that will predict variations in the behavior of the material.

Unfortunately, the current data base is not sufficient to clearly identify the effects of factors such as composition and grain size on the creep behavior. Previously results on types 304 and 316 stainless steel[20,23,30,31] and on 2 1/4 Cr-1 Mo steel[24] have shown that the elevated-temperature ultimate tensile strength for material of a given heat and heat treatment can be an effective indicator of variations in creep strength. However, the current creep data for alloy 800H show little or no correlation between tensile strength and creep strength, as shown in Fig. 14. This lack of correlation is possibly because the time period involved in a tensile test is too brief for the effects of precipitation on the creep strength to appear.

Thus, the 55 available experimental stress-rupture data were analyzed merely as functions of stress and temperature by the regression techniques described in ref. 31. Considering the large uncertainties involved, the data could be adequately described by a simple Larson-Miller[32] paramater of the form

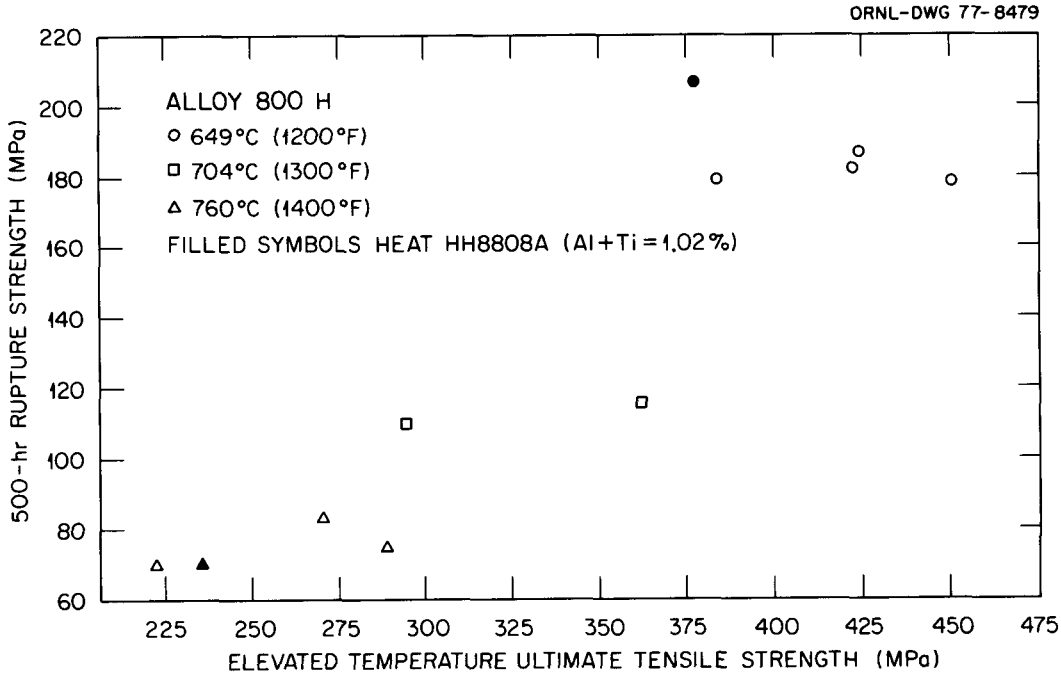

Fig. 14. Relationship Between Ultimate Tensile Strength and 500-hr Creep Rupture Strength for Alloy 800H.

$$\log t_r = -18.45 + 3402/T - (6430/T)\log \sigma \ , \tag{11}$$

where t_r is the rupture life in hours, T is the temperature (K), and σ is the stress (MPa). Figure 15 compares the fit of Eq. (11) with the experimental data. Defining the goodness of fit in terms of R^2, the coefficient of determination,[31] the value was 88.4%. Thus 88.4% of the variations in the data were described by the simple form of Eq. (11). More complicated models fit slightly better (R^2 for the best five-term model was 90.9%), but this improvement was judged to be insignificant. The data simple do not warrant use of a more complicated model.

Define the standard error of estimate, SEE, as

$$\text{SEE} = \sqrt{\sum_i (y_i - \hat{y}_i)^2/(n - \nu)} \ , \tag{12}$$

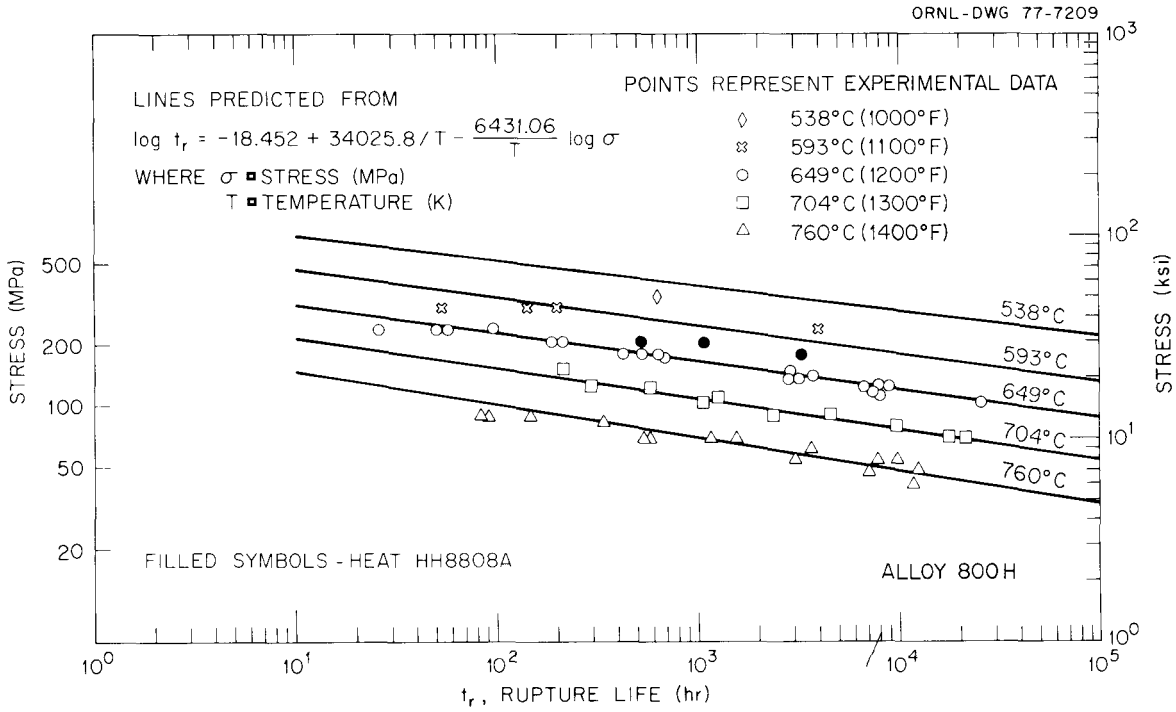

Fig. 15. Comparison of Experimental Stress-Rupture Data with Predicted Behavior for Alloy 800H.

where the y_i are the experimental values of the dependent variable (here log t_r) and the $\hat{y}_i$ are the corresponding values predicted by the model. The number of terms in the model is given by ν, while n is the number of data. The scatter band of behavior could be described by the value of log t_r predicted by Eq. (11) ± 2SEE. Here, SEE was 0.272. Thus, the scatter in behavior about the mean t_r could be described approximately by a factor of 3.5 up or down. Figure 16 compares the available data with limits obtained this way. It should be emphasized that these limits are merely empirical descriptions of the width of the scatter band and that they have no real statistical meaning.

The only apparent systematic deviation of the data from the predicted lines occurs in the data for Heat HH8808A at 649°C. Table 3 shows the chemical compositions of the heats of material used in this analysis. Heat HH8808A has a high combined aluminum and titanium content of 1.02%. Thus, it might be expected to be unusually strong at 649°C because of γ' precipitation.

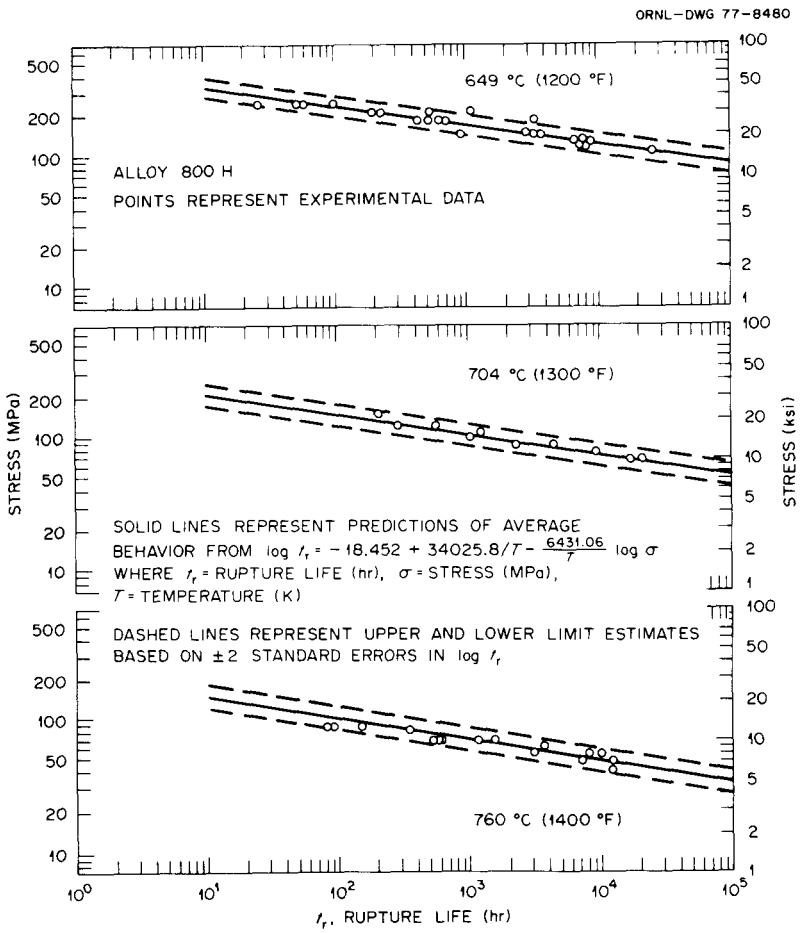

Fig. 16. Comparison of Experimental Data with Predicted Mean Behavior and ± 2SEE Upper and Lower Limit Behavior for Alloy 800H.

Table 3. Heats of Material Used in Analysis of the Creep Properties of Alloy 800H

Heat	Chemical Composition, wt %									
	C	Mn	Fe	S	Si	Cu	Ni	Cr	Al	Ti
HH8735A	0.04	0.55	45.28	0.007	0.41	0.41	31.31	21.29	0.29	0.39
HH8808A	0.05	0.83	45.15	0.009	0.42		31.06	21.46	0.51	0.51
HH7686A	0.07	0.97	45.88	0.007	0.47	0.38	30.94	21.26	0.39	0.49
HH3603A	0.06	1.03	46.42	0.007	0.41	0.30	31.33	20.42	0.39	0.46
HH8416A	0.10	0.88	45.31	0.007	0.29	0.44	31.99	20.96	0.48	0.37
HH8285A	0.08	0.80	45.55	0.007	0.37	0.40	32.20	20.75	0.50	0.41
HH7534A	0.06	0.98	45.70	0.007	0.42	0.33	31.35	21.13	0.43	0.52

Heat-to-heat variations in creep strength can be qualitatively examined by reference to some recent data from Huntington Alloys.[6] These data were obtained on some experimental heats with the specific goal of examining the effects of composition and processing on the creep behavior of solution annealed alloy 800 (not all heats meet the specifications for alloy 800H). These heats were not used in the current analysis because of their experimental nature. Table 4 shows the chemical compositions of these heats.

Again, an analysis of composition effects is beyond the scope of this report. Huntington[6] work has involved such an investigation, including a thermodynamic model for the precipitation of various

Table 4. Experimental Heats Tested in Huntington Program

Heat	Chemical Composition, wt %										
	C	Mn	S	Si	Cu	Ni	Cr	Al	Ti	N	O
HF5978	0.057	0.90	0.004	0.44	0.52	33.09	22.16	0.29	0.39	0.021	0.060
HF5979	0.061	0.89	0.004	0.60	0.51	32.87	22.00	0.45	0.12	0.053	0.040
HF5980	0.062	0.90	0.004	0.47	0.50	33.15	22.51	0.73	0.51	0.036	0.030
HF5981	0.065	0.94	0.003	0.44	0.51	32.81	21.69	1.27	0.61	0.037	0.040
HF5982	0.063	0.94	0.004	0.47	0.52	32.74	21.80	1.61	0.70	0.027	0.020
HF5983	0.080	0.92	0.004	0.44	0.50	32.67	21.33	0.16	0.45	0.041	0.050
HF5984	0.070	0.95	0.003	0.49	0.50	32.76	21.79	0.22	0.87	0.020	0.050
HF5985	0.064	0.95	0.004	0.50	0.50	32.68	21.23	0.28	1.51	0.010	0.050
HF5986	0.066	0.94	0.003	0.49	0.51	32.91	21.86	0.31	1.82	0.014	0.040
HF5997	0.029	1.65	0.004	0.62	0.42	32.61	21.32	0.34	0.59	0.035	
HF5998	0.028	0.99	0.004	0.50	0.42	32.62	21.92	0.33	0.62	0.037	
HF5999	0.061	0.94	0.004	0.52	0.42	32.77	21.57	0.35	0.59	0.035	
HF6000	0.098	0.95	0.004	0.45	0.41	32.88	21.83	0.37	0.60	0.047	
HF6061	0.010	0.85	0.004	0.40	0.42	33.73	20.74	0.16	0.48	0.037	
HF6119	0.090	0.99	0.005	0.57	0.51	33.44	21.99	0.20	0.85	0.021	0.028
HF6134	0.007	0.87	0.005	0.47	0.37	33.14	21.68	0.27	0.64	0.012	0.023
HF6135	0.012	0.89	0.005	0.57	0.45	33.38	21.54	0.20	0.80	0.026	0.040
HV2968	0.020	0.91	0.003	0.57	0.29	32.87	20.71	0.11	0.20	0.019	
HV2969	0.020	0.91	0.004	0.61	0.31	32.59	21.62	0.56	0.64	0.016	0.020
HV2970	0.020	0.89	0.003	0.57	0.27	32.55	21.87	0.61	0.25	0.043	0.017
HV2771	0.020	0.90	0.003	0.60	0.33	32.37	21.76	0.20	0.60	0.037	0.017
HV2972	0.070	0.89	0.003	0.55	0.33	32.65	21.40	0.63	0.24	0.011	0.013
HV2973	0.080	0.89	0.003	0.62	0.34	32.24	21.97	0.22	0.64	0.008	0.017
HV2974	0.080	0.87	0.003	0.54	0.27	32.62	21.80	0.20	0.22	0.040	0.016
HV2975	0.070	0.90	0.003	0.59	0.32	32.56	21.66	0.64	0.64	0.039	0.018
HV3105	0.017	0.99	0.003	0.63	0.48	32.82	20.74	0.40	0.41	0.016	0.016
HV3106	0.050	0.89	0.002	0.71	0.46	32.42	21.26	0.11	0.64	0.018	0.037
HV3107	0.130	0.91	0.002	0.66	0.51	32.07	21.46	0.13	0.27	0.014	0.023
HV3108	0.130	0.89	0.003	0.66	0.53	32.19	21.07	0.57	0.69	0.013	0.039
HV3114	0.050	0.87	0.003	0.58	0.51	32.57	21.39	0.01	0.53	0.012	0.034
HV3115	0.090	0.88	0.003	0.60	0.52	32.14	20.78	0.01	0.61	0.014	0.031
HV3185	0.020	0.93	0.005	0.64	0.33	35.07	20.40	0.03	0.60	0.007	0.035

phases and the subsequent effects on creep rupture strength and ductility. The γ' phase was the most potent strengthener, but carbides and nitrides can also be important. More work is needed in this area, but the currently available results all appear consistant with the theory that γ' precipitation is extremely important to the behavior of this material.

Another aspect of the data for the heats in Table 4 is that room-temperature tensile data were obtained on aged as well as on as-annealed material. As shown in Fig. 17, little correlation appears between room-temperature tensile strength and 500-hr rupture strength at 649°C, even for heats specifically designed for the study of heat-to-heat variations. However, when the tensile strengths are obtained on material aged 1000 hr at 649°C, a strong positive correlation appears between tensile strength and creep strength. Figure 18 shows that the effects of aging at 593°C are similar to those at 649°C. Figures 19 and 20 show that the correlation between aged tensile strength and creep strength begins to deteriorate at creep test temperatures of 704°C and above. For instance, at 760°C only three heats show unusually strong 500-hr creep strengths. These are Heat HF5982 with an extremely high aluminum content and Heats HF5985 and HF5986 with extremely high titanium contents. All results are again consistent with the explanation that precipitated phases (particularly γ') are the primary reason for heat-to-heat variability in this material.

The heats in the experimental program of ref. 6 vary beyond the bounds of the specifications on composition of alloy 800H and were specifically designed to produce variations in creep strength. Still, the large variations in those data compared with the limited scope of the data used to develop Eq. (11) raise two questions. First, are the data used for Eq. (11) typical and does Eq. (11) predict approximately average behavior? Second, do the limits in Fig. 16 adequately bracket the behavior that might be displayed by the material? Figure 21 compares the predictions from Eq. (11), including the log t_r − 2SEE lower limits, with the data for the experimental heats in ref. 6. The average predicted values appear to be reasonable for the entire data set, although the material meeting the alloy 800H specifications on composition (no grain sizes were given) appears to be consistently weaker than

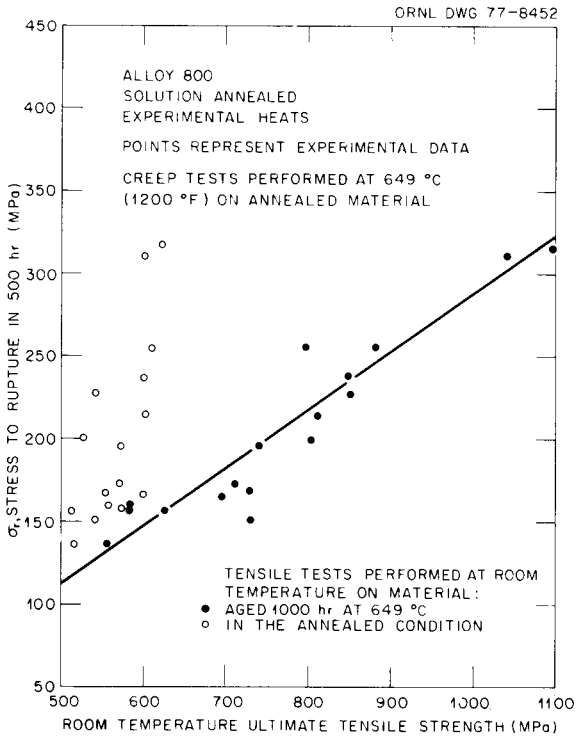

Fig. 17. Relationship Between Room-Temperature Ultimate Tensile Strength of Solution Annealed and of Aged Alloy 800 and the 500-hr Creep Rupture Strength of Solution Annealed Alloy 800 at 649°C (1200°F).

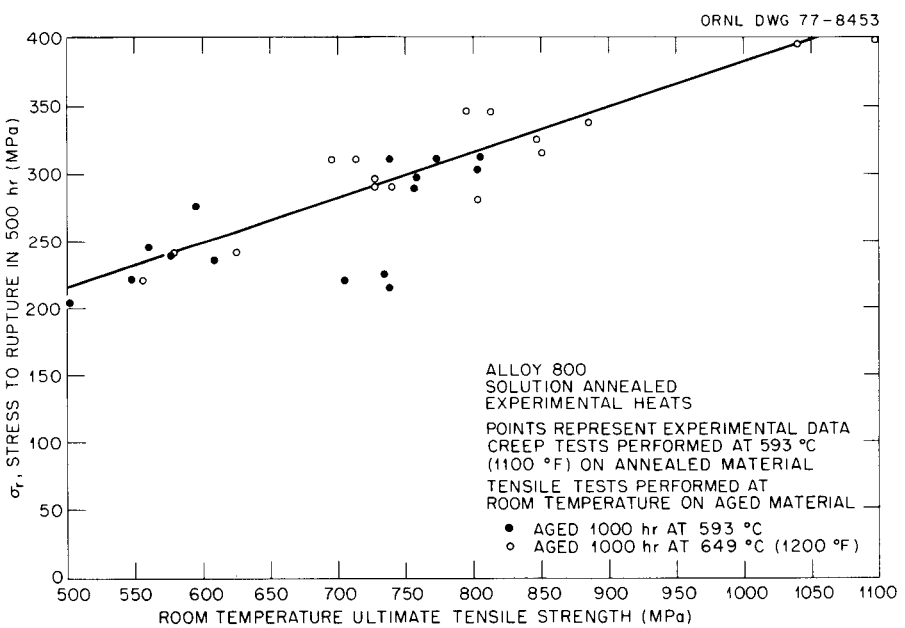

Fig. 18. Relationship Between Room-Temperature Ultimate Tensile Strength of Alloy 800 Aged at 593 or 649°C (1100 or 1200°F) and the 500-hr Creep Rupture Strength of Solution Annealed Alloy 800 at 593°C (1100°F).

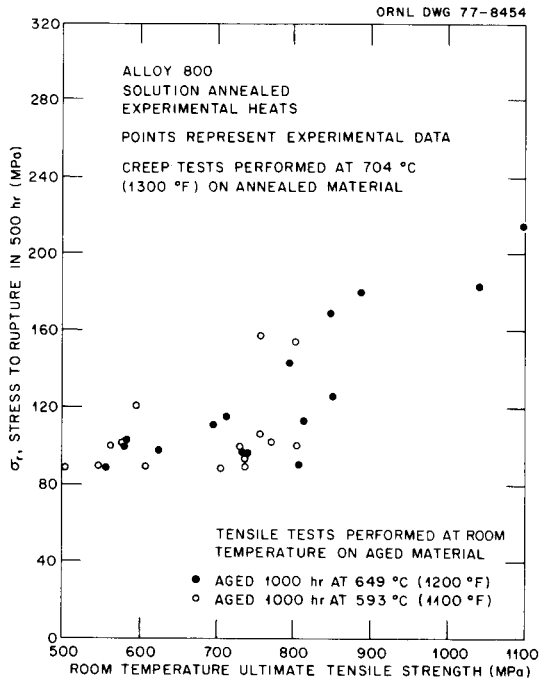

Fig. 19. Relationship Between Room-Temperature Ultimate Tensile Strength of Alloy 800 Aged at 593 or 649°C (1100 or 1200°F) and the 500-hr Creep Rupture Strength of Solution Annealed Alloy 800 at 704°C (1300°F).

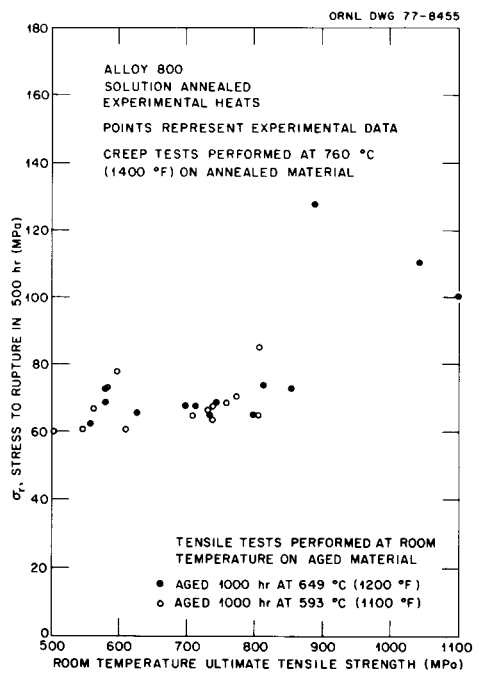

Fig. 20. Relationship Between Room-Temperature Ultimate Tensile Strength of Alloy 800 Aged at 593 or 649°C (1100 or 1200°F) and the 500-hr Creep Rupture Strength of Solution Annealed Alloy 800 at 760°C (1400°F).

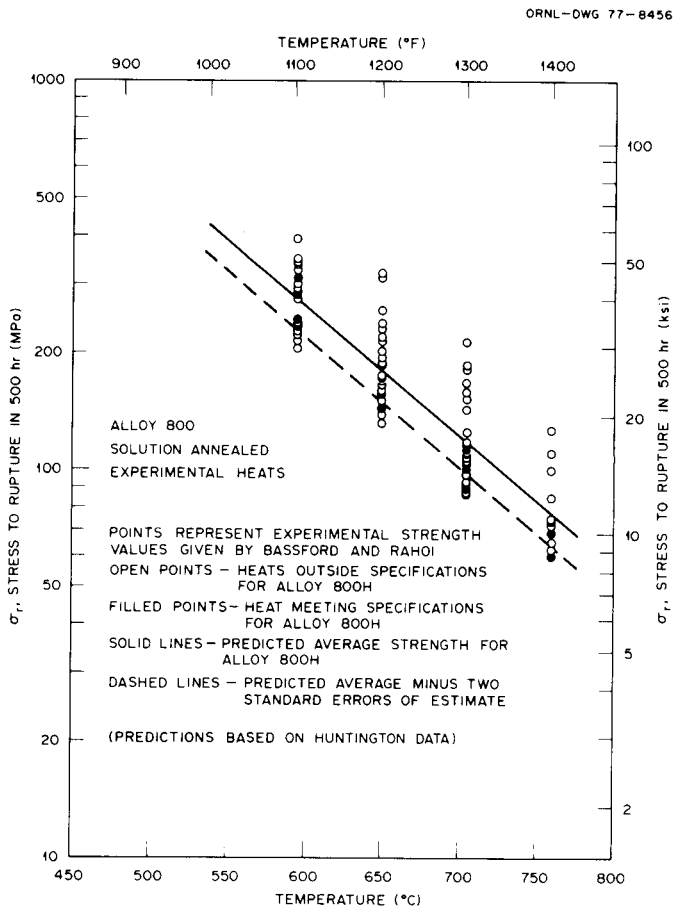

Fig. 21. Comparison Between the 500-hr Creep Strengths of Experimental Heats of Solution Annealed Alloy 800 and Behavior Predicted from the Alloy 800H Data (Fig. 16).

predicted. The width of the ± 2SEE scatter band appears too small for the entire data set. It is about right for the material meeting alloy 800H specifications, except the predicted magnitudes are again consistently high.

A final source of information about the rupture behavior of annealed alloy 800H is the extensive package of data prepared by Sandvik[13] for Sanicro 31. These data are especially relevant since they range from 550 to 700°C, with a significant number at 550 and 600°C. The package includes data for the effects of product form (bar or tube), composition, and solution treatment temperature. Detailed discussions of the Sandvik work can be found in refs. 7 and 33–36. A cursory examination of the data showed no trends that would lead to changing the model used above

to describe the rupture behavior of alloy 800H. The only obvious trend observed was that the Sanicro 31 appears consistently weaker than the alloy 800H. One cause of this weakness may be that many of the solution treatment temperatures were lower than 1150°C (as low as 980°C). These lower temperatures would tend to create a smaller grain size and thus lower strength.[7] Also, the thermodynamic model developed in ref. 6 indicates that the compositions of the Sanicro 31 are generally such that the tendency to form γ' would be smaller than is generally[6] the case for alloy 800H. In an attempt to evaluate these factors, the Sandvik data were analyzed by the procedures used above for the Huntington data. The analysis was performed in three ways. First, the entire package of data[7] was analyzed. Second, only those data for heats that were solution annealed at about 1150°C were analyzed. No data on the grain size of these heats were available, but this high solution treatment temperature should create a reasonably coarse grain structure. Finally, reference to Table 5 shows that several of the Sanicro 31 heats did not meet the composition[1] specifications given in Table 1 for alloy 800H. Thus, a final analysis was conducted with only data for material that was solution annealed at about 1150°C and that met the alloy 800H composition specifications.

The equations chosen to represent these three data sets were as follows:

$$\log t_r = -1.075 + 15300/T - 5.84 \log \sigma \ , \tag{13}$$

for the complete Sanicro 31 data set;

$$\log t_r = -1.655 + 16300/T - 6.03 \log \sigma \ , \tag{14}$$

for the complete 1150°C solution annealed data; and

$$\log t_r = -1.4560 + 15820/T - 5.88 \log \sigma \ , \tag{15}$$

for the 1150°C solution annealed data meeting the alloy 800H composition specifications. Note that Eqs. (13) through (15) are all forms of the

Table 5. Chemical Composition of Sandvik Sanicro Test Material

Melt	Chemical Composition, wt %									
	C	Si	Mn	P	S	Cr	Ni	Ti	Al	N
5.67078	0.042	0.58	1.06	0.009	0.005	21.0	34.0	0.31	0.31	0.022
5.67107	0.036	0.32	1.12	0.010	0.005	20.3	33.65	0.47	0.49	0.018
7.07711	0.040	0.45	1.12	0.008	0.005	21.05	33.8	0.52	0.58	0.016
7.06863	0.041	0.70	0.43	0.011	0.007	21.5	33.7	0.47	0.25	
7.06745	0.045	0.38	0.40	0.009	0.009	19.7	34.4	0.39	0.18	
7.52399	0.046	0.54	0.48	0.013	0.012	20.2	34.8	0.31	0.11	
7.52438	0.043	0.75	0.66	0.010	0.006	19.7	34.8	0.33	0.085	
7.05801	0.045	0.55	0.57	0.010	0.006	19.9	35.2	0.34	0.12	
7.53088	0.041	0.48	0.45	0.007	0.009	20.1	33.9	0.29	0.26	
7.53353	0.055	0.51	0.50	0.009	0.005	21.5	30.8	0.41	0.24	0.030
7.53723	0.048	0.30	0.49	0.009	0.005	21.10	30.8	0.35	0.26	0.016
7.07766	0.035	0.29	1.31	0.008	0.005	20.47	33.45	0.47	0.49	0.018
7.54214	0.042	0.63	0.46	0.010	0.005	20.51	31.15	0.36	0.28	0.035
5.68012	0.041	0.52	0.50	0.007	0.004	19.85	30.55	0.40	0.26	0.007
5.68981	0.042	0.52	0.52	0.008	0.006	21.18	31.20	0.36	0.30	0.032
4.98195	0.052	0.60	0.59	0.020	0.003	20.93	30.80	0.42	0.16	0.026
4.98198	0.056	0.48	0.57	0.014	0.005	21.0	30.76	0.39	0.23	0.033
7.72471	0.055	0.56	0.59	0.007	0.008	20.96	30.92	0.35	0.24	0.020
7.54802	0.046	0.47	0.48	0.009	0.003	20.52	31.10	0.35	0.34	0.049
4.98180	0.075	0.68	0.54	0.011	0.003	21.14	30.96	0.31	0.19	0.029
6.26772	0.085	0.65	0.59	0.007	0.005	20.8	30.67	0.48	0.26	0.022
6.27461	0.076	0.53	0.53	0.009	0.006	20.5	30.99	0.56	0.15	0.009
7.73697	0.062	0.58	0.55	0.007	0.008	20.4	31.0	0.39	0.34	0.012
6.27271	0.111	0.68	0.61	0.010	0.006	19.7	29.47	0.38	0.56	0.021
6.27272	0.113	0.66	0.57	0.010	0.006	20.4	30.08	0.32	0.53	0.025
6.27273	0.103	0.63	0.56	0.009	0.006	20.2	30.15	0.33	0.49	0.024
7.76025	0.068	0.60	0.57	0.010	0.005	20.4	30.5	0.43	0.41	0.012
7.76211	0.070	0.61	0.59	0.010	0.005	20.4	30.7	0.42	0.37	0.018
7.76411	0.068	0.68	0.58	0.009	0.005	20.3	30.5	0.39	0.29	0.018
7.76412	0.068	0.56	0.58	0.008	0.004	20.7	30.8	0.39	0.33	0.016
6.53433	0.054	0.72	0.66	0.007	0.003	21.6	33.2	0.57	0.52	0.015
4.81837	0.078	0.71	0.63	0.013	0.005	20.4	30.3	0.36	0.34	0.016
7.73207	0.058	0.53	0.56	0.011	0.005	20.9	31.3	0.32	0.41	0.018
7.74129	0.043	0.59	0.56	0.010	0.007	21.7	33.2	0.33	0.20	0.019
7.76025	0.065	0.56	0.56	0.008	0.005	20.8	30.5	0.43	0.47	0.014
6.53434	0.041	0.62	0.62	0.008	0.005	21.7	33.8	0.18	0.14	0.026
6.53435	0.055	0.56	0.56	0.008	0.005	21.5	33.4	0.23	0.17	0.024
6.53436	0.058	0.59	0.57	0.008	0.005	21.8	33.4	0.24	0.12	0.014
6.53438	0.068	0.71	0.65	0.008	0.005	21.6	33.5	0.35	0.27	0.014

Orr-Sherby-Dorn[37] time-temperature parameter. Table 6 summarizes the fits of Eqs. (11) and (13) through (15) to the respective data sets.

Figure 22 shows the complete Sanicro 31 data set, including predicted behavior from Eq. (13) and predicted behavior for alloy 800H from Eq. (11). Equation (11) clearly predicts longer lives than Eq. (13). Figure 23 shows the data for the 1150°C solution annealed Sanicro 31 material meeting the composition specifications for alloy 800H. Included in the figure are predicted behavior from Eq. (15) and ±2 standard error of estimate limits as described above.

The results in Table 6 indicate that omission of Sanicro 31 data with nonstandard heat treatments or chemical compositions tends to decrease the amount of scatter in the data. However, the predicted strength (Table 7) of the complete data set is only slightly below

Table 6. Summary of Fits to the Various Rupture Life Data Sets Examined

Data Set	Number of Data	Equation in Text	Standard Error of Estimate (log t_r)	Coefficient of Determination (%)
Alloy 800H	55	(11)	0.271	88.36
Sanicro 31[a]	485	(13)	0.327	70.14
Sanicro 31[b]	291	(14)	0.305	73.44
Sanicro 31[c]	156	(15)	0.244	76.37

[a]Complete Sanicro 31 data set.

[b]1150°C solution annealed material only.

[c]1150°C solution annealed material meeting alloy 800H composition specifications only.

that of the 1150°C solution annealed data set. The two 1150°C solution annealed data sets (standard and nonstandard compositions) have virtually identical predicted strengths. All the Sanicro 31 data sets display somewhat lower creep rupture strengths than the alloy 800H data. Interestingly, the 1150°C solution annealed data sets display strengths roughly equivalent to those of the alloy 800H heats in Fig. 21.

The implication is that the data used in deriving Eq. (11) may well be representative of stronger than average heats of alloy 800H. If this is the case, the predictions of Eq. (11) could be nonconservative. At present, Eq. (11) is recommended to describe the stress-rupture behavior of this material. A further investigation of the differences between the alloy 800H data and the Sanicro 31 data does appear to be indicated, however. The collection of more data on alloy 800H at temperatures of 593°C and below should also be given priority attention.

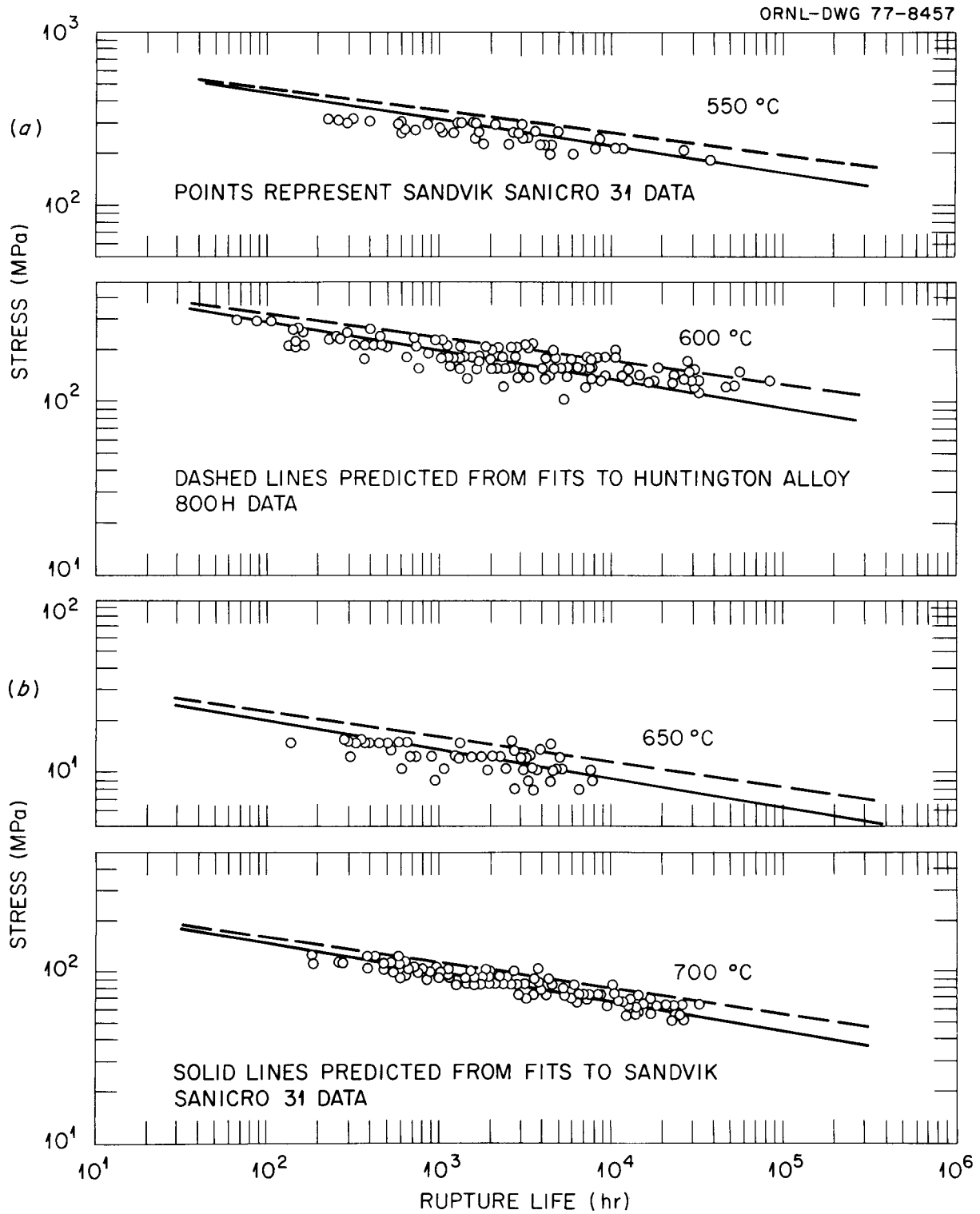

Fig. 22. Comparison Among the Experimental Sandvik Sanicro 31 Stress-Rupture Data and the Predicted Behavior Based on These Data and on the Huntington Data for Alloy 800H.

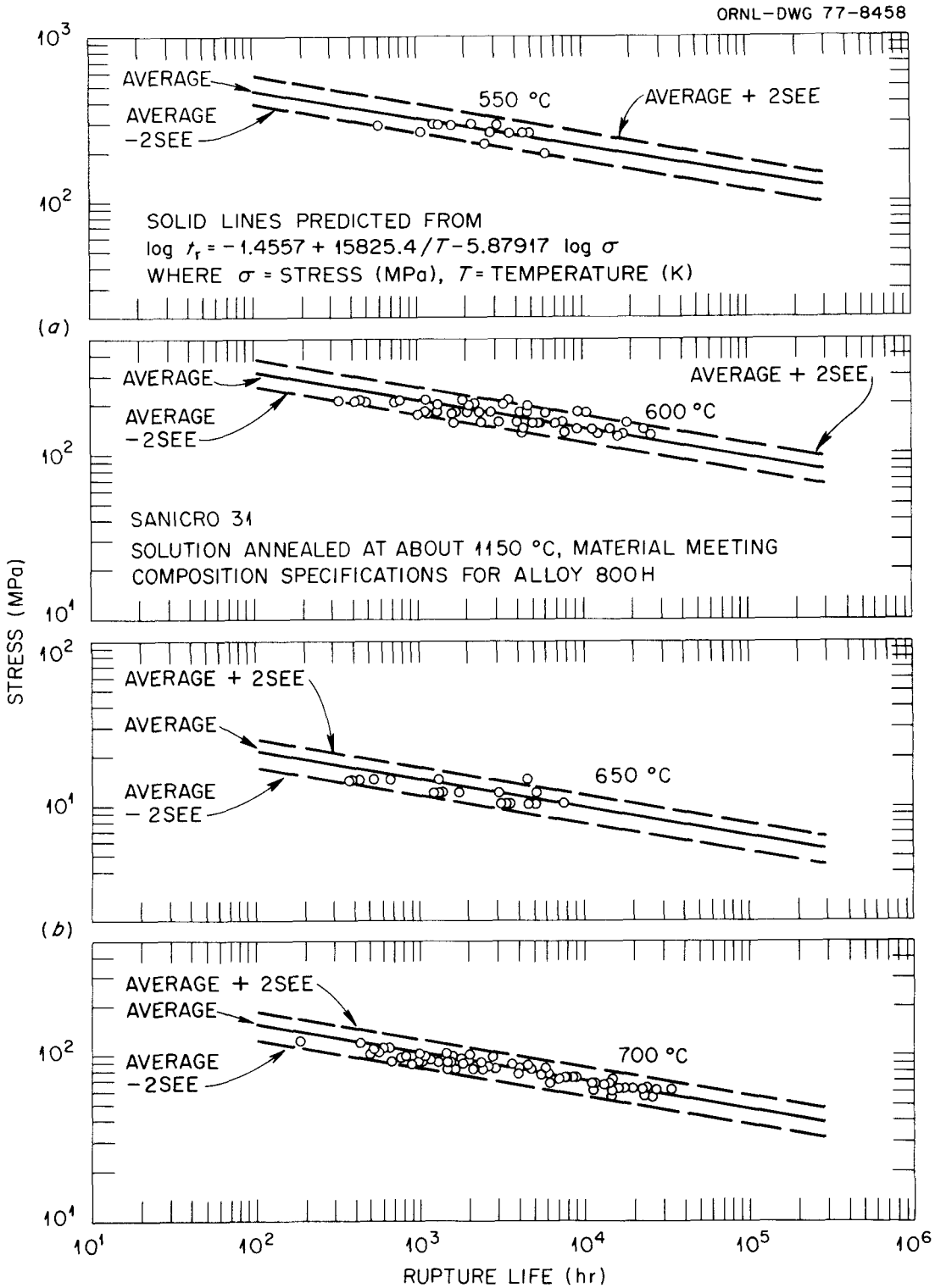

Fig. 23. Comparison of the Experimental 1150°C Solution Annealed Sanicro 31 Data Meeting Alloy 800H Composition Specifications with Predicted Average Behavior for Those Data and ± 2SEE Limits.

Table 7. Estimated Rupture Strengths for the Various Rupture Life Data Sets Examined

Temperature		10^3-hr Rupture Strength, MPa (ksi)		10^5-hr Rupture Strength, MPa (ksi)	
(°C)	(°F)	Average	Lower Limit[a]	Average	Lower Limit[a]
		Alloy 800H[b]			
427	800	903 (131)	788 (114)	547 (79.3)	478 (69.2)
482	900	592 (85.9)	511 (74.2)	345 (50.0)	298 (43.2)
538	1000	385 (55.8)	329 (47.7)	215 (31.2)	184 (26.7)
593	1100	252 (36.6)	213 (30.9)	136 (19.7)	115 (16.6)
649	1200	164 (23.8)	137 (19.9)	85 (12.3)	71 (10.3)
704	1300	108 (15.6)	69 (12.9)	53 (7.8)	44 (6.4)
760	1400	70 (10.2)	57 (8.5)	33 (4.8)	27 (4.0)
		Sanicro 31 Complete Data Set[c]			
427	800	1120 (162)	866 (126)	509 (73.8)	393 (57.0)
482	900	597 (86.6)	462 (67.0)	271 (39.3)	210 (30.4)
538	1000	344 (49.9)	266 (38.6)	156 (22.6)	121 (17.5)
593	1100	214 (31.0)	166 (24.1)	97 (14.1)	75 (10.9)
649	1200	140 (20.3)	108 (15.7)	64 (9.2)	49 (7.1)
704	1300	97 (14.1)	75 (10.9)	44 (6.4)	34 (4.9)
760	1400	69 (10.1)	54 (7.8)	32 (4.6)	24 (3.5)
		Sanicro 31 1150°C Solution Annealed[d]			
427	800	1217 (176)	964 (140)	567 (82.2)	450 (65.3)
482	900	637 (92.4)	505 (73.2)	297 (43.1)	235 (34.1)
538	1000	361 (52.4)	286 (41.5)	168 (24.4)	133 (19.3)
593	1100	222 (32.2)	176 (25.5)	103 (14.9)	82 (11.9)
649	1200	143 (20.7)	114 (16.5)	67 (9.7)	53 (7.7)
704	1300	98 (14.2)	78 (11.3)	46 (6.6)	36 (5.2)
760	1400	70 (10.1)	55 (8.0)	32 (4.7)	26 (3.7)
		Sanicro 31 1150°C Solution Annealed Meeting Alloy 800H Specifications[e]			
427	800	1223 (177)	1010 (146)	559 (81.1)	462 (67.0)
482	900	642 (93.1)	530 (76.9)	293 (42.5)	242 (35.1)
538	1000	364 (52.8)	301 (43.6)	166 (24.1)	137 (19.9)
593	1100	224 (32.5)	185 (26.8)	102 (14.8)	85 (12.3)
649	1200	145 (21.0)	120 (17.4)	66 (9.6)	55 (8.0)
704	1300	99 (14.4)	82 (11.9)	45 (6.6)	38 (5.4)
760	1400	70 (10.2)	58 (8.4)	32 (4.7)	27 (3.9)

[a]Estimate from log t_r − 2SEE lower limits.

[b]Predictions from Eq. (11).

[c]Predictions from Eq. (13).

[d]Predictions from Eq. (14).

[e]Predictions from Eq. (15).

TIME TO TERTIARY CREEP

Since structural instabilities must be avoided in component design, the time to the onset of tertiary creep can be an important design criterion. Methods for the analysis of the time to tertiary creep, t_3, are discussed in ref. 38. These methods consist of two basic types: (1) analyze the data for t_3 by methods analogous to those for t_r and (2) express t_3 as a function of t_r. Both approaches have been used here.

As shown in Fig. 12, the values for t_3 used here were obtained from experimental curves by a 0.2% strain offset from the linear secondary creep line and will be referred to as t_{ss}. The data roughly correspond to the same tests used above in the analysis of rupture life data, the total number of available data being 55 for temperatures from 538 to 760°C. Data for t_2, the time to first deviation from linear secondary ceeep, will be discussed later in this report.

Direct analysis of the available data for t_{ss} yielded an equation of the form

$$\log t_{ss} = -18.95 + 32160/T - (5510/T) \log \sigma \ , \tag{16}$$

which is again a Larson-Miller parameter.[32] The fit to the data (R^2 = 77.76%) is reasonably good, as can be seen from Fig. 24. However, Eq. (16) predicts an anomaly at low temperatures ($T \leqslant 593$°C) in that the predicted values of t_{ss} can be larger than those for t_r from Eq. (11). Thus, either the predicted values of t_{ss} are too large or the predicted values of t_r are too small in this temperature region (which represents an extrapolation beyond the data base). The discussion in the last section indicated that the predicted values of t_r are too large, if anything. It thus appears that Eq. (16) overestimates the values of t_{ss} in the low temperature region.

A possible solution to the above anomaly is to express t_{ss} as a function of t_r. Following the procedure used previously[38] for types 304 and 316 stainless steels, 2 1/4 Cr-1 Mo steel, and Inconel alloy 718, this relationship was found to be

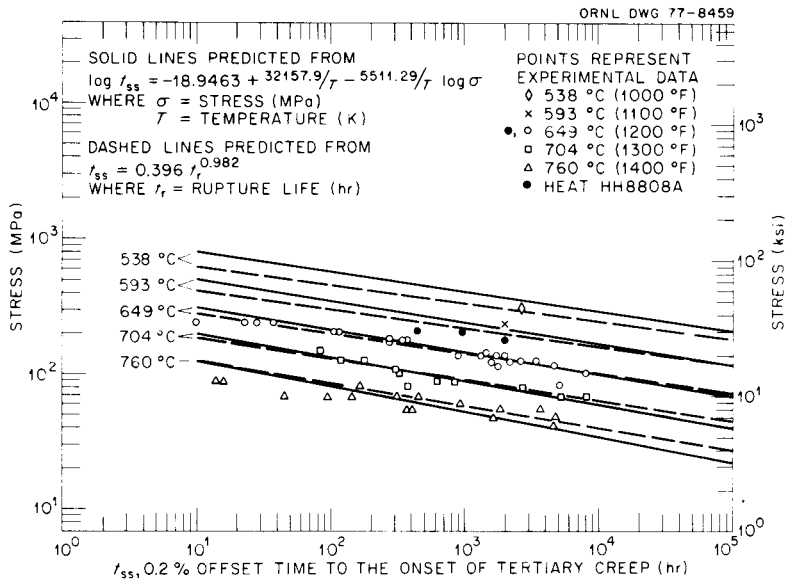

Fig. 24. Comparison of Available Experimental Data for Time to Tertiary Creep (0.2% Offset) for Alloy 800H with Predicted Behavior from Direct Fits to the Data and from a Temperature-Independent Relationship Between the Time to Tertiary Creep and the Rupture Life.

$$t_{ss} = 0.396 t_r^{0.982} , \tag{17}$$

as illustrated in Fig. 25.

The value of R^2 for Eq. (17), based on 50 data, was 91.9%. The predictions from Eq. (17) [using Eq. (11) to estimate t_r] are also shown in Fig. 24.

A close examination of the data, such as described in ref. 39, showed that the ratio of t_{ss}/t_r clearly increased as the test temperature decreased. Following previous results in similar situations[39,40] a temperature dependence was introduced, leading to

$$t_{ss} = 0.000628 e^{6108}/T t_r^{0.996} , \tag{18}$$

as shown in Fig. 26.

Equation (18) yielded an R^2 value of 95.3%. However, rewriting Eq. (18) as $t_{ss} = F(T) t_r^{0.996}$, the value of F reaches and exceeds unity as the temperature decreases below 828 K. Above about 866 K (593°C),

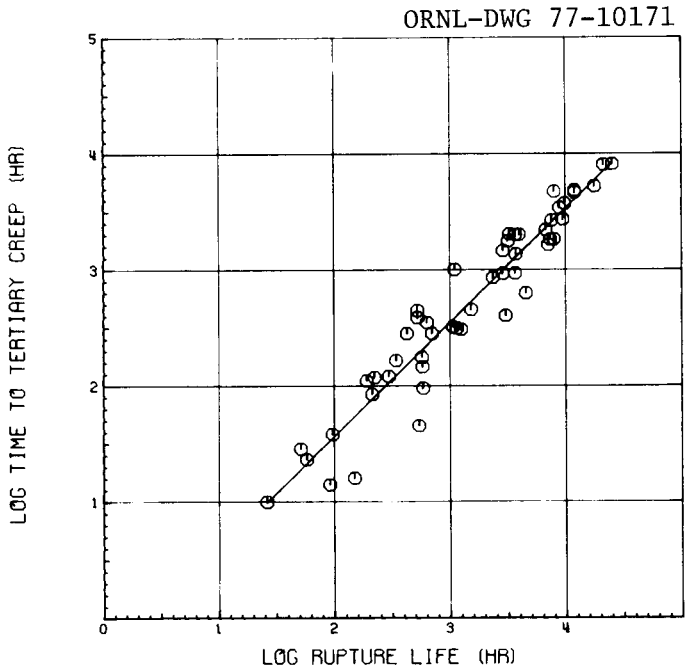

Fig. 25. Temperature-Independent Relationship Between Rupture Life and Time to Tertiary Creep (0.2% Offset) for Alloy 800H.

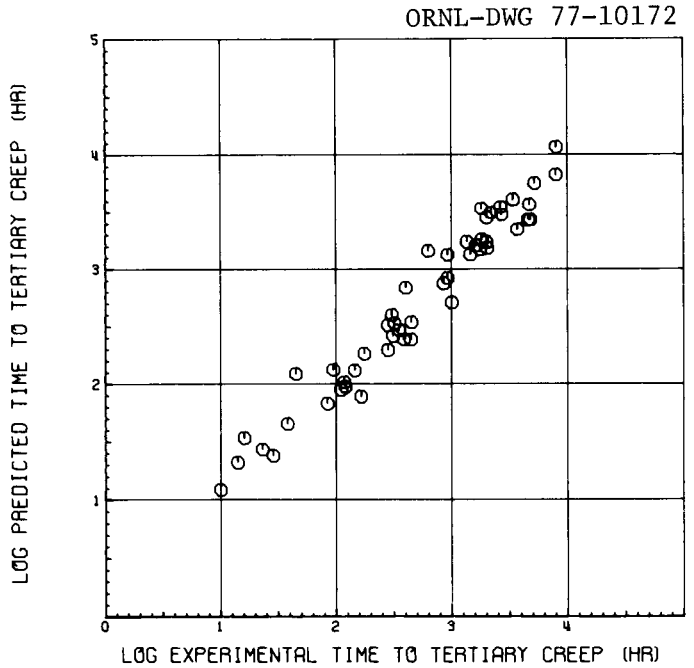

Fig. 26. Relationship Between Experimental Values of Time to Tertiary Creep (0.2% Offset) for Alloy 800H and Values Predicted from a Temperature-Dependent Relationship Between Time to Tertiary Creep and Rupture Life.

Eq. (18) appears to provide the best available description for the data. Interestingly, the value of F at 593°C is 0.726, which corresponds closely to that found previously for type 304 stainless steel. The recommended procedure is to use Eq. (18) at 593°C and above. At lower temperatures, the predicted behavior should be given by

$$t_{ss} = 0.726 t_r^{0.996} \quad . \tag{19}$$

These predictions are compared with the experimental data in Fig. 27. Note that the predictions of Eqs. (16) and (18) are virtually identical at temperatures of 593°C or above, whereas Eq. (19) resolves the low temperature anomalies in those equations.

To predict "minimum" values of t_{ss}, first calculate a mean value for log t_{ss} by the above procedure. Then, subtract two standard errors from Eq. (11) to account for uncertainties in t_r at a given σ and T. Finally, subtract two standard errors from Eq. (18) (SEE = 0.17) to account for uncertainties in t_{ss} at a given t_r. The resulting value is the log t_{ss} value corresponding to the lower limit estimate at the stress and temperature of interest. A similar procedure has been used successfully for 2 1/4 Cr-1 Mo steel,[17] although there tolerance limits were used at each step rather than 2SEE limits. Predicted minimum curves are included in Fig. 27, while Table 8 shows the estimated average and minimum stresses to cause onset of tertiary creep in 10^3 and 10^5 hr.

No other data for t_{ss} were available than those discussed above. Conceivably, the Sanicro 31 rupture data discussed in the last section could be used in conjunction with Eqs. (18) and (19) to estimate tertiary creep behavior. However, having no concrete tertiary creep data for the Sanicro 31, such estimation would be largely conjecture.

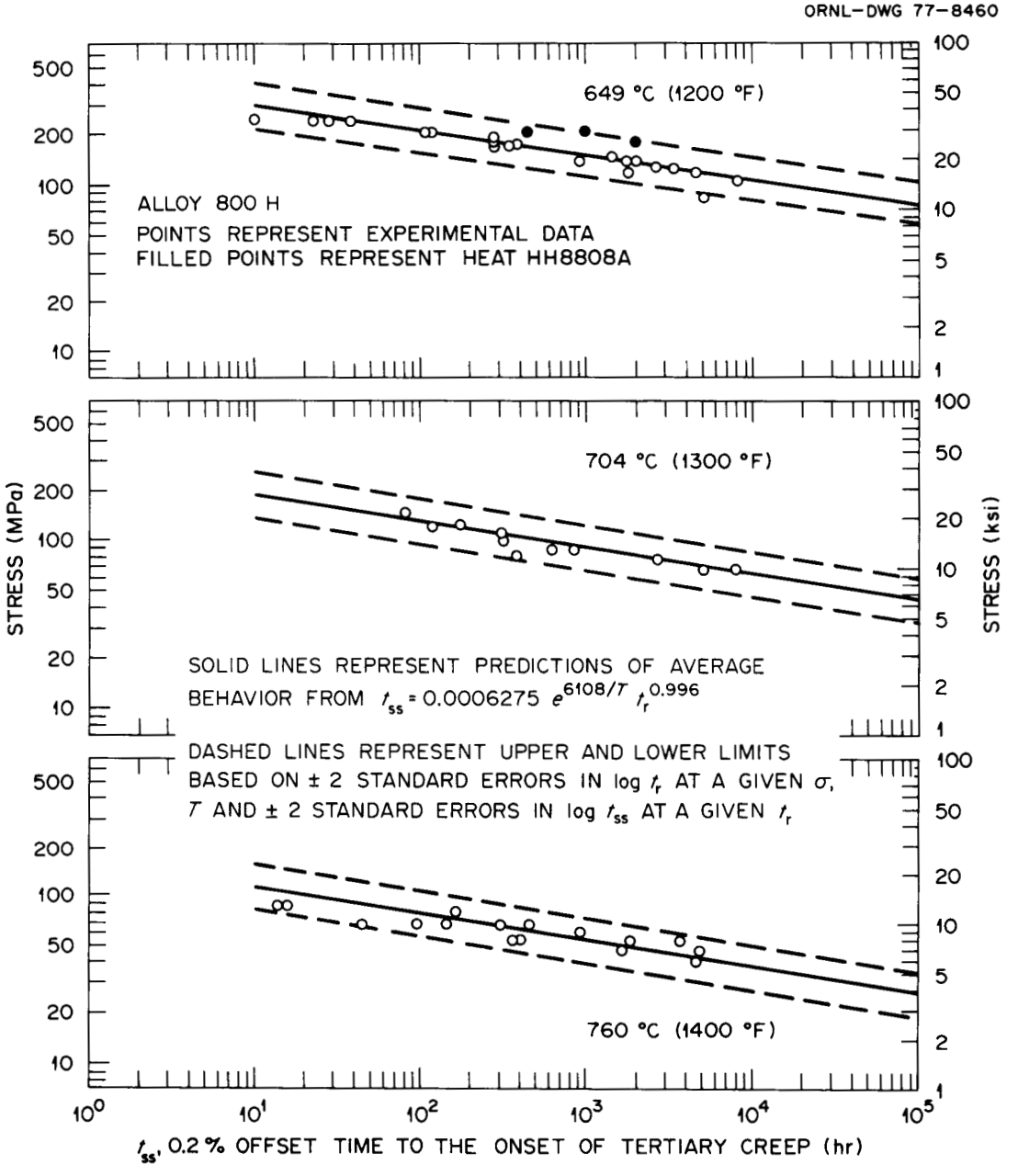

Fig. 27. Comparison Between Experimental Time to Tertiary Creep (0.2% Offset) Data for Alloy 800H and Predicted Behavior from the Recommended Temperature-Dependent Relationship Between Rupture Life and Time to Tertiary Creep. Included are ±2SEE limits.

Table 8. Estimated Tertiary Creep Strength for Alloy 800H (0.2% Offset)

Temperature		10^3-hr Tertiary Creep Strength, MPa (ksi)		10^5-hr Tertiary Creep Strength, MPa (ksi)	
(°C)	(°F)	Average	Lower Limit	Average	Lower Limit
427	800	870 (126)	697 (101)	526 (76.2)	421 (61.1)
482	900	568 (82.4)	448 (64.9)	330 (47.9)	260 (37.7)
538	1000	368 (53.4)	285 (41.4)	206 (29.8)	159 (23.1)
593	1100	241 (34.9)	183 (26.6)	129 (18.7)	98 (14.2)
649	1200	147 (21.3)	110 (15.9)	76 (11.0)	57 (8.2)
704	1300	90 (13.1)	66 (9.6)	45 (6.5)	33 (4.8)
760	1400	55 (8.0)	40 (5.8)	26 (3.8)	19 (2.7)

STRAIN TO RUPTURE

Since long-term ductility is of particular concern in materials such as alloy 800H, the available data for the total strain to creep rupture were examined. These data included roughly the same as those used above in the analysis of rupture life, including the Sandvik Sanicro 31 data.

The method used to analyze these data was similar to that proposed first by Smith[41], expanded by Goldhoff,[42] and applied in detail by Booker et al.[43] Denoting the strain to rupture as e_t, the average strain rate to rupture $\dot{e}_t$ is defined by

$$\dot{e}_t = e_t/t_r \ . \tag{20}$$

Although the scatter in e_t is generally too great to permit a meaningful direct analysis such as used above for t_r and t_3, the quantity $\dot{e}_t$ often does permit such an analysis. Having estimates for $\dot{e}_t$ and t_r, one then simply multiplies these values to yield an estimate for e_t. Analysis of the Huntington alloy 800H data yielded a final selected equation similar to that used above for rupture life:

$$\log \dot{e}_t = 25.18 - 41200/T + \frac{7410}{T} \log \sigma \ . \tag{21}$$

Figure 28 compares the predictions of Eq. (21) with the experimental data.

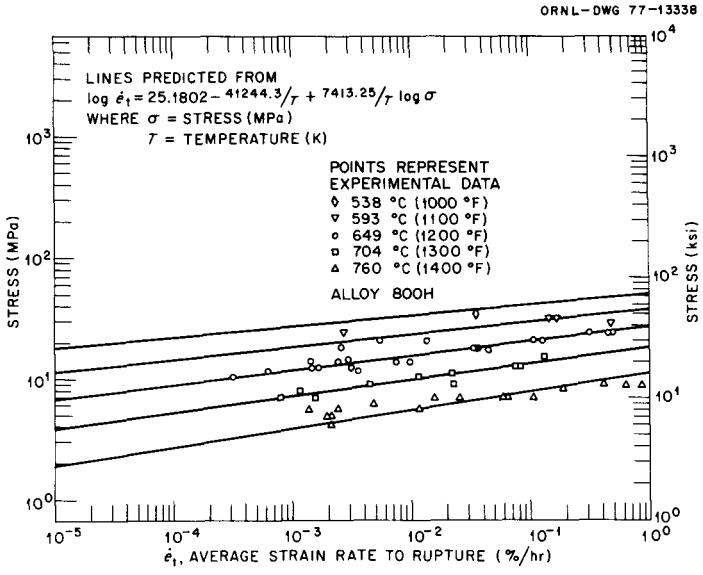

Fig. 28. Comparison Between Experimental Average Strain Rate to Rupture Data for Alloy 800H and Predicted Behavior.

The three Sanicro 31 data sets described above were fit by equations of the form:

$$\log \dot{e}_t = 5.061 - 18900/T + 6.52 \log \sigma \ , \tag{22}$$

for the complete Sanicro 31 data set;

$$\log \dot{e}_t = 6.218 - 20330/T + 6.63 \log \sigma \ , \tag{23}$$

for the complete 1150°C solution annealed data set; and

$$\log \dot{e}_t = 5.494 - 19900/T + 6.74 \log \sigma \ , \tag{24}$$

for the 1150°C solution annealed material meeting the alloy 800H composition specifications. Table 9 summarizes the fits of Eqs. (21) through (24) to the respective data sets.

Equations (21) through (24) can be combined with the corresponding Eqs. (11) and (13) through (15) for rupture life to express the models directly in terms of log e_t as:

Table 9. Summary of Fits to the Various Average Creep Strain to Rupture Data Sets Examined

Data Set	Number of Data	Equation Number in Text	Standard Error of Estimate ($\log \dot{e}_t$)	Coefficient of Determination (%)
Alloy 800H	55	25	0.454	77.72
Sanicro 31[a]	484	26	0.539	51.96
Sanicro 31[b]	290	27	0.509	55.67
Sanicro 31[c]	155	28	0.386	63.52

[a]Complete Sanicro 31 data set.

[b]1150°C solution annealed material only.

[c]1150°C solution annealed material meeting alloy 800H chemistry specifications only.

$$\log e_t = 6.728 - 7218/T + \frac{982}{T} \log \sigma \ , \tag{25}$$

for the Huntington alloy 800H data;

$$\log e_t = 3.986 - 3635/T + 0.684 \log \sigma \ , \tag{26}$$

for the complete Sanicro 31 data set;

$$\log e_t = 4.563 - 4039/T + 0.593 \log \sigma \ , \tag{27}$$

for the 1150°C solution annealed material; and

$$\log e_t = 4.038 - 4065/T + 0.857 \log \sigma \ , \tag{28}$$

for the 1150°C solution annealed material meeting the alloy 800H composition specifications.

Figures 29 and 30 compare the predictions of these equations with the experimental data. Table 10 compares the predicted average and "minimum" values of e_t corresponding to rupture lives of 10^3 and 10^5 hr for the various data sets. Since the rupture lives are assumed, there

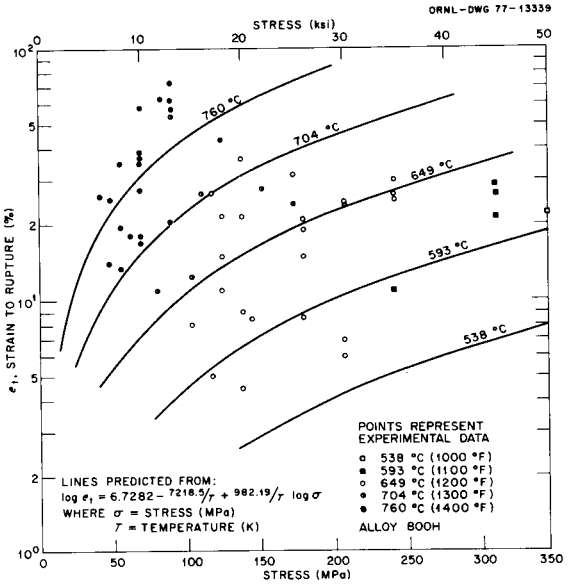

Fig. 29. Comparison Between Experimental and Predicted Values of Total Elongation to Creep Rupture for Alloy 800H.

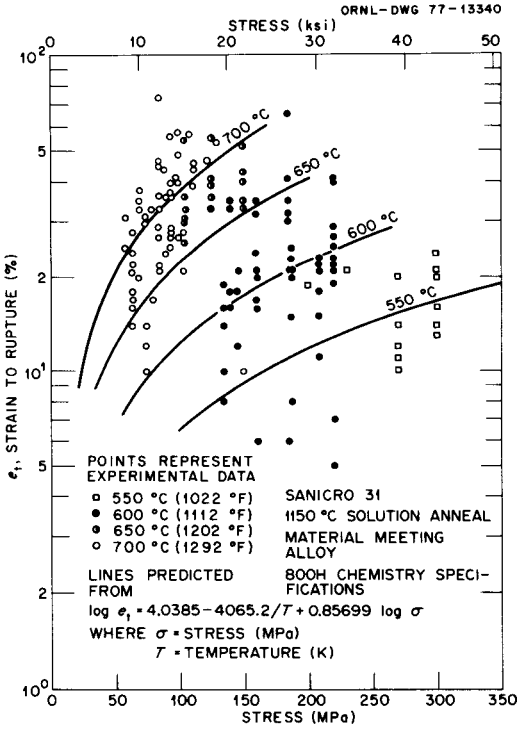

Fig. 30. Comparison Between Experimental and Predicted Values of Total Elongation to Creep Rupture for Sanicro 31 1150°C Solution Annealed Material Meeting Alloy 800H Composition Specifications.

Table 10. Estimated Values of Total Elongation to Creep Rupture for the Various Data Sets Examined

Temperature		10^3-hr Rupture Elongation, %		10^5-hr Rupture Elongation, %	
(°C)	(°F)	Average	Lower Limit[a]	Average	Lower Limit
			Alloy 800H[b]		
427	800	3.6	0.4	1.8	0.2
482	900	5.9	0.7	2.9	0.4
538	1000	9.1	1.1	4.5	0.6
593	1100	13.1	1.6	6.5	0.8
649	1200	18.1	2.2	9.0	1.1
704	1300	24.2	3.4	11.8	1.4
760	1400	31.2	3.8	15.3	1.9
			Sanicro 31 Complete Data Set[c]		
427	800	7.5	0.6	4.4	0.4
482	900	11.7	1.0	6.8	0.6
538	1000	17.3	1.4	10.1	0.8
593	1100	24.1	2.0	14.0	1.2
649	1200	32.4	2.7	19.0	1.6
704	1300	42.0	3.5	24.5	2.0
760	1400	53.0	4.4	31.3	2.6
			Sanicro 31 1150°C Solution Annealed[d]		
427	800	4.2	0.4	2.6	0.2
482	900	7.5	0.7	4.8	0.5
538	1000	12.5	1.2	8.0	0.8
593	1100	19.4	1.9	12.3	1.2
649	1200	28.8	2.8	18.3	1.8
704	1300	40.6	3.9	25.9	2.5
760	1400	55.7	5.4	35.0	3.4
			Sanicro 31 1150°C Solution Annealed Meeting Alloy 800H Specifications[e]		
427	800	7.5	1.3	3.8	0.6
482	900	11.5	1.9	5.9	1.0
538	1000	16.6	2.8	8.5	1.4
593	1100	22.8	3.8	11.6	2.0
649	1200	30.3	5.1	15.4	2.6
704	1300	38.7	6.5	19.7	3.3
760	1400	48.4	8.2	24.7	4.2

[a]Estimated from log e_t − 2SEE in log $\dot{e}_t$.

[b]Predictions from Eq. (25).

[c]Predictions from Eq. (26).

[d]Predictions from Eq. (27).

[e]Predictions from Eq. (28).

is no error in t_r for these predictions. Thus, the minimum values of e_t were obtained simply by subtracting 2SEE for the various log $\dot{e}_t$ fits (Table 9) from the predicted values of log e_t.

Briefly, the results of the current analysis of the data for total elongation for creep rupture can be summarized as follows:

1. The three Sanicro 31 data sets all yield similar results, and all predict greater ductility than the alloy 800H data at 593°C and above.

2. The scatter is large, but Eqs. (25) through (28) appear to adequately describe the trends apparent in the data. These trends include a tendency for ductility to increase as temperature increases and to decrease as the rupture life increases (stress and creep rate decrease).

3. The low predicted values of e_t below about 593°C cannot be totally substantiated by concrete data, but they appear consistent with the data that are available. These low values, together with the decrease in e_t as t_r increases, again indicate a need for more long time and low temperature test data for this material. Such data would permit a better quantitative estimate of any possible design problems due to a lack of creep ductility.

CREEP STRAIN TO TERTIARY CREEP

The amount of creep strain that a material can withstand can also be an important ductility criterion in elevated-temperature design.[40] Therefore, the available data for e_3, the creep strain to tertiary creep (corresponding to the above data for t_3, the time to tertiary creep), have been analyzed as described below.

The method of analysis is similar to that used previously.[40—43] First, the average creep rate to tertiary creep, $\dot{e}_3$, is defined by

$$\dot{e}_3 = e_3/t_3 \ . \tag{29}$$

Then, separate analysis of $\dot{e}_3$ and t_3, followed by a multiplication of the results, yields an estimate for e_3 as a function of stress and temperature. (The 0.2% offset strain to tertiary creep will be referred to as e_{ss}.)

The data for $\dot{e}_{ss}$ have been analyzed in two ways. First, the 55 available data were directly fit by the same procedures used above for t_r, t_{ss}, and $\dot{e}_t$. Then, available data for the minimum creep rate, $\dot{e}_m$, were analyzed. Values of $\dot{e}_{ss}$ were then estimated as functions of $\dot{e}_m$ analogous to the relationship between rupture life and time to tertiary creep used above.

The direct analysis of the data for $\dot{e}_{ss}$ yielded an equation of the form

$$\log \dot{e}_{ss} = 24.81 - 40520/T + (6955/T) \log \sigma \ , \tag{30}$$

which had an R^2 value of 76.34%. The predictions of this equation are compared with the experimental data in Fig. 31.

Minimum creep rate data were analyzed on 73 available data. (Many values of $\dot{e}_m$ were estimated for tests that appeared to be well into secondary creep but had not reached tertiary creep — thus the larger number of data.) The final equation chosen was

$$\log \dot{e}_m = 28.84 - 46080/T + (7610/T) \log \sigma \ , \tag{31}$$

with an R^2 value of 75.73%. The predictions of Eq. (31) are compared with the experimental data in Fig. 32.

The relationship between $\dot{e}_m$ and $\dot{e}_{ss}$ was reasonably independent of temperature, the data being well described (R^2 = 94.5%) by

$$\dot{e}_{ss} = 0.80\dot{e}_m^{\,0.839} \ , \tag{32}$$

as shown in Fig. 33. Predictions from Eq. (32) are also shown in Fig. 32. The predicted values from Eqs. (30) and (32) are quite similar, although Eq. (30) appears to fit the data slightly better.

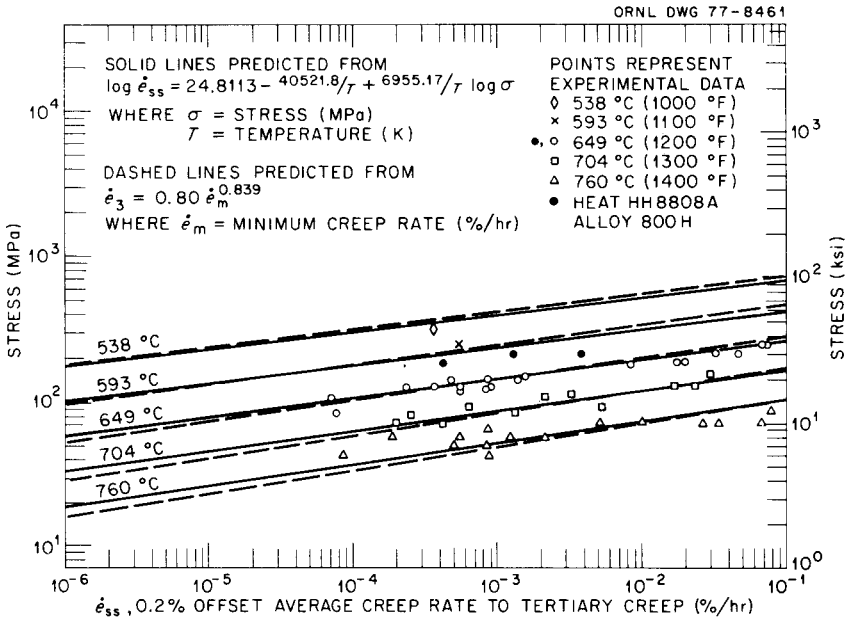

Fig. 31. Comparison Between Experimental and Predicted Values of Average Creep Rate to Tertiary Creep (0.2% Offset) for Alloy 800H.

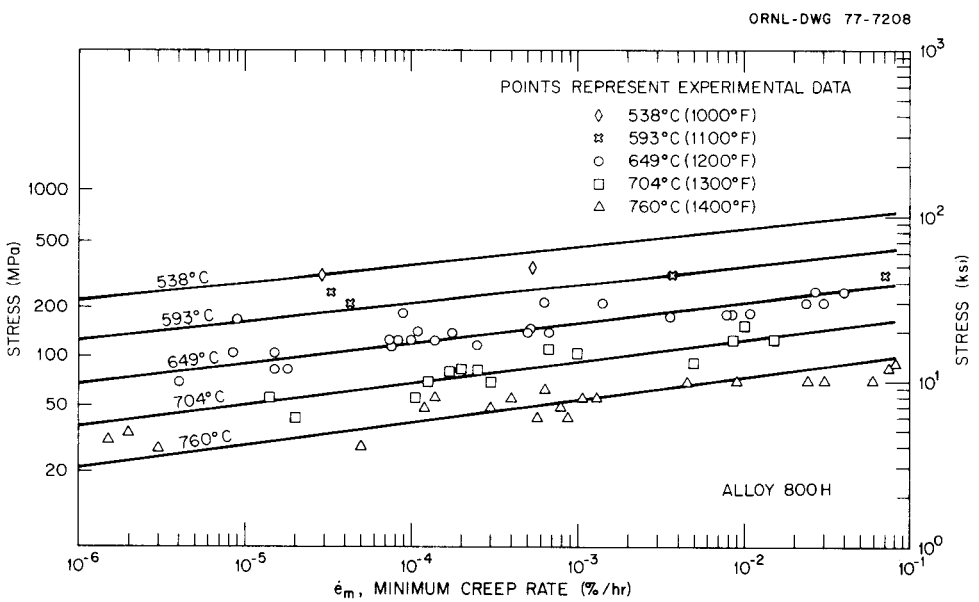

Fig. 32. Comparison Between Experimental Data and Predicted Values of Minimum Creep Rate for Alloy 800H. Lines predicted from $\log \dot{e}_m = 28.84 - 46080/T + (7610/T) \log \sigma$, where σ = stress (MPa), and T = temperature (K).

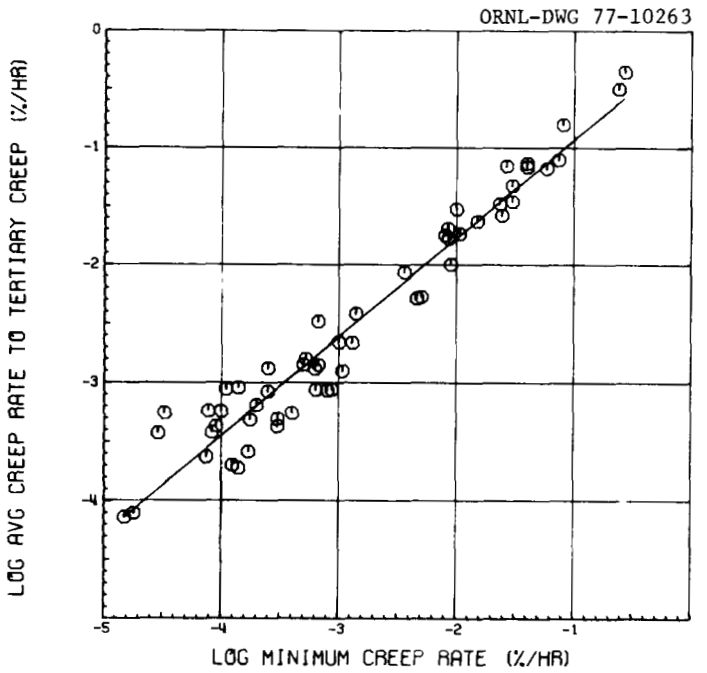

Fig. 33. Relationship Between Minimum Creep Rate and Average Creep Rate to Tertiary Creep (0.2% Offset) for Alloy 800H.

This advantage may be due to a slight tempertaure dependence in the relationship between $\dot{e}_m$ and $\dot{e}_{ss}$. Thus, we decided to use Eq. (30) to predict $\dot{e}_{ss}$.

To develop an analytical expression for e_{ss}, note that the above Eqs. (11), (18), and (19) can be rearranged to yield

$$\log t_{ss} = -18.53 + 33910/T - (6410/T) \log \sigma \ , \tag{33}$$

for $T < 593°C$, and

$$\log t_{ss} = -21.59 + 36560/T - (6410/T) \log \sigma \ , \tag{34}$$

for $T \geqslant 593°C$. Thus, e_3 is given by

$$\log e_{ss} = 6.284 - 6615/T + (547/T) \log \sigma \ , \tag{35}$$

for $T < 593°C$, and

$$\log e_{ss} = 3.221 - 3962/T + (547/T) \log \sigma \ , \tag{36}$$

for $T \geqslant 593°C$.

Figure 34 compares the predictions from Eqs. (35) and (36) with the experimental data for e_{ss}. Unfortunately, the prediction of e_{ss} by these equations probably introduces certain biases into the predictions. These biases occur because Eq. (18) and (19) alter the predictions for

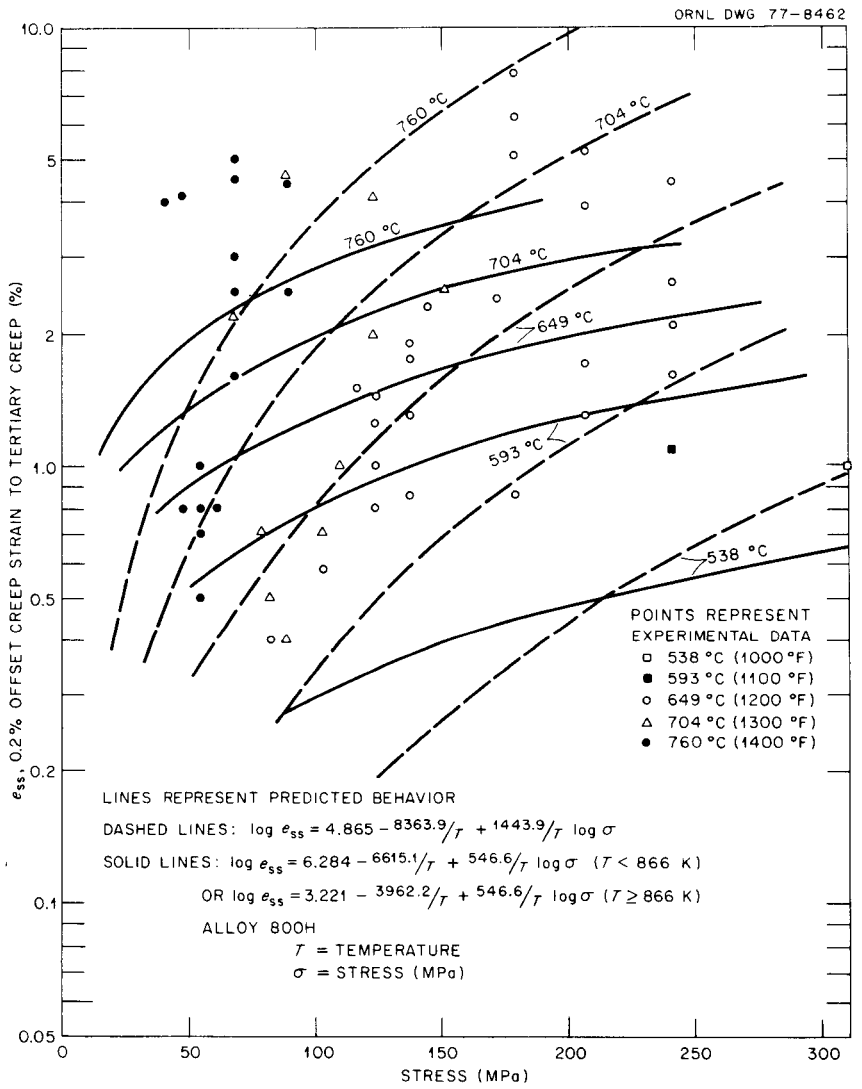

Fig. 34. Predicted and Experimental Values of Strain to the Onset of Tertiary Creep (0.2% Offset) for Alloy 800H.

t_{ss} to reflect variations in t_r. Equation (30) includes no such alterations in the predictions for $\dot{e}_{ss}$. Rather, the tertiary creep data themselves determine the trends in the predictions for $\dot{e}_{ss}$. Attempts at predicting $\dot{e}_{ss}$ from t_r or from t_{ss} proved unsatisfactory. Thus, the most unbiased prediction for e_{ss} can probably be obtained by combining Eqs. (16) and (30), even though Eqs. (18) and (19) yield the best predictions for t_{ss} itself. Thus, we have

$$\log e_{ss} = 4.865 - 8360/T + (1440/T) \log \sigma \ , \tag{37}$$

the predictions from which are also shown in Fig. 34.

Equations (35) through (37) all lead to analytical anomalies at low stresses and temperatures. This region represents a large extrapolation beyond the data base, and the predicted values of e_{ss} can be quite small. However, if e_{ss} is less than 0.2%, the predicted value of e_2 (creep strain to first deviation from linear secondary creep) becomes negative. This anomaly can be solved by a slightly different treatment of the data for e_{ss}, or the strain to tertiary creep can be analyzed with data for e_2. Using techniques analogous to those used above, these analyses yielded equations of the form:

$$\log t_2 = -17.080 + 28940/T - (4890/T) \log \sigma \ , \tag{38}$$

$$t_2 = 0.414 t_r^{\,0.935} \ , \tag{39}$$

and

$$t_2 = 0.00135 e^{5480/T} t_r^{\,0.940} \ , \tag{40}$$

corresponding to Eqs. (16) through (18) above (Figs. 35—38), and

$$\log \dot{e}_2 = 24.31 - 40240/T + (7040/T) \log \sigma \ , \tag{41}$$

and

$$\dot{e}_2 = 0.762 \dot{e}_m^{\,0.836}, \tag{42}$$

corresponding to Eqs. (30) and (32) above (Figs. 39 and 40).

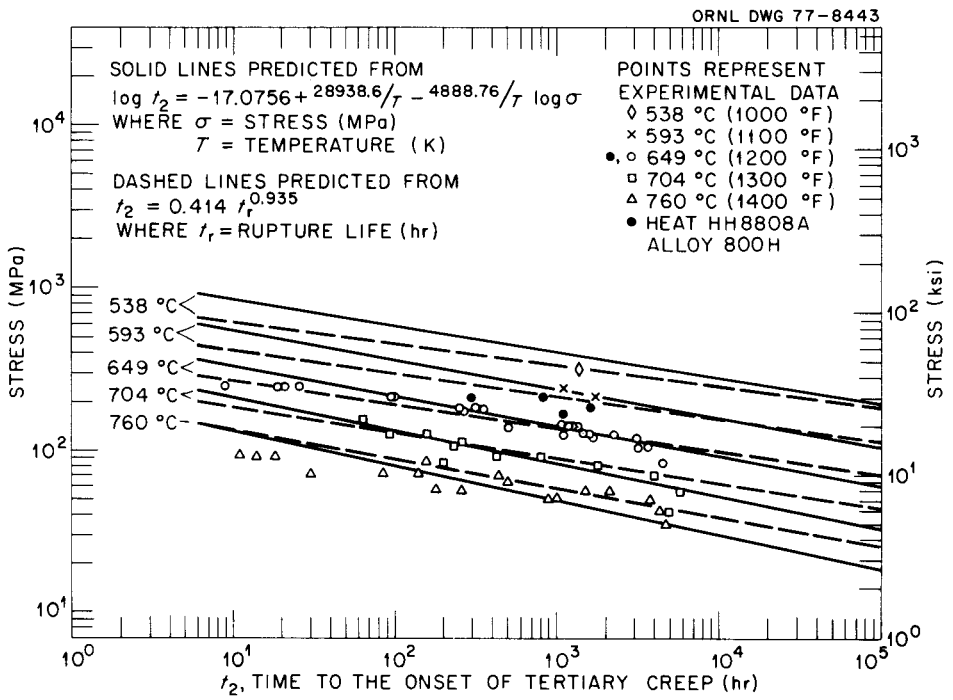

Fig. 35. Comparison of Available Experimental Data for Time to Tertiary Creep (No Offset) for Alloy 800H with Predicted Behavior from Direct Fits to the Data, and from a Temperature-Independent Relationship Between the Time to Tertiary Creep and the Rupture Life.

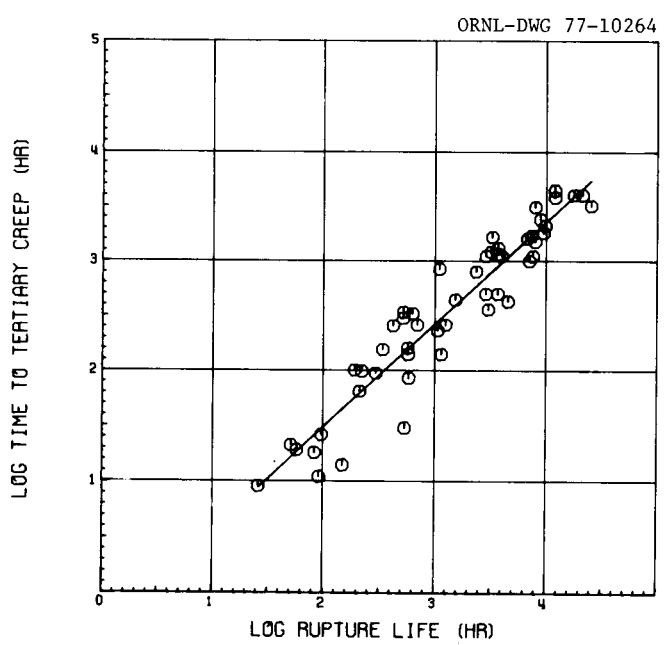

Fig. 36. Temperature-Independent Relationship Between Rupture Life and Time to Tertiary Creep (No Offset) for Alloy 800H.

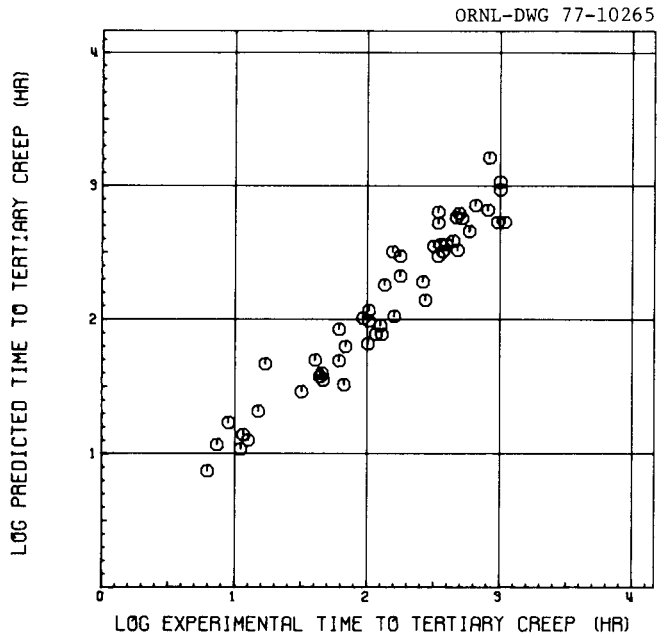

Fig. 37. Relationship Between Experimental Values of Time to Tertiary Creep (No Offset) for Alloy 800H and Values Predicted from a Temperature-Dependent Relationship Between Time to Tertiary Creep and Rupture Life.

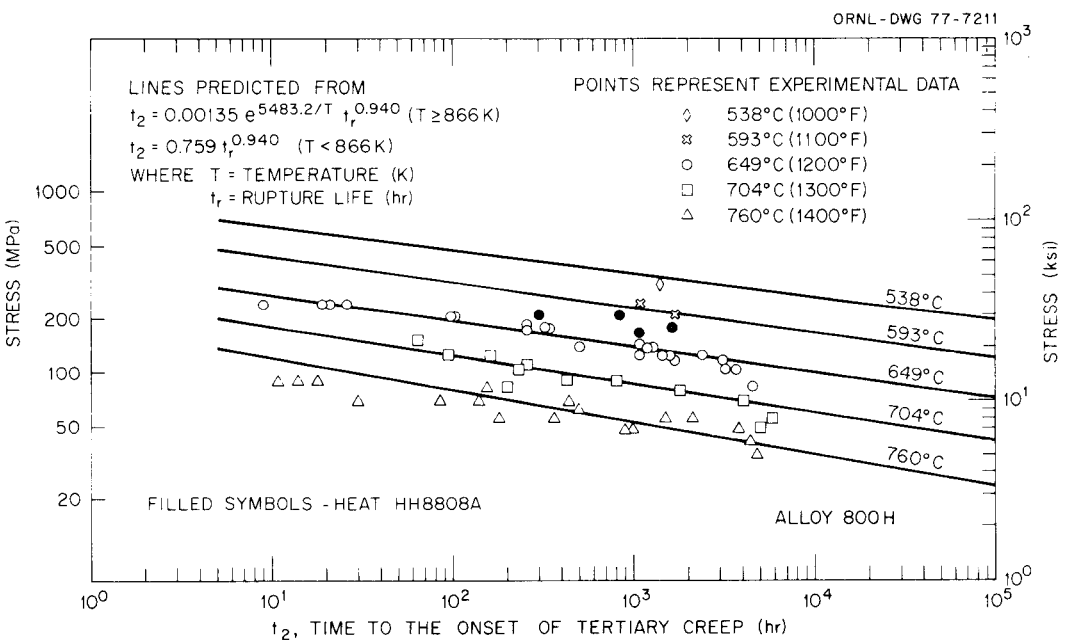

Fig. 38. Comparison Between Experimental Time to Tertiary Creep (No Offset) Data for Alloy 800H and Predicted Behavior from the Recommended Temperature-Dependent Relationship Between Rupture Life and Time to Tertiary Creep.

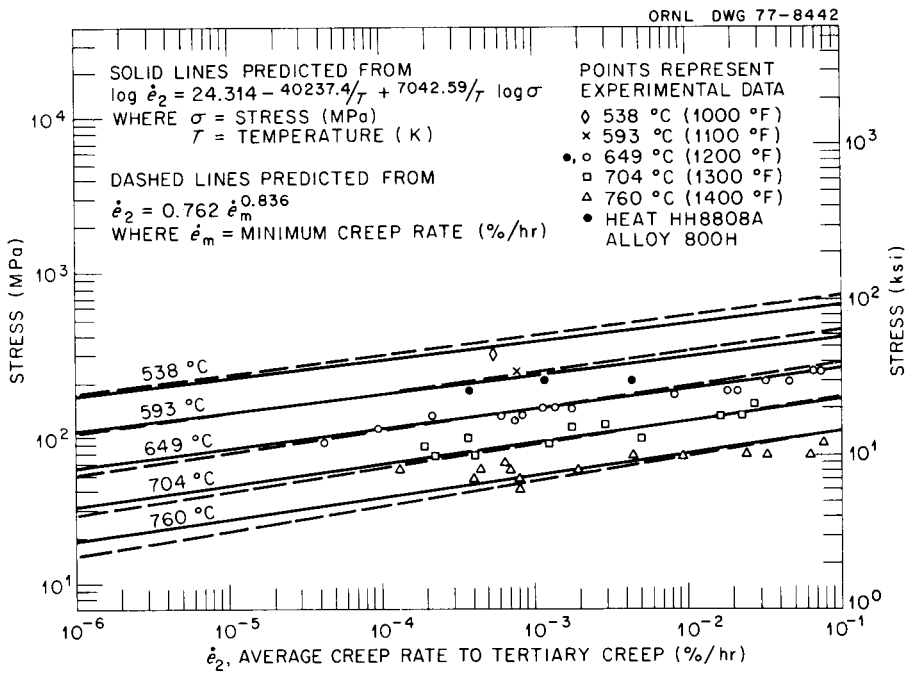

Fig. 39. Comparison Between Experimental and Predicted Values of Average Creep Rate to Tertiary Creep (No Offset) for Alloy 800H.

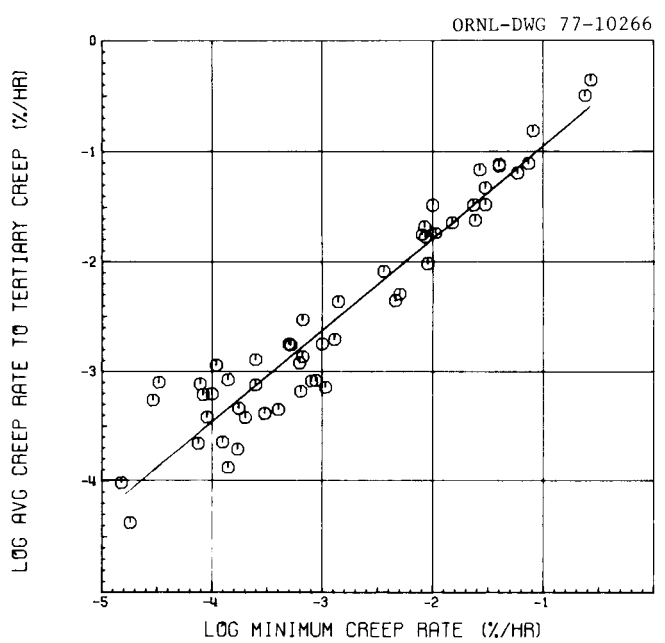

Fig. 40. Relationship Between Minimum Creep Rate and Average Creep Rate to Tertiary Creep (No Offset) for Alloy 800H.

Like Eq. (18), Eq. (40) is valid only at 593°C (866 K) and above. At lower temperatures, 866 should be substituted for T in that equation, yielding

$$t_2 = 0.759 t_r^{0.940} \quad . \tag{43}$$

Equations (40) and (43) yield the recommended predictions for t_2, while Eq. (41) yields the recommended predictions for $\dot{e}_2$. However, as with e_{ss} above, e_2 should be predicted from Eqs. (38) and (41) by

$$\log e_2 = 7.238 - 11300/T + (2150/T) \log \sigma \ , \tag{44}$$

as shown in Fig. 41. Table 11 shows predicted average and minimum values for the 10^3- and 10^5-hr tertiary creep strength based on t_2.

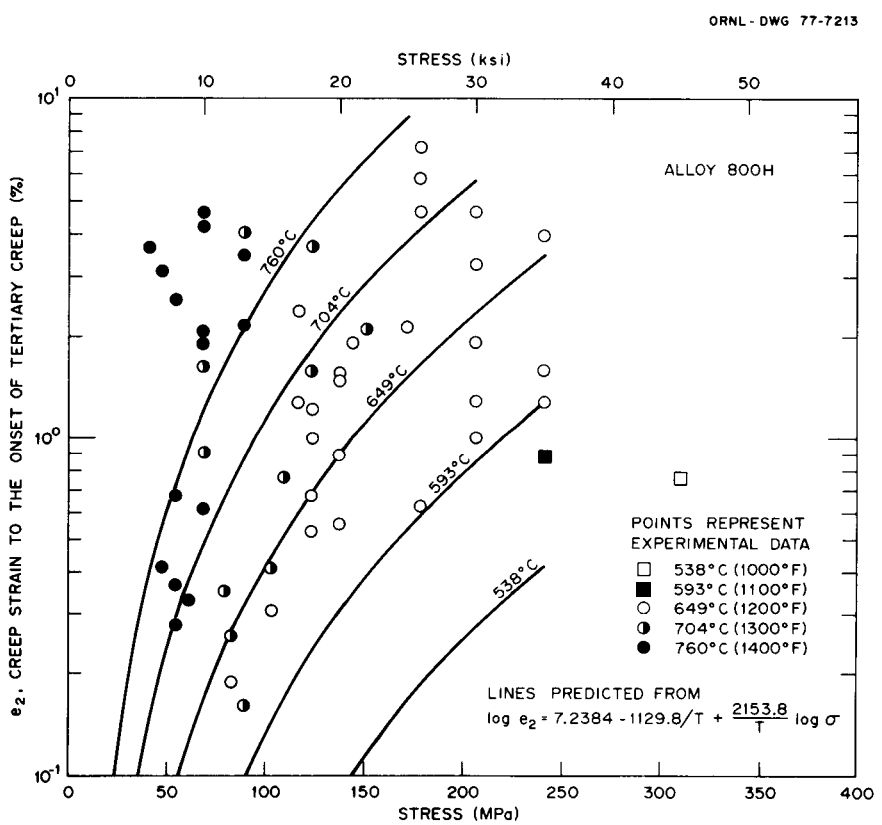

Fig. 41. Comparison Between Experimental Data and Predicted Values of Creep Strain to Tertiary Creep for Alloy 800H.

Table 11. Estimated Tertiary Creep Strength for Alloy 800H (No Offset)

Temperature		10^3-hr Tertiary Creep Strength, MPa (ksi)		10^5-hr Tertiary Creep Strength, MPa (ksi)	
(°C)	(°F)	Average	Lower Limit	Average	Lower Limit
427	800	834 (121)	683 (99.1)	489 (71.0)	401 (58.2)
482	900	543 (78.8)	438 (63.6)	306 (44.3)	246 (35.8)
538	1000	351 (50.9)	279 (40.4)	189 (27.4)	150 (21.8)
593	1100	229 (33.2)	179 (25.9)	118 (17.1)	92 (13.4)
649	1200	139 (20.2)	107 (15.6)	69 (10.0)	53 (7.7)
704	1300	86 (12.4)	65 (9.4)	41 (5.9)	31 (4.5)
760	1400	52 (7.6)	39 (5.6)	24 (3.4)	18 (2.6)

A final possible method to estimate the strain to tertiary creep is to use $e_s = \dot{e}_m t_r$, the "plasticity resource."[39,40,43–45] This quantity was originally proposed[44,45] as an estimate of the strain to tertiary creep. Its use as such is discussed further in refs. 39, 40, and 43. Equations (11) and (31) can be combined to yield predictions for the plasticity resource by

$$\log e_s = 10.39 - 12060/T + (1180/T) \log \sigma \ . \tag{45}$$

Table 12 compares predicted values of e_2 and e_s.

Table 12. Predicted Values of the Strain to Tertiary Creep (e_2) and the Plasticity Resource (e_s) for Alloy 800H

Temperature		Value, %, Based on t_2 =			
		10^3 hr		10^5 hr	
(°C)	(°F)	e_s	e_2	e_s	e_2
427	800	0.012	1.22	0.0049	0.24
482	900	0.049	1.19	0.020	0.23
538	1000	0.16	1.16	0.067	0.22
593	1100	0.47	1.15	0.19	0.22
649	1200	1.12	0.98	0.46	0.19
704	1300	2.40	0.87	0.98	0.17
760	1400	4.70	0.76	1.95	0.15

It is clear that for the current data e_s is not a good approximation for e_2. At low temperatures e_s tends to significantly underestimate e_2, while at high temperatures e_s is considerably greater than e_2. We have shown[39] that e_s and e_2 are related by

$$e_s = \frac{t_r}{t_2} (e_2 - e_p) \ , \tag{46}$$

where e_p is the total amount of primary creep strain. Thus, the relationship between e_s and e_2 is determined by the ratio t_r/t_2 and by the shape of the creep curve. From Eq. (40), t_r/t_2 tends to decrease as temperature decreases down to 593°C. Moreover, e_p becomes an increasingly larger function of e_2 as temperature decreases. (The creep strain-time behavior of alloy 800H is analyzed in the next section.)

The best estimate of the strain to tertiary creep for alloy 800H is thus given by Eq. (44). The predicted trends (see Fig. 41 and Table 12) are somewhat similar to those given above for e_t. At a given stress, e_2 increases with temperature; at a given temperature, e_2 increases with stress. At long times, e_2 can be quite small ($e_2 \approx 0.2\%$ in 10^5 hr at all temperatures).

CREEP STRAIN-TIME BEHAVIOR

For inelastic design analysis, one needs to be able to estimate the amount of creep strain that will be incurred by a material as a function of time, stress, and temperature. The current limited set of available creep curves for alloy 800H make a precise analysis of such a complicated phenomenon quite difficult. However, reasonable estimates of creep strain-time behavior can be obtained by making certain assumptions and approximations. A previous analysis[46] of creep strain-time behavior falls into this category. The present analyses will be used here to develop an alternative simplified equation, and the two equations will be compared with available experimental data.

Sterling[46] analyzed the creep strain-time behavior of alloy 800H as follows. First, he assumed that t_x, the time to the accumulation of X% creep strain, could be described by a linear (log σ vs log t_x) Larson-Miller[32] parameter. Then, he assumed that the relationship between creep strain and time can be described by a simple power law equation

$$e_c = \alpha\sigma^n t^m \ . \tag{47}$$

Combining these equations yields

$$\log t = \frac{a_1}{T} \log \sigma + \left(\frac{a_2}{T} + a_3\right) \log e_c + \left(\frac{a_4}{T} + a_5\right) \ , \tag{48}$$

where $a_1 - a_s$ are constants to be estimated by least squares. This equation can be rewritten in the simple power law form $e_c = \beta t^K$, where now

$$\beta = 10 - \frac{(a_1/T) \log \sigma + a_4/T + a_5}{a_2/T + a_3} \ , \tag{49a}$$

and

$$K = 1/(a_2/T + a_3) \ . \tag{49b}$$

While the Sterling approach is very simple, it does contain several disadvantages, which are discussed elsewhere.[24] The analysis was done by fitting Eq. (48) to data for the time to 0.02, 0.05, 0.1, 0.15, 0.2, 0.25, 0.3, 0.4, 0.5, 0.7, 1.0, and 2% creep strain. Whole creep curves were never fit. As a result, there is some question where the predictions of Eq. (48) will yield creep curves whose shapes reflect the true shapes of the experimental creep curves. Our analyses have shown, in fact. that the experimental curve shapes are inconsistent with the power law form. Moreover, that form is intended for the description of primary creep only, whereas Sterling used it for primary and secondary creep. Garofalo[47] suggests addition of a linear secondary term to make the equation applicable in that region.

The simplified nature of the Sterling approach can be partially justified by the limited nature of the available creep data. However, our analyses showed that the individual experimental creep curves could be described much better by a rational polynomial creep equation. The many advantages of this equation form are discussed elsewhere.[25] Also, as in refs. 20 and 23, the nature of this equation is such that its stress and temperature dependence can often be determined by very simplified methods.

As used here, the rational polynomial is given by

$$e_c = \frac{Cpt}{1 + pt} + \dot{e}_m t \ , \tag{50}$$

where e_c is the creep strain, t is the time, $\dot{e}_m$ is the minimum creep rate (%/hr), and C is the limiting value of the transient primary term (corresponding to e_p above). The parameter p is related to the sharpness of the curvature of the primary creep region. From Eq. (50), the instantaneous creep rate $\dot{e}_c$ is given by

$$\dot{e}_c = \frac{Cp}{(1 + pt)^2} + \dot{e}_m \ , \tag{51}$$

and the initial creep rate $\dot{e}_0$ is given by

$$\dot{e}_0 = Cp + \dot{e}_m \ . \tag{52}$$

Figure 42 summarizes the properties of the equation, while refs. 17, 20, and 22 through 25 describe previous recent use of the equation for the analysis of creep data.

From Fig. 42, it can easily be verified that the value of C (%) is given by

$$C = e_2 - \dot{e}_m t_2 \ , \tag{53}$$

ORNL-DWG 76-3986

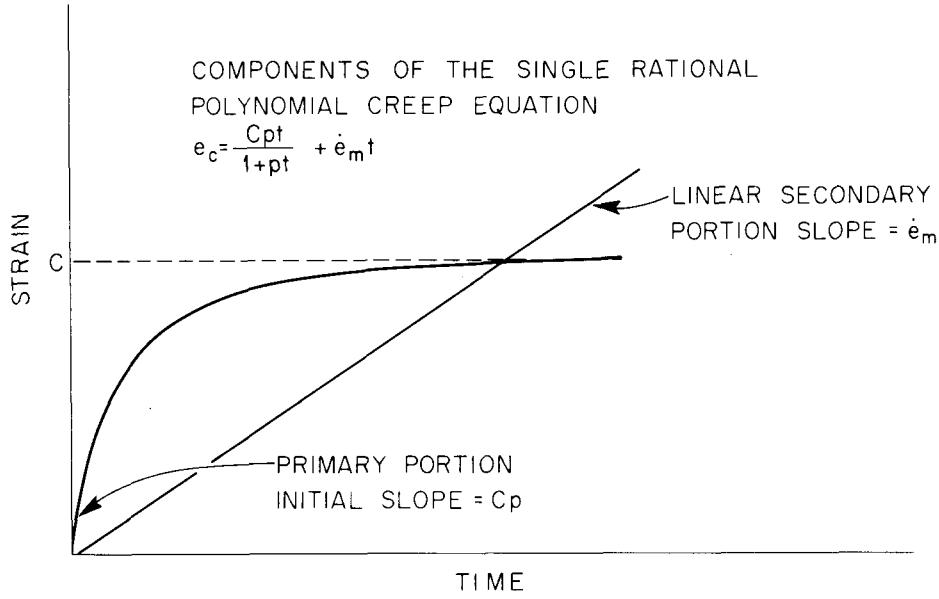

ORNL-DWG 76-3985R

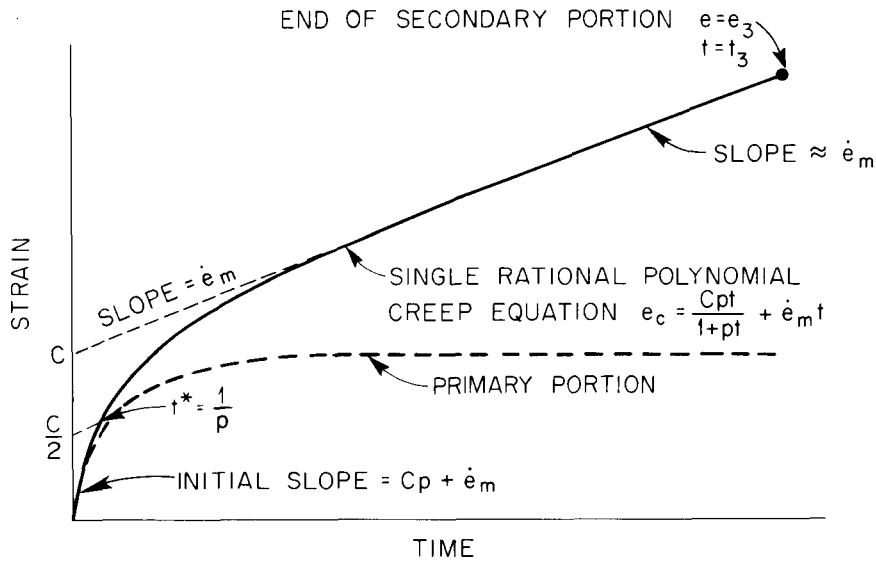

Fig. 42. Schematic Illustrations of the Properties of the Rational Polynomial Creep Equation.

where e_2 and t_2 are, as above, the strain (%) and the time (hr) to the onset of tertiary creep. Methods for the estimation of e_2, t_2, and e_m are given in previous sections of this report. These estimates can thus be used to derive a prediction for C.

Note that at any time t, we have

$$\frac{Cpt}{1 + pt} = FC \ , \tag{54}$$

where F is the fraction of the total C of the primary strain that has been exhausted ($F = 0$ at $t = 0$, $F = 1$ at $t = \infty$). Equation (54) can be arranged to yield

$$p = F/(1 - F)t \ . \tag{55}$$

Reasonably good results were obtained for several materials[39] by assuming that 98% of the transient strain was exhuasted by the onset of tertiary creep ($F = 0.98$ at $t = t_2$). Thus, $p = 49/t_2$. The shapes of the creep curves for alloy 800H vary considerably (perhaps as a reflection of the complex precipitation processes that occur in this material). Therefore, we could not estimate p from t_2 alone.

As an alternative procedure, we analyzed data for the time to the onset of secondary creep, t_1, obtaining an equation of the form

$$\log t_1 = -35.51 + 45300/T + 8.71 \log \sigma - (12980/T) \log \sigma \ . \tag{56}$$

Figure 43 illustrates the fit of Eq. (56) to the available data. Next, we assumed that at $t = t_1$, $F = 0.95$, leading to

$$p = 19/t_1 \ . \tag{57}$$

Comparison of this equation with experimental curves led to generally good results. Having estimates for C, p, and $\dot{e}_m$, we can predict the creep strain-time behavior of alloy 800H as a function of stress and temperature.

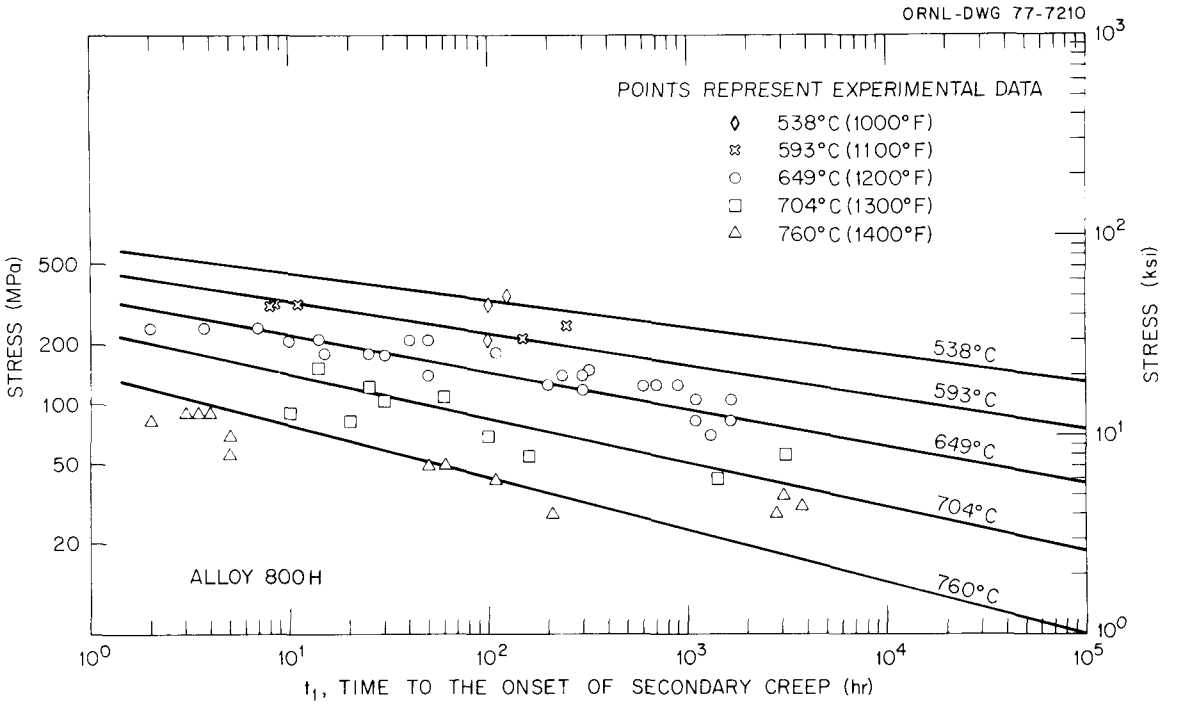

Fig. 43. Comparison Between Experimental Data and Predicted Values of Time to Secondary Creep for Alloy 800H. Lines predicted from $\log t_1 = -35.51 + 45300/T + 8.71 \log \sigma - (12980/T) \log \sigma$, where σ = stress (MPa), and T = temperature (K).

Typical comparisons of the predictions from this approach and from the Sterling equation with experimental curves are shown in Appendix B. The prediction involves a great deal of uncertainty, and some method of predicting strength variations would obviously be desirable. For instance, Heat HH8808A creeps far less at 649°C than would be predicted. Still, the current results are generally acceptable, although the magnitude of predicted strain appears only slightly more accurate than that from the Sterling equation. In fact, the predictions from the Sterling equation are quite similar to those of the current equation in most cases. The main difference between the two is that the current equation appears to depict more accurately the shapes of the individual creep curves. This advantage may be a small one, but with the large uncertainties involved in the extrapolation of results, any advantage is welcome.

A convenient format for presenting the general predictions of a creep equation is through the use of isochronous stress-strain curves. Figures 44 through 49 compare isochronous stress-strain curves predicted from the current equation and from the Sterling equation with those appearing in Code Case 1592 (ref. 1) for this material. These curves, of course, reflect total accumulated strain (time-dependent creep strain and instantaneous strain incurred upon loading). In Figs. 44—49, the loading strains for all three sets of curves were calculated from the monotonic tensile stress-strain curves given in Code Case 1592 so that the variations among the curves are due solely to differences in the predictions of creep behavior from the three sources — the creep predictions in Code Case 1592 having been made by the parametric technique described in ref. 48. Considering the uncertainties involved, the predictions from the three sources appear to be quite similar. The only marked differences occur at 538 and 593°C, where the current equation predicts more creep in the initial part of the creep curve but less creep after long times (10^5 hr). This difference is due to the fact that the current equation predicts a comparatively large initial transient term, but very little beyond that. The very limited data at these temperatures appear consistent with this sort of behavior.

The results presented earlier in this report include the development of an analytical representation for monotonic tensile stress-strain behavior. Figures 50 through 55 compare the Code Case 1592 isochronous stress-strain curves with curves predicted from the current creep and tensile stress-strain equations (using average values for yield strength). In this case, the current curves can lie somewhat below those given in the Code Case because the estimated yield strengths from the current analysis are lower than those used in the Code Case. (Note that construction of monotonic stress-strain curves to 2.0% represents an extrapolation of the current results. These extrapolations appear reasonable. Moreover, in most cases the extrapolated portions do not affect the 10^3- and 10^5-hr curves.)

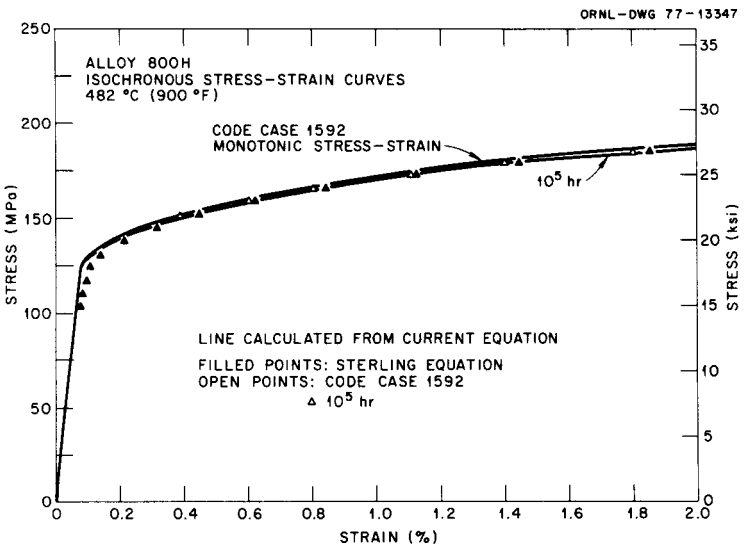

Fig. 44. Isochronous Stress-Strain Curves for Alloy 800H at 482°C (900°F) Calculated by the Current Equation and by the Sterling Equation, and Taken from ASME Code Case 1592. Loading strains were calculated from the monotonic tensile stress-strain curve given in Code Case 1592.

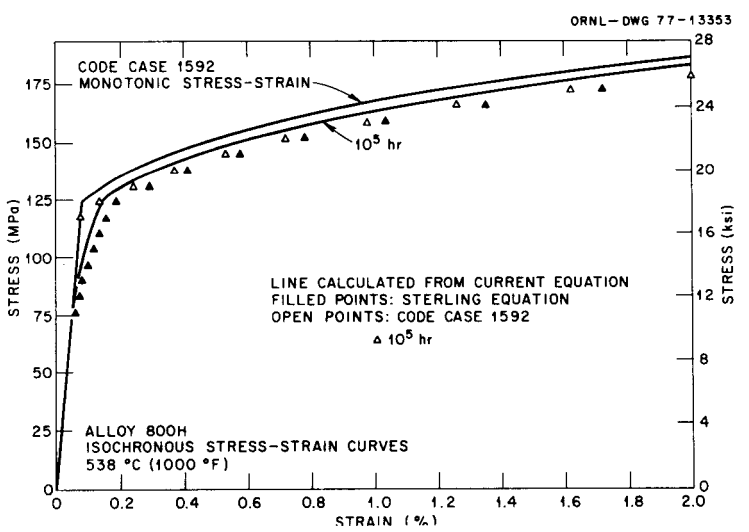

Fig. 45. Isochronous Stress-Strain Curves for Alloy 800H at 538°C (1000°F) Calculated by the Current Equation and by the Sterling Equation, and Taken from ASME Code Case 1592. Loading strains were calculated from the monotonic tensile stress-strain curve given in Code Case 1592.

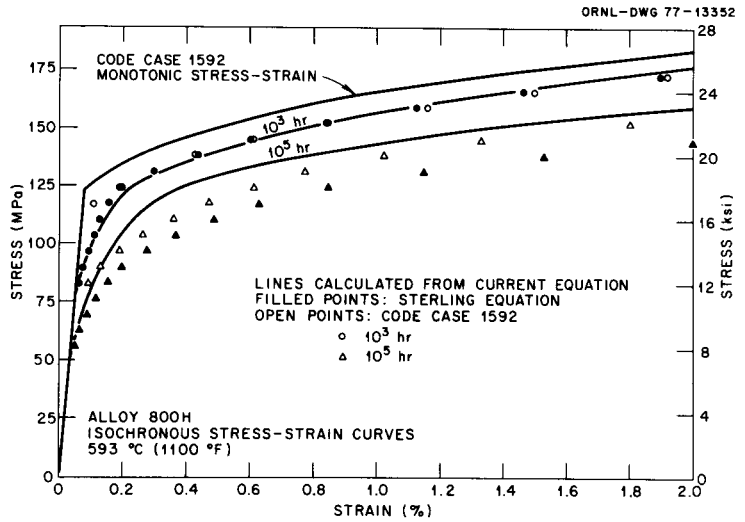

Fig. 46. Isochronous Stress-Strain Curves for Alloy 800H at 593°C (1100°F) Calculated by the Current Equation and by the Sterling Equation, and Taken from ASME Code Case 1592. Loading strains were calculated from the monotonic tensile stress-strain curve given in Code Case 1592.

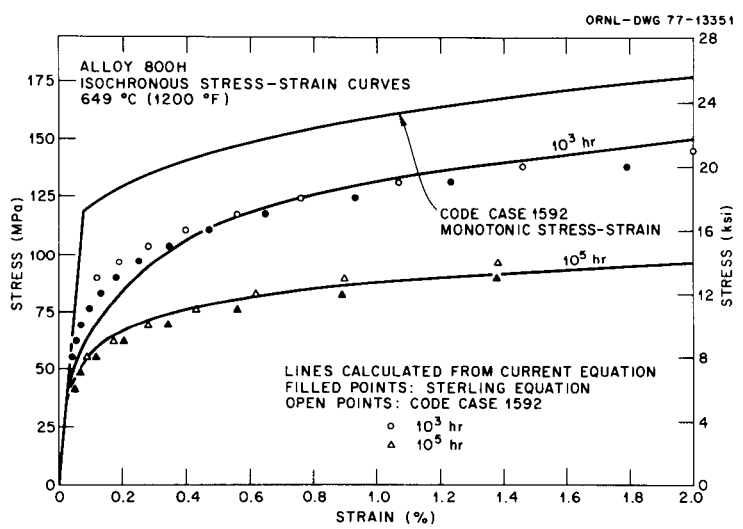

Fig. 47. Isochronous Stress-Strain Curves for Alloy 800H at 649°C (1200°F) Calculated by the Current Equation and by the Sterling Equation, and Taken from ASME Code Case 1592. Loading strains were calculated from the monotonic tensile stress-strain curve given in Code Case 1592.

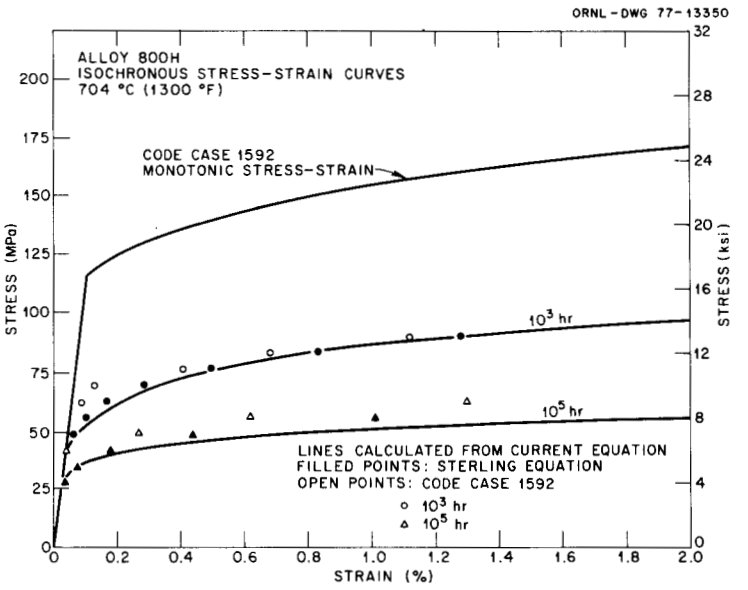

Fig. 48. Isochronous Stress-Strain Curves for Alloy 800H at 704°C (1300°F) Calculated by the Current Equation and by the Sterling Equation, and Taken from ASME Code Case 1592. Loading strains were calculated from the monotonic tensile stress-strain curve given in Code Case 1592.

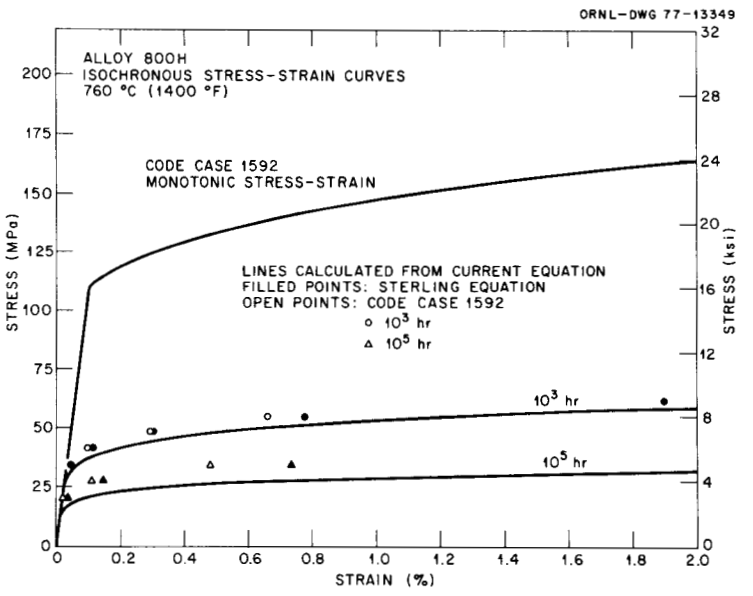

Fig. 49. Isochronous Stress-Strain Curves for Alloy 800H at 760°C (1400°F) Calculated by the Current Equation and by the Sterling Equation, and Taken from ASME Code Case 1592. Loading strains were calculated from the monotonic tensile stress-strain curve given in Code Case 1592.

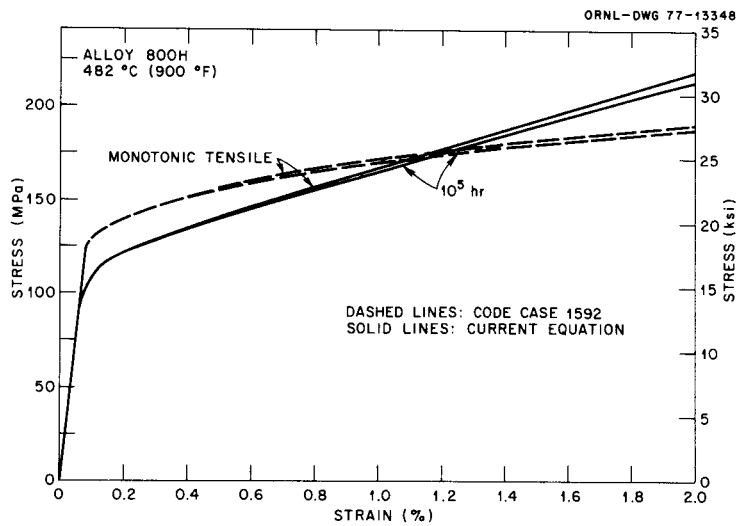

Fig. 50. Isochronous Stress-Strain Curves for Alloy 800H at 482°C (900°F) from the Current Creep and Tensile Equations and from ASME Code Case 1592.

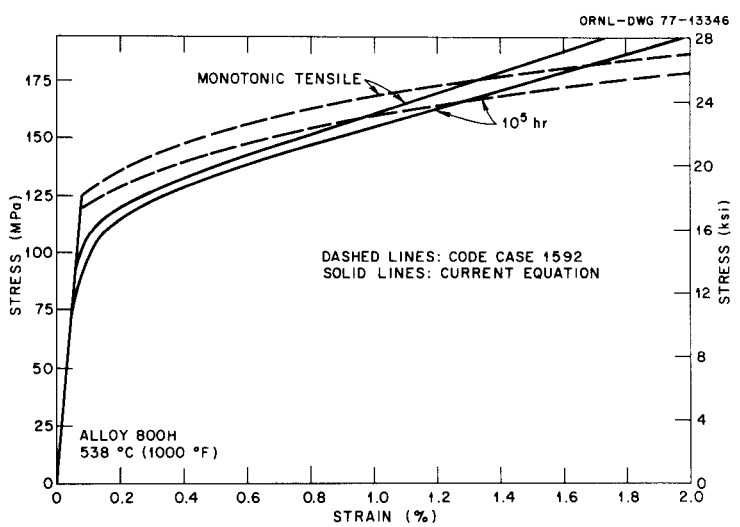

Fig. 51. Isochronous Stress-Strain Curves for Alloy 800H at 538°C (1000°F) from the Current Creep and Tensile Equations and from ASME Code Case 1592.

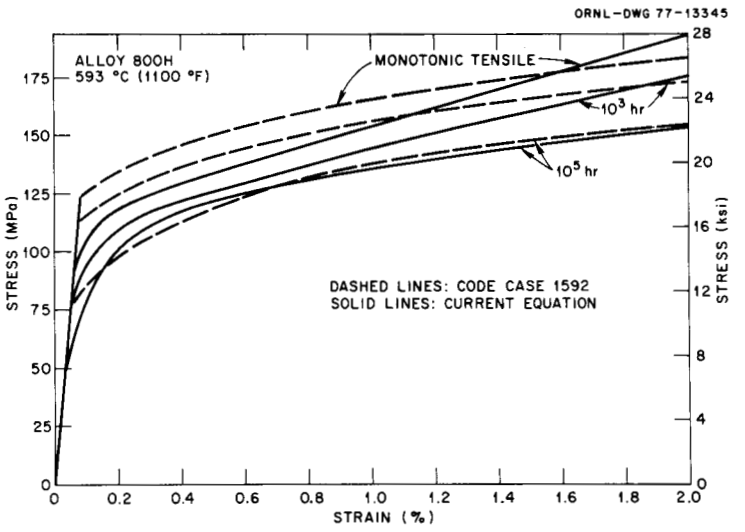

Fig. 52. Isochronous Stress-Strain Curves for Alloy 800H at 593°C (1100°F) from the Current Creep and Tensile Equations and from ASME Code Case 1592.

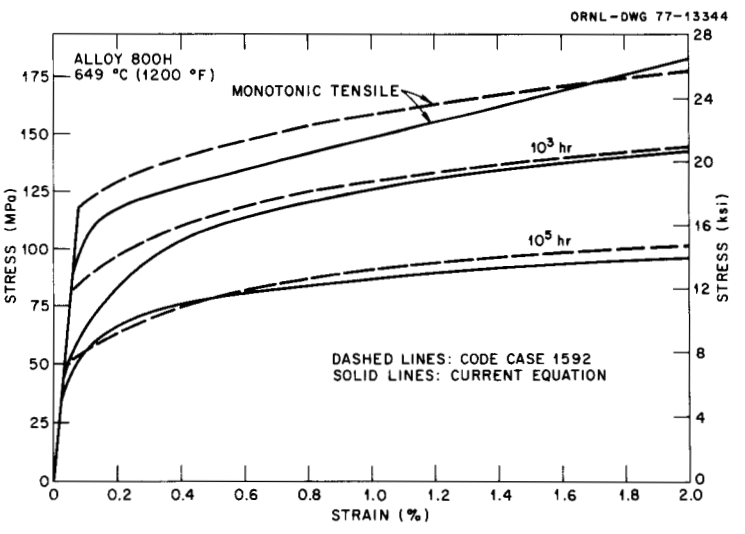

Fig. 53. Isochronous Stress-Strain Curves for Alloy 800H at 649°C (1200°F) from the Current Creep and Tensile Equations and from ASME Code Case 1592.

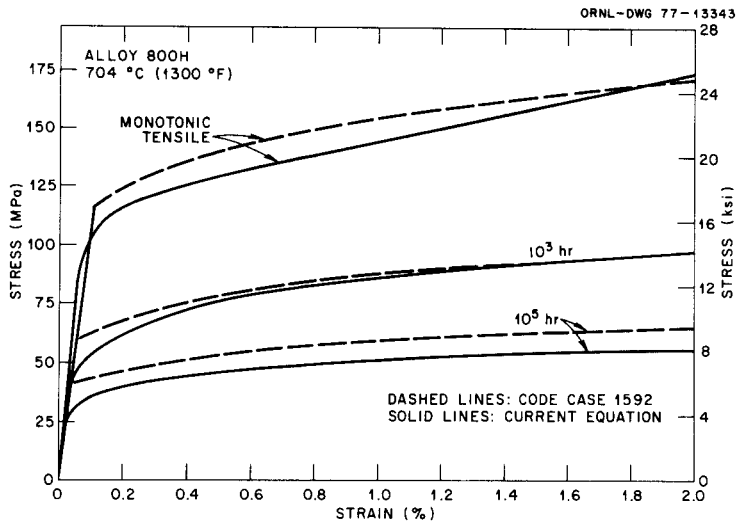

Fig. 54. Isochronous Stress-Strain Curves for Alloy 800H at 704°C (1300°F) from the Current Creep and Tensile Equations and from ASME Code Case 1592.

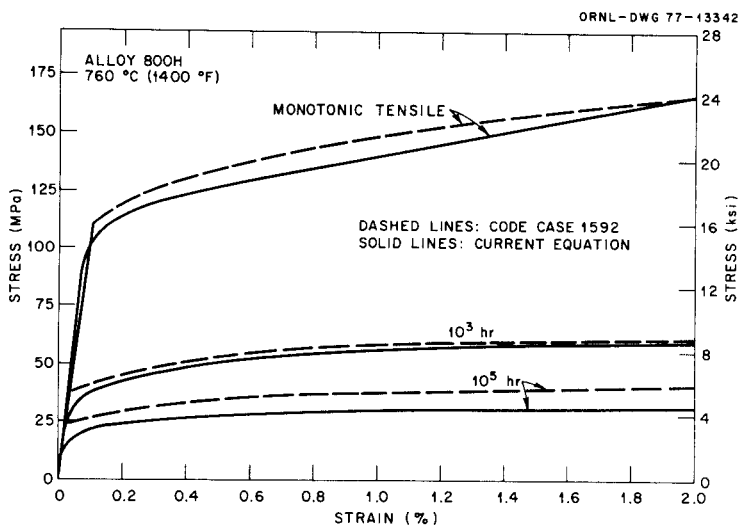

Fig. 55. Isochronous Stress-Strain Curves for Alloy 800H at 760°C (1400°F) from the Current Creep and Tensile Equations and from ASME Code Case 1592.

Limitations

The above creep predictions are analytically valid under the following ranges of conditions:

Stress: 0 MPa < σ < ultimate tensile strength,

Temperature: 427°C (800°F) $\leqslant T \leqslant$ 760°C (1400°F),

Time: 0 hr $\leqslant t \leqslant$ time to tertiary creep.

It must be realized, however, that the actual validity of any equation beyond the range of existing data cannot be verified in the absence of a detailed physical theory for the subject process. No such theory exists for the creep of this material. In addition, actual behavior can show wide variations, whereas the current equations yield predictions for typical behavior. It is hoped that further studies can yield a quantitative understanding of these variations. Still, based on the currently available data, it is felt that the equations developed here yield a reasonable representation of the behavior of this material.

Calculation of Allowable Stress Values

The allowable stress levels for a given material at elevated temperature are given in ASME Code Case 1592 (ref. 1). The allowable stress for service in a time t is denoted by S_{mt}. S_{mt} is the lower of two components — a time-independent allowable stress (S_m) and a time-dependent allowable stress (S_t).

The time-independent allowable stress intensity, S_m, is given by the lowest of the following four values:

1. 1/3 of the specified minimum tensile strength at room temperature,
2. 1.1/3 times the minimum tensile strength at the operating temperature,
3. 2/3 of the specified minimum yield strength at room temperature, and
4. 90% of the minimum yield strength at the operating temperature.

The time-dependent allowable stress intensity, S_t, is given by the lowest of:

1. 2/3 of the minimum stress (S_r) to cause rupture in time t,
2. 80% of the minimum stress (S_3) to cause onset of tertiary creep in time t,
3. the minimum stress ($S_{1\%}$) to cause 1% accumulated strain in time t.

Due to difficulties in defining minimum strain-time behavior, $S_{1\%}$ is often defined merely as 80% of the average stress to cause 1% accumulated strain in time t. That definition will be used here. Tables 13 and 14 summarize the calculation of S_m and S_t values from the current results, while Table 15 compares those values with the ones given in Code Case 1592.

For the values from the current analysis, S_m is in all cases controlled by the minimum yield strength at temperature. These values can lie significantly below those given in Code Case 1592. The S_t values are a little more complicated, being controlled at the lowest temperatures by $S_{1\%}$, at intermediate temperatures by S_r, and at the highest temperatures by S_3. However, $S_{1\%}$ controls only in regions where most of the strain is instantaneous, and where S_m determines S_{mt}. The current values generally fall slightly below those given in the code case. The largest differences are those between the minimum yield strengths from the current analysis and from the code case.

Table 13. Calculation of Time-Independent Allowable Stresses for Alloy 800H from the Current Analysis

Temperature		Stresses, MPa (ksi)				
(°C)	(°F)	$(1/3)\sigma_u$ (Room Temperature)	$(1.1/3)\sigma$ (At Temperature)[a]	$(2/3)\sigma_y$ (Room Temperature)	$0.9\sigma_y$ (At Temperature)[a]	S_m
427	800	161 (23.3)	163 (23.7)	115 (16.7)	72 (10.4)	72 (10.4)
482	900	161 (23.3)	161 (23.4)	115 (16.7)	69 (10.0)	69 (10.0)
538	1000	161 (23.3)	156 (22.6)	115 (16.7)	66 (9.6)	66 (9.6)
593	1100	161 (23.3)	146 (21.2)	115 (16.7)	65 (9.4)	65 (9.4)
649	1200	161 (23.3)	131 (19.0)	115 (16.7)	63 (9.2)	63 (9.2)
704	1300	161 (23.3)	109 (15.8)	115 (16.7)	62 (9.0)	62 (9.0)
760	1400	161 (23.3)	78 (11.3)	115 (16.7)	61 (8.9)	61 (8.9)

[a]Minimum values calculated by mean value − 2 standard errors.

Table 14. Calculation of Time-Dependent Allowable Stresses for Alloy 800H from the Current Analysis

Temperature (°C)	Temperature (°F)	Stresses, MPa (ksi) $(2/3)S_r$	$0.8S_3$ (0.2% Offset)	$S_{1\%}$	S_t
			10^3 hr		
427	800	580 (84.1)	558 (80.9)	141 (20.5)	141 (20.5)
482	900	379 (55.0)	358 (51.9)	133 (19.3)	133 (19.3)
538	1000	245 (35.5)	228 (33.1)	125 (18.2)	125 (18.2)
593	1100	161 (23.4)	146 (21.2)	115 (16.7)	115 (16.7)
649	1200	98 (14.2)	88 (12.8)	101 (14.6)	88 (12.8)
704	1300	60 (8.7)	53 (7.7)	69 (10.0)	53 (7.7)
760	1400	37 (5.3)	32 (4.6)	45 (6.6)	32 (4.6)
			10^5 hr		
427	800	319 (46.1)	337 (48.9)	141 (20.5)	141 (20.5)
482	900	199 (28.8)	208 (30.2)	132 (19.2)	132 (19.2)
538	1000	123 (17.8)	127 (18.5)	124 (18.0)	123 (17.8)
593	1100	77 (11.1)	78 (11.4)	108 (15.7)	77 (11.1)
649	1200	47 (6.9)	46 (6.6)	70 (10.1)	46 (6.6)
704	1300	29 (4.3)	26 (3.8)	41 (5.9)	26 (3.8)
760	1400	18 (2.7)	15 (2.2)	24 (3.5)	15 (2.2)

Table 15. Comparison of Allowable Stress Values from the Current Analysis with Those Given in ASME Code Case 1592

Temperature (°C)	Temperature (°F)	Stresses, MPa: Current Analysis S_m	S_t 10^3 hr	S_t 10^5 hr	S_{mt} 10^3 hr	S_{mt} 10^5 hr	Code Case 1592 S_{mt} 10^3 hr	Code Case 1592 S_{mt} 10^5 hr
427	800	72	141	141	72	72		
482	900	69	133	132	69	69	102	102
538	1000	66	125	123	66	66	99	99
593	1100	65	115	77	65	65	97	81
649	1200	63	88	46	63	46	86	50
704	1300	62	53	26	53	26	54	32
760	1400	61	32	15	32	15	36	21

Figure 56 compares these values with actual experimental data. The figure indicates that Code Case 1592 results may indeed be nonconservative in terms of yield strength in the temperature range from about 427 to 593°C.

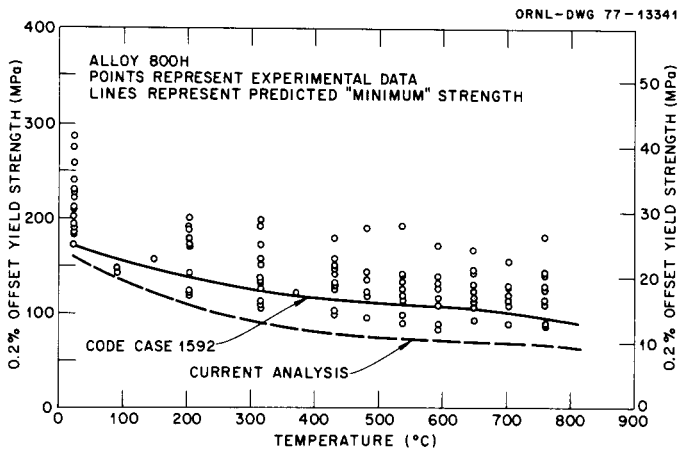

Fig. 56. Comparison of Experimental Data for 0.2% Offset Yield Strength for Alloy 800H with Predicted Minimum Values from the Current Analysis and from Code Case 1592.

SUMMARY

Available tensile and creep data for alloy 800H have been collected and analyzed to yield analytical representations for the behavior of this important material. It is recognized that precipitation processes and other metallurgical phenomena play an important role in determining the behavior of this material. However, the current data base and the current understanding of the metallurgy of alloy 800H dictate that the analyses be empirical in nature. Specific results of the current study are listed below.

1. The 0.2% offset yield strength, ultimate tensile strength, total elongation, and reduction of area from monotonic tensile tests were expressed as simple polynomial functions of temperature.

2. The engineering stress-strain behavior to 0.4% plastic strain was expressed using the rational polynomial tensile equation,

$$\sigma - \sigma_0 = \frac{abe_p}{1 + e_p} + \dot{h}_m \dot{e}_p \ , \tag{58}$$

where σ is the stress and e_p is the plastic strain. The remaining parameters are given by:

$$\sigma_0 = 0.7\sigma_y \text{ (0.2\% offset yield strength)} \ , \tag{59}$$

$$b = 40 \ , \tag{60}$$

$$\dot{h}_m = 186e^{-0.00261T_c} \ , \tag{61}$$

where T_c = temperature (°C), and

$$a = 9/8(\sigma_y - \sigma_0 - 0.2\ h_m) \ . \tag{62}$$

Thus, the stress-strain behavior is given as a function of temperature and yield strength. Average, minimum and maximum values of σ_y can be used to yield predicted stress-strain curves for average, minimum, and maximum strength material.

3. Several creep properties were expressed as simple functions of stress and temperature. These properties include time (t_r) and strain (e_t) to rupture, time (t_3) and creep strain (e_3) to tertiary creep (both 0.2% offset and first deviation from linearity), minimum creep rate ($\dot{e}_m$), plasticity resource ($e_s = \dot{e}_m t_r$), and time to the onset of secondary creep (t_1). Although the available data are sparse (particularly at lower temperatures), the equations developed appear to describe the data well.

4. Rupture data for Sanicro 31 material indicate consistently lower strength and higher ductility than those for the alloy 800H material, even when the Sanicro 31 material meets specifications for alloy 800H. These differences need to be examined further.

5. The creep strain-time behavior of alloy 800H was expressed using the rational polynomial creep equation,

$$e_c = \frac{Cpt}{1 + pt} + \dot{e}_m t \ , \tag{63}$$

where e_c is the creep strain and t is the time. The parameter $\dot{e}_m$ is the minimum creep rate mentioned above. The remaining parameters are given by

$$C = e_3 - \dot{e}_m t_3 \ , \tag{64}$$

and

$$p = 19/t_1 \ . \tag{65}$$

6. The predictions from the current creep equation are generally somewhat similar to those of the previously developed Sterling equation, although the current predicted curve shapes are more consistent with the shapes of available experimental creep curves.

7. The current results were used to calculate allowable stress values such as those given in ASME Code Case 1592. The current values were generally slightly lower than those of Code Case 1592.

REFERENCES

1. *Interpretations of the ASME Boiler and Pressure Vessel Code, Case 1592,* American Society of Mechanical Engineers, New York, 1974.
2. J. F. King, *Behavior and Properties of Welded Transition Joints Between Austenitic Stainless Steels and Ferritic Steels — A Literature Review,* ORNL/TM-5163 (November 1975).
3. R. L. Klueh and J. F. King, "Creep and Tensile Properties of Transition Weld Joint Materials," *Mechanical Properties Test Data for Structural Materials Quart. Prog. Rep. Oct. 31, 1976,* ORNL-5237, pp. 211—13.
4. S. J. Rosenberg, *Nickel and Its Alloys,* National Bureau of Standards Monograph 106, U.S. Department of Commerce, Washington, D.C., 1968, pp. 72—73.

5. R. T. King et al., "Intermediate Nickel Alloys, Solid Solution Strengthened: Alloy 800H and Alloy 800," p. 108 in *Report of Task Force on Alternate Structural Materials for Liquid Metal Fast Breeder Reactors*, ORNL-5076 (May 1976).
6. T. H. Bassford and D. W. Rahoi, "Effect of Composition and Processing on the Mechanical Properties of Incoloy Alloy 800 and Similar Ni-Fe-Cr Alloys," *Metallurgy of Alloy 800 and Implication for Use in LMFBR Steam Generators*, WTD-AMD-76-048 (minutes of meeting at Westinghouse-Tampa Division, November 1976).
7. L. Egnell and N. G. Persson, "Creep-Rupture Ductility of Alloy 800," paper presented at the 18 ème Colloque de Métallurgie — Le Nickel et Son Rôle Spécifique Dans Certains Types D'Alliage, Saclay, June 23–25, 1975.
8. M. K. Booker and B.L.P. Booker, *Development and Implementation of a Mechanical Properties Data Storage and Retrieval System*, ORNL/TM-5330 (June 1976).
9. J. M. Martin, *Incoloy Alloy 800 Data for Use in Design of Gas-Cooled and Liquid Metal Fast Reactors*, Trip Report, INCO/ORNL/RRD/WR&D/WTD Meeting on Development of an Advanced Material for Sodium-Heated Steam Generators, Jan. 17, 1975.
10. J. B. Conway, *Short-Term Tensile and Low-Cycle Fatigue Studies of Incoloy 800*, GEMP-732 (December 1969).
11. C. E. Jaske, H. Mindlin, and J. S. Perrin, *Low-Cycle Fatigue and Creep Fatigue of Incoloy Alloy 800*, BMI-1921 (February 1972).
12. D. L. Keller, *Progress on LMFBR Cladding, Structural, and Component Materials Studies During July 1971 Through June 1972*, BMI-1928 (July 1972).
13. L. Egnell and N. G. Persson, "Creep-Rupture Data for Sanicro 30/31," data package privately supplied to ORNL by Sandvik AB, Sanviken, Sweden.
14. G. T. Leiberman and R. G. Miller, Jr., "Simultaneous Tolerance Intervals in Regression," *Biometrika* 50: 155–68 (1963).
15. G. V. Smith, "Evaluation of Elevated-Temperature Strength Data," *J. Mater.* 4: 878–908 (1969).

16. V. K. Sikka, T. L. Hebble, M. K. Booker, and C. R. Brinkman, *Influence of Laboratory Annealing on Tensile Properties and Time-Independent Design Stress Intensity Limits for Type 304 Stainless Steel*, ORNL-5175 (December 1976).

17. M. K. Booker, T. L. Hebble, D. O. Hobson, and C. R. Brinkman, *Mechanical Property Correlations for 2 1/4 Cr-1 Mo Steel in Support of Nuclear Reactor Systems Design*, ORNL/TM-5329 (June 1976).

18. K. D. Challenger, General Electric Company, Fast Breeder Reactor Development, private communication (October 1975).

19. R. L. Klueh and T. L. Hebble, "A Mathematical Description for the Stress-Strain Behavior of Annealed 2 1/4 Cr-1 Mo Steel," *J. Press. Vess. Technol.* 98: 118–25 (May 1976).

20. M. K. Booker and V. K. Sikka, *Analysis of the Creep Strain-Time Behavior of Type 304 Stainless Steel*, ORNL-5190 (October 1976).

21. J. P. Hammond and V. K. Sikka, *Heat-to-Heat Variations of Total Strain (to 5%) at Discrete Stress Levels in Types 316 and 304 Stainless Steel from 24 to 316°C*, ORNL/NUREG/TM-57 (November 1976).

22. W. E. Stillman, M. K. Booker, and V. K. Sikka, "Mathematical Description of the Creep Strain-Time Behavior of Type 316 Stainless Steel," pp. 424–28 in *Proc. 2nd Int. Conf. Mechanical Behavior of Materials*, Metals Park, Ohio, 1976.

23. M. K. Booker, *Mathematical Description of the Elevated-Temperature Creep Behavior of Type 304 Stainless Steel*, ORNL/TM-6110 (in press).

24. M. K. Booker, *An Interim Analysis of the Creep Strain-Time Characteristics of Annealed and Isothermally Annealed 2 1/4 Cr-1 Mo Steel* (in preparation).

25. D. O. Hobson and M. K. Booker, *Materials Applications and Mathematical Properties of the Rational Polynomial Creep Equation*, ORNL-5202 (December 1976).

26. R. L. Klueh, *Creep and Rupture Behavior of Annealed 2 1/4 Cr-1 Mo Steel*, ORNL-5219 (December 1976).

27. J. D. Baird and A. Jamieson, "High-Temperature Tensile Properties of Some Synthesized Iron Alloys Containing Molybdenum and Chromium," *J. Iron Steel Inst. (London)* 210: 841–46 (1972).

28. F. N. Rhines and P. J. Wray, "Investigation of the Intermediate Temperature Ductility Minimum in Metals," *ASM Trans. Q.* 54: 117–28, (1961).

29. C. E. Sessions, G. Grotke, A. Vaia, and I.L.W. Wilson, *Review of the Behavior of Alloy 800 for Use in LMFBR Steam Generators,* WNET-115 (July 1975).

30. V. K. Sikka, M. K. Booker, and C. R. Brinkman, *Use of Ultimate Tensile Strength to Correlate and Predict Creep and Creep-Rupture Behavior of Types 304 and 316 Stainless Steel*, ORNL-5285 (October 1977).

31. M. K. Booker, *Regression Analysis of Creep-Rupture Data — A Practical Approach* (in preparation).

32. F. R. Larson and J. Miller, "A Time-Temperature Relationship for Rupture and Creep Stresses," *Trans. ASME* 74: 765–71 (1952).

33. L. Egnell, "Design Data," Paper 21 in *British Nuclear Energy Society Materials Conference — Status Review of Alloy 800,* University of Reading, England, Sept. 25–26, 1974.

34. N. G. Persson and L. Egnell, "Creep Rupture Characteristics of Alloy 800 at Around 600°C," Sandvik AB, Sandviken, Sweden, unpublished document.

35. L. E. Svensson, G. L. Dunlop, and N. G. Persson, "Creep Fracture Modes in a Ti-Stabilized 20 Cr-30 Ni Austenitic Alloy," *Scand. J. Metall.* 5: 166–73 (1976).

36. A. Plumtree and N. G. Persson, "Influence of γ' Precipitation on the Creep Strength and Ductility of an Austenitic Fe-Ni-Cr Alloy," to be published in *Metallurgical Transactions.*

37. R. L. Orr, O. D. Sherby, and J. E. Dorn, "Correlations of Rupture Data for Metals at Elevated Temperatures," *ASM Trans. Q.* 46: 113–28 (1954).

38. M. K. Booker and V. K. Sikka, "Interrelationships Between Creep Life Criteria for Four Nuclear Structural Materials," *Nucl. Technol.* 30: 52–64 (1976).

39. M. K. Booker and V. K. Sikka, *Empirical Relationships Among Creep Properties of Four Elevated-Temperature Structural Materials,* ORNL/TM-5399 (June 1976).

40. M. K. Booker and V. K. Sikka, *Predicting the Strain to Tertiary Creep for Elevated-Temperature Structural Materials*, ORNL/TM-5403 (July 1976).

41. G. V. Smith, *Properties of Metals at Elevated Temperatures*, McGraw-Hill, New York, 1950, p. 151.

42. R. M. Goldhoff, "A Method for Extrapolating Rupture Ductility," pp. 82–94 in *Elevated Temperature Testing Problem Areas*, *Spec. Tech. Publ.* 488, American Society for Testing and Materials, Philadelphia, 1971.

43. M. K. Booker, C. R. Brinkman, and V. K. Sikka, "Correlation and Extrapolation of Creep Ductility Data for Four Elevated-Temperature Structural Materials," pp. 108–45 in *Structural Materials for Service at Elevated Temperatures in Nuclear Power Generation*, MPC-1, ed. by A. O. Schaffer, The American Society of Mechanical Engineers, New York, 1975.

44. V. S. Ivanova, "Creep Ductility Criterion for Metals,"*Zavod. Lab.* 21(2): 212–16 (1955), Brutcher Translation No. 4210.

45. I. A. Oding and V. S. Ivanova, "Analysis and Application of Certain Creep Criteria," *Vestn. Mashinostr.* 35(5): 62–66 (1955), Brutcher Translation No. 4211.

46. S. A. Sterling, *A Temperature-Dependent Power Law for Monotonic Creep*, GA-A13027 (June 1974, revised March 1976).

47. F. Garofalo, *Fundamentals of Creep and Creep Rupture in Metals*, McMillan, New York, 1965, p. 16.

48. D. I. Roberts and S. A. Sterling, "A Parametric Method for the Development of Isochronous Stress-Strain Curves," pp. 1–14 in *The Generation of Isochronous Stress-Strain Curves*, ed. by A. O. Schaffer, The American Society of Mechanical Engineers, New York, 1972.

APPENDIX A

Table A1. Alloy 800H Tensile Data

HEAT NUMBER	TEMP (C)	YIELD STRENGTH (PSI)	ULTIMATE STRESS (PSI)	TOTAL ELONG.	RED. IN AREA (%)
	25.	30600.	82900.	54.000	
	25.	30800.	82500.	53.000	72.90
HH1022A	25.	32500.	81500.	57.000	
HH1026A	25.	35000.	80000.	55.000	
HH3603A	25.	28300.	81700.	51.000	73.60
HH4391A	25.	27600.	76900.	53.000	74.80
HH5171A	25.	27200.	72000.	55.000	68.00
HH5342A	25.	29500.	78300.	54.000	69.30
HH5356A	25.	37600.	77000.	56.000	73.50
HH5432A	25.	41700.	84500.	47.000	68.50
HH5853A	25.	27500.	77700.	58.000	73.70
HH6279A	25.	28000.	85700.	43.000	
HH6738A	25.	28200.	75100.	56.000	73.00
HH7262A	25.	26800.	75600.	57.000	
HH7534A	25.	26700.	75000.	53.000	71.00
HH7686A	25.	35000.	83500.	48.000	75.00
HH7686A	25.	33500.	81500.	50.000	73.50
HH7686A	25.	33000.	80000.	49.000	70.50
HH7686A	25.	28500.	81000.	52.000	76.00
HH8285A	25.	40000.	82000.	48.000	66.00
HH8416A	25.	33000.	82500.	50.000	64.00
HH8646A	25.	33400.	83400.	52.000	74.80
HH8808A	25.	29500.	79000.	51.000	72.00
HH8808A	25.	27900.	81000.	49.000	72.20

Table A1. (Continued)

HEAT NUMBER	TEMP (C)	YIELD STRENGTH (PSI)	ULTIMATE STRESS (PSI)	TOTAL ELONG.	RED. IN AREA (%)
HH8808A	25.	25000.	78500.	52.000	76.50
HH8808A	93.	20900.	72300.	52.500	72.20
HH8808A	93.	21300.	71600.	50.000	67.30
HH8808A	93.	21000.	73000.	52.500	70.00
HH6279A	149.	22700.	77700.	37.000	
	204.	25100.	74500.	48.000	71.10
	204.	24800.	74500.	48.500	71.10
HH1022A	204.	26100.	72500.	46.000	
HH1026A	204.	27900.	69600.	48.500	
HH3603A	204.	20700.	73700.	48.500	71.10
HH7686A	204.	27400.	72300.	43.000	69.00
HH7686A	204.	25200.	72000.	43.000	68.00
HH8416A	204.	29300.	74500.	45.000	64.70
HH8808A	204.	17400.	67400.	49.000	70.30
HH8808A	204.	17500.	68000.	47.000	66.50
HH8808A	204.	17900.	67700.	50.000	71.50
HH1022A	316.	22100.	77300.	49.000	
HH1026A	316.	25000.	69500.	47.000	
HH3603A	316.	20200.	75000.	52.000	65.50
HH6279A	316.	20000.	76700.	38.000	
HH6279A	316.	20300.	70700.	36.000	
HH7262A	316.	19100.	65000.	54.000	67.00
HH7686A	316.	22800.	71500.	44.000	67.00
HH7686A	316.	22800.	72500.	44.000	71.00

Table A1. (Continued)

HEAT NUMBER	TEMP (C)	YIELD STRENGTH (PSI)	ULTIMATE STRESS (PSI)	TOTAL ELONG.	RED. IN AREA (%)
HH8416A	316.	27900.	74000.	50.000	57.00
HH8416A	316.	28500.	74300.	53.000	62.00
HH8808A	316.	15800.	66800.	52.000	62.00
HH8808A	316.	18300.	68500.	49.000	59.50
HH8808A	316.	15300.	66800.	53.000	60.00
HH8808A	316.	16300.	68500.	56.000	67.30
HH3603A	371.	17800.	75000.	55.500	66.00
	427.	23000.	76000.	56.000	62.90
	427.	21500.	75000.	56.000	63.00
HH1022A	427.	22000.	69700.	44.500	
HH1026A	427.	22400.	68800.	52.000	
HH3603A	427.	18100.	75000.	53.500	61.50
HH7686A	427.	21600.	72500.	48.000	55.00
HH7686A	427.	21400.	72500.	44.000	56.00
HH8416A	427.	26100.	75600.	55.000	58.50
HH8808A	427.	14400.	65700.	53.000	62.50
HH8808A	427.	15000.	65500.	48.500	45.00
HH8808A	427.	14300.	66500.	51.500	58.50
HH8808A	427.	18800.	67500.	52.000	64.50
HH1022A	482.	20900.	69500.	51.000	
HH3603A	482.	17800.	73500.	52.500	60.50
HH3603A	482.	17800.	73500.	52.500	60.50
HH6279A	482.	17200.	73700.	48.000	
HH6279A	482.	17900.	76700.	36.000	

Table A1. (Continued)

HEAT NUMBER	TEMP (C)	YIELD STRENGTH (PSI)	ULTIMATE STRESS (PSI)	TOTAL ELONG.	RED. IN AREA (%)
HH6279A	482.	17800.	75300.	40.000	
HH6279A	482.	17100.	75000.	40.000	
HH7686A	482.	20600.	71500.	46.000	59.50
HH7686A	482.	19800.	72000.	44.000	64.50
HH8416A	482.	27800.	75400.	52.000	55.70
HH8808A	482.	13800.	65300.	52.000	58.20
HH1022A	538.	20200.	72000.	53.500	
HH1026A	538.	20400.	65500.	50.000	
HH3603A	538.	16600.	72000.	53.500	61.00
HH3603A	538.	16600.	73000.	53.500	61.00
HH6279A	538.	17200.	74300.	40.000	
HH7262A	538.	16400.	62500.	57.000	61.00
HH7686A	538.	19400.	69000.	44.000	49.00
HH7686A	538.	18400.	68500.	46.000	54.50
HH8416A	538.	28200.	73000.	53.000	56.00
HH8808A	538.	13000.	62700.	54.000	60.00
HH8808A	538.	13000.	63400.	53.000	63.00
HH8808A	538.	14300.	62600.	51.000	58.30
HH1022A	593.	19000.	64100.	50.000	
HH1026A	593.	20200.	63100.	47.000	
HH3603A	593.	15900.	70000.	52.000	63.00
HH3603A	593.	15900.	70000.	52.000	63.00
HH5206A	593.	18300.	65300.	45.000	54.60
HH6279A	593.	18700.	70700.	37.000	

Table A1. (Continued)

HEAT NUMBER	TEMP (C)	YIELD STRENGTH (PSI)	ULTIMATE STRESS (PSI)	TOTAL ELONG.	RED. IN AREA (%)
HH6279A	593.	18200.	69700.	36.000	
HH6279A	593.	16900.	69000.	38.000	
HH7262A	593.	15800.	57200.	55.000	62.50
HH7686A	593.	16800.	62000.	46.000	57.50
HH7686A	593.	16600.	62500.	46.000	64.00
HH8416A	593.	24900.	70000.	51.000	58.50
HH8808A	593.	12000.	59400.	54.000	57.00
HH8808A	593.	12800.	59500.	55.500	62.00
HH8808A	593.	16500.	59800.	51.000	63.00
HH1022A	649.	18800.	58000.	47.500	
HH1026A	649.	20800.	57600.	48.000	
HH3603A	649.	17200.	61500.	45.000	54.50
HH3603A	649.	17200.	61500.	45.000	54.50
HH5206A	649.	17500.	61600.	42.000	52.70
HH6279A	649.	17000.	65500.	40.000	
HH6279A	649.	18700.	64300.	36.000	
HH7262A	649.	17600.	53600.	50.000	62.30
HH7686A	649.	16700.	62700.	39.000	53.00
HH7686A	649.	17600.	59800.	39.000	46.50
HH7686A	649.	15800.	61500.	45.000	61.50
HH7686A	649.	16000.	62000.	47.000	64.50
HH8416A	649.	24100.	65400.	46.000	50.50
HH8808A	649.	13500.	54800.	50.000	65.00
HH8808A	649.	15500.	56500.	45.500	53.50

Table A1. (Continued)

HEAT NUMBER	TEMP (C)	YIELD STRENGTH (PSI)	ULTIMATE STRESS (PSI)	TOTAL ELONG.	RED. IN AREA (%)
HH8808A	649.	13400.	55700.	53.000	63.60
HH8808A	649.	21000.	61400.	34.500	36.00
HH1022A	704.	18800.	50000.	46.000	
HH1026A	704.	18500.	49300.	48.000	
HH3603A	704.	16500.	53900.	41.500	49.50
HH3603A	704.	16500.	53900.	41.500	49.50
HH6279A	704.	17300.	55300.	39.500	
HH7686A	704.	17500.	53500.	33.000	39.00
HH7686A	704.	17000.	52000.	33.000	47.00
HH8416A	704.	22500.	52500.	33.000	36.50
HH8808A	704.	13100.	44100.	43.000	47.50
HH8808A	704.	15800.	47700.	50.000	49.30
	760.	26200.	34200.	41.000	64.20
	760.	20700.	32900.	51.000	70.00
HH1022A	760.	18200.	40000.	52.000	
HH1026A	760.	18600.	36200.	51.500	
HH3603A	760.	15900.	39200.	53.000	57.50
HH3603A	760.	15900.	39200.	53.000	57.50
HH6279A	760.	16500.	42000.	41.000	
HH7686A	760.	18200.	38500.	47.000	57.00
HH7686A	760.	16400.	39000.	48.000	64.00
HH8416A	760.	20500.	41800.	29.000	35.00
HH8808A	760.	13100.	34200.	41.000	56.00
HH8808A	760.	12700.	34000.	55.500	60.50

Table A2. Alloy 800 Grade 2 Tensile Data

HEAT NUMBER	TEMP (C)	YIELD STRENGTH (PSI)	ULTIMATE STRESS (PSI)	TOTAL ELONG.	RED. IN AREA (%)
FY0531/1	25.	32800.	82200.	35.000	
FY0531/6/1	25.	43500.	91900.	37.000	
HH1736A	25.	29100.	78400.	52.000	76.20
HH3113A	25.	27600.	79200.		
HH3113A	25.	27600.	79200.		75.00
HH323A	25.	38000.	79400.	43.000	
HH4060A	25.	25563.	79371.	61.000	56.60
HH4101A	25.	24845.	73499.	67.500	59.00
HH462A	25.	27000.	76500.	64.000	
HH5118A	25.	28600.	78700.	54.000	75.80
HH5754A	25.	37200.	75500.	52.000	68.30
HH5756A	25.	36000.	80000.	54.000	75.00
HH5856A	25.	27300.	77700.	56.000	75.50
HH6071A	25.	28000.	78000.	52.000	69.50
HH6072A	25.	31400.	77400.	57.000	75.60
HH7493A	25.	27000.	77000.	51.000	73.40
HH7493A	25.	27000.	80000.	51.000	69.20
HH8735A	25.	28300.	76300.	52.000	76.50
HH8735A	25.	28800.	76500.	53.500	67.50
HH8735A	25.	27400.	75500.	51.000	64.50
HH8872A	25.	26300.	75000.		
HH9374A	25.	28500.	75300.	52.000	77.60
HH9945A	25.	25200.	74300.	58.000	77.10
LC0111XT	25.	32300.	81500.	36.400	

Table A2. (Continued)

HEAT NUMBER	TEMP (C)	YIELD STRENGTH (PSI)	ULTIMATE STRESS (PSI)	TOTAL ELONG.	RED. IN AREA (%)
570594	25.	49500.		32.000	
A*	26.	26750.	81000.	38.500	74.16
A*	26.	26033.	80165.	40.590	72.73
A*	26.	26446.	94380.	37.260	70.24
A*	26.	26942.	86776.	35.880	69.42
D*	26.	35537.	104132.	34.660	48.76
D*	26.	39836.	113524.	29.670	54.90
D*	26.	25819.	92377.	36.360	62.29
D*	26.	25246.	91147.	37.760	58.19
G*	26.	30492.	95082.	30.590	46.72
G*	26.	29180.	93442.	30.950	42.62
G*	26.	29504.	92810.	30.170	43.80
G*	26.	30578.	95867.	30.670	49.58
H*	26.	31147.	95082.	29.060	47.54
H*	26.	30488.	94471.	30.640	48.78
H*	26.	29339.	85950.	36.770	55.37
H*	26.	27272.	83884.	36.220	59.50
J*	26.	28925.	93388.	31.480	45.45
J*	26.	29173.	94380.	30.930	41.87
J*	26.	27851.	88100.	34.080	51.24
J*	26.	31818.	92561.	31.630	50.41
HH4060A	93.	23299.	73821.	60.200	57.51
HH4101A	93.	23106.	69145.	64.700	55.04
HH8735A	93.	24100.	71000.	53.000	75.60

Table A2. (Continued)

HEAT NUMBER	TEMP (C)	YIELD STRENGTH (PSI)	ULTIMATE STRESS (PSI)	TOTAL ELONG.	RED. IN AREA (%)
FY0531/1	100.	28700.	74300.	37.000	
FY0531/6/1	100.	40500.	85500.	38.000	
LC0111XT	100.	30200.			
FY0531/1	200.	24300.	70200.	35.000	
FY0531/6/1	200.	37300.	81000.	35.000	
LC0111XT	200.	25600.	30800.	71.200	40.00
HH4060A	204.	19534.	69713.	55.800	47.53
HH4101A	204.	19764.	64667.	60.900	45.49
HH8735A	204.	21000.	65400.	49.500	64.50
FY0531/1	300.	24900.	70400.		
FY0531/1	300.	24400.	69300.	34.000	
FY0531/6/1	300.	35100.	80500.	31.000	
LC0111XT	300.	24700.	69900.	37.500	
HH4060A	316.	17524.	69090.	58.500	42.75
HH4101A	316.	17361.	63715.	65.900	50.63
FY0531/1	400.	23900.	69400.		
FY0531/6/1	400.	32900.	79600.	32.000	
LC0111XT	400.	24300.	70200.	41.000	
HH3113A	427.	22600.	71500.		
HH3113A	427.	22900.	72400.		51.00
HH4060A	427.	15744.	69375.	61.400	45.76
HH4101A	427.	15358.	63412.	66.300	47.20
HH462A	427.	18000.	67000.	56.000	66.50
HH8735A	427.	18100.	65800.	53.000	62.50

Table A2. (Continued)

HEAT NUMBER	TEMP (C)	YIELD STRENGTH (PSI)	ULTIMATE STRESS (PSI)	TOTAL ELONG.	RED. IN AREA (%)
HH4060A	482.	17748.	69559.	62.600	41.95
HH4101A	482.	15183.	63525.	70.500	47.05
HH8735A	482.	14900.	66000.	56.000	65.50
FY0531/1	500.	21800.	67900.	39.000	
FY0531/6/1	500.		76000.	33.000	
LC0111XT	500.	21300.	65900.	37.000	
A*	538.	16363.	67685.	31.420	61.98
A*	538.	16363.	64628.	38.350	73.55
A*	538.	16156.	65451.	35.730	74.32
A*	538.	16116.	64545.	31.200	58.68
D*	538.	22131.	78114.	38.570	49.18
D*	538.	19586.	76373.	39.770	48.76
D*	538.	27934.	85124.	33.860	34.66
D*	538.	14590.	71557.	36.020	60.65
G*	538.	19008.	81405.	36.250	30.58
G*	538.	17520.	80661.	37.810	33.88
G*	538.	17459.	79098.	37.280	33.60
G*	538.	16311.	78688.	37.600	31.97
H*	538.	21885.	84426.	26.940	22.95
H*	538.	18016.	75702.	49.660	56.19
H*	538.	20248.	77273.	42.000	52.89
HH3113A	538.	21600.	69700.		
HH3113A	538.	17700.	64800.		
HH3113A	538.	23600.	67200.		

Table A2. (Continued)

HEAT NUMBER	TEMP (C)	YIELD STRENGTH (PSI)	ULTIMATE STRESS (PSI)	TOTAL ELONG.	RED. IN AREA (%)
HH3113A	538.	21000.	67200.		64.00
HH4060A	538.	14127.	65451.	59.000	39.81
HH4101A	538.	13523.	68481.	68.100	40.08
HH462A	538.	16750.	65000.	56.000	64.50
HH6733A	538.	15800.	68300.	54.000	44.00
HH8735A	538.	16500.	63500.	51.000	59.00
HH8968A HOT-FIN. 3/4 IN. DIA. ROUND	538.	14200.	63200.		46.00
HH8968A HOT-FIN. 3/4 IN. DIA. ROUND	538.	17000.	63000.		56.00
HH9374A	538.	23400.	61000.	45.000	55.00
J*	538.	18760.	87603.	38.480	44.62
J*	538.	22705.	87705.	36.020	34.43
J*	538.	21557.	79918.	38.040	31.14
HH4060A	593.	13839.	62545.	62.700	40.04
HH4101A	593.	13222.	57585.	69.400	41.79
HH8735A	593.	14200.	60000.	50.500	53.50
	649.	14900.	41800.		38.00
	649.	17100.	47200.		46.00
	649.	13300.	48700.		58.00
HH3113A	649.	18000.	59900.		
HH3113A	649.	17100.	59700.		
HH3113A	649.	16700.	59800.		69.00

Table A2. (Continued)

HEAT NUMBER	TEMP (C)	YIELD STRENGTH (PSI)	ULTIMATE STRESS (PSI)	TOTAL ELONG.	RED. IN AREA (%)
HH4101A	649.	16084.	50350.	59.000	39.68
HH462A	649.	16050.	56250.	37.000	36.00
HH8735A	649.	14800.	55700.	50.000	60.70
HH8968A HOT-FIN. 3/4 IN. DIA. ROUND	649.	15900.	51900.		59.00
HH8968A HOT-FIN. 3/4 IN. DIA. ROUND	649.	13500.	53900.		58.00
HH9374A	649.	22100.	52500.	45.000	55.00
HH4101A	704.	13482.	41869.	48.400	34.54
HH8735A	704.	14200.	42700.	43.000	42.80
HH8968A HOT-FIN. 3/4 IN. DIA. ROUND	704.	16200.	40700.		52.00
HH8968A HOT-FIN. 3/4 IN. DIA. ROUND	704.	11900.	46000.		52.00
HH3113A	760.		43800.		
HH3113A	760.	18600.	45600.		
HH3113A	760.	13400.	45700.		
HH3113A	760.	16400.	45000.		70.00
HH4101A	760.	13556.	41536.	48.600	28.81
HH462A	760.	14500.	34250.	56.500	45.50
HH8735A	760.	15400.	32300.	78.000	60.00

Table A2. (Continued)

HEAT NUMBER	TEMP (C)	YIELD STRENGTH (PSI)	ULTIMATE STRESS (PSI)	TOTAL ELONG.	RED. IN AREA (%)
HH8968A HOT-FIN.3/4 IN. DIA. ROUND	760.	13000.	31200.		64.00
HH8968A HOT-FIN. 3/4 IN. DIA. ROUND	760.	13200.	39400.		64.00
HH9374A	760.	17800.	35000.	56.000	54.50

Table A3. Data Used in Tensile Stress-Strain Analysis

HEAT NO.	TEMP C	STRESS AT A PLASTIC STRAIN OF 0%	0.02%	0.2%	0.4%
HH8808A	93.	97.	115.	144.	160.
HH8808A	93.	121.	131.	147.	160.
HH8808A	93.	59.	100.	145.	162.
HH6279A	149.	99.	133.	157.	165.
HH8808A	204.	85.	101.	120.	128.
HH8808A	204.	79.	96.	120.	141.
HH8808A	204.	69.	98.	123.	135.
HH1022A	204.	111.	138.	180.	194.
HH8808A	316.	76.	88.	109.	123.
HH8808A	316.	86.	97.	113.	124.
HH8808A	316.	62.	76.	126.	150.
HH8808A	316.	60.	77.	105.	119.
HH6279A	316.	100.	117.	140.	152.
HH1026A	316.	114.	135.	172.	187.
HH1022A	316.	102.	117.	153.	165.
HH8808A	427.	73.	81.	100.	109.
HH8808A	427.	91.	123.	176.	206.
HH8808A	427.	65.	79.	103.	121.
HH8808A	427.	60.	79.	99.	113.
HH1026A	427.	97.	119.	155.	166.
HH1022A	427.	94.	117.	152.	165.
HH6279A	482.	89.	101.	117.	129.
HH3603A	482.	98.	103.	122.	141.
HH6279A	482.	58.	82.	122.	136.
HH6279A	482.	76.	103.	122.	131.
HH6279A	538.	89.	103.	120.	127.
HH3603A	538.	74.	90.	115.	131.
HH1022A	538.	96.	114.	144.	151.
HH8808A	538.	62.	69.	90.	100.
HH8808A	538.	66.	77.	98.	110.
HH1026A	538.	87.	104.	144.	159.
HH8735A	538.	86.	97.	114.	131.
HH8808A	538.	72.	74.	90.	103.
HH6279A	593.	113.	118.	129.	135.
HH3603A	593.	66.	84.	110.	122.
HH1022A	593.	85.	98.	133.	151.
HH8808A	593.	52.	62.	86.	95.
HH8808A	593.	52.	64.	87.	98.
HH6279A	593.	110.	118.	126.	131.
HH6279A	593.	98.	109.	118.	124.
HH1026A	593.	93.	111.	141.	154.
HH8735A	593.	52.	66.	99.	117.
HH3603A	649.	78.	92.	119.	129.
HH6279A	649.	99.	106.	119.	127.
HH1022A	649.	76.	96.	131.	144.

Table A3. (Continued)

HEAT NO.	TEMP C	STRESS AT A PLASTIC STRAIN OF 0%	0.02%	0.2%	0.4%
HH8808A	649.	57.	69.	107.	122.
HH8808A	649.	67.	80.	93.	98.
HH8808A	649.	119.	128.	145.	156.
HH6279A	649.	104.	114.	130.	136.
HH1026A	649.	85.	104.	144.	157.
HH8735A	649.	69.	81.	103.	112.
HH8808A	649.	69.	78.	93.	103.
HH6279A	704.	91.	108.	121.	129.
HH3603A	704.	95.	102.	114.	121.
HH1022A	704.	91.	103.	129.	137.
HH8808A	704.	67.	74.	90.	97.
HH1026A	704.	80.	97.	126.	137.
HH8735A	704.	79.	83.	99.	105.
HH6279A	760.	97.	103.	114.	125.
HH3603A	760.	71.	85.	111.	122.
HH1022A	760.	83.	97.	126.	134.
HH8808A	760.	62.	72.	88.	97.
HH1026A	760.	87.	101.	128.	138.
HH8735A	760.	86.	96.	134.	183.
HH8808A	760.	76.	83.	90.	93.

Table A4. Alloy 800H Creep Data Used[a]

Heat No.	Temp. (°C)	Stress (MPa)	$\dot{e}_m$	t_1	t_2	t_{ss}	t_r	e_t	e_{ss}
HH8735A	538.	310.	0.000029	100.0	1400.0	2700.0	0.0	19.50	1.00
HH8735A	538.	345.	0.000530	125.0	0.0	0.0	632.4	22.00	0.0
HH8735A	538.	207.	0.0	100.0	0.0	0.0	0.0	4.60	0.0
HH8735A	593.	310.	0.070000	8.5	0.0	0.0	53.5	26.50	0.0
HH8735A	593.	207.	0.000043	150.0	1700.0	0.0	0.0	5.45	0.0
HH8735A	593.	241.	0.000033	250.0	1100.0	2000.0	3974.6	11.00	1.10
HH8808A	593.	310.	0.003750	8.0	0.0	0.0	198.7	28.50	0.0
HH8808A	593.	310.	0.0	11.0	0.0	0.0	142.4	21.50	0.0
HH7686A	649.	138.	0.000110	240.0	1300.0	2000.0	3710.0	9.00	1.75
HH8808A	649.	179.	0.000090	300.0	1650.0	2020.0	3273.7	8.50	0.86
HH8808A	649.	165.	0.000009	400.0	1100.0	0.0	0.0	0.0	0.0
HH7686A	649.	124.	0.000083	600.0	1100.0	2650.0	7617.1	11.00	1.00
HH7686A	649.	145.	0.000520	320.0	1100.0	1450.0	2877.9	8.50	2.30
HH7686A	649.	103.	0.000015	1100.0	3200.0	8050.0	25354.0	8.00	0.58
HH7686A	649.	207.	0.023500	14.0	98.0	118.0	221.9	24.00	3.90
HH8735A	649.	241.	0.270000	3.7	9.0	10.0	26.0	30.00	4.40
HH8735A	649.	69.	0.000004	1300.0	0.0	0.0	0.0	0.17	0.0
HH8735A	649.	117.	0.000250	10.0	1700.0	1800.0	7385.5	26.50	1.50
HH8735A	649.	172.	0.003600	30.0	260.0	280.0	695.3	31.50	2.40
HH8735A	649.	138.	0.000500	50.0	500.0	920.0	2879.1	21.50	1.30
HH8735A	649.	207.	0.030000	10.0	100.0	110.0	190.1	24.50	5.20
HH7686A	649.	83.	0.000015	1650.0	0.0	0.0	0.0	0.20	0.0
HH7686A	649.	124.	0.000075	200.0	2400.0	3400.0	8866.7	15.00	0.80
HH7686A	649.	179.	0.008400	15.0	340.0	385.0	522.4	19.00	7.80
HH7686A	649.	241.	0.040000	7.0	21.0	28.5	51.2	25.00	2.10

Table A4. (Continued)

Heat No.	Temp. (°C)	Stress (MPa)	$\dot{e}_m$	t_1	t_2	t_{ss}	t_r	e_t	e_{ss}
HH8808A	649.	207.	0.000625	50.0	840.0	1000.0	1099.0	6.00	1.30
HH8808A	649.	207.	0.001400	40.0	300.0	445.0	522.0	7.00	1.70
HH8416A	649.	103.	0.000008	1650.0	3700.0	0.0	0.0	0.05	0.0
HH8416A	649.	241.	0.026700	2.0	19.0	23.0	57.7	26.00	1.60
HH8416A	649.	179.	0.010600	25.0	255.0	280.0	421.7	15.00	5.10
HH8416A	649.	117.	0.000078	300.0	3100.0	4700.0	7999.3	5.00	2.70
HH8416A	649.	138.	0.000175	240.0	1210.0	1760.0	3190.5	4.50	0.85
HH3603A	649.	179.	0.008000	110.0	330.0	350.0	632.3	21.00	6.20
HH3603A	649.	83.	0.000018	1100.0	4500.0	5100.0	0.0	0.50	0.40
HH3603A	649.	241.	0.040000	2.0	26.0	38.0	96.1	30.00	2.60
HH3603A	649.	124.	0.000140	700.0	1460.0	1600.0	0.0	1.80	1.44
HH3603A	649.	138.	0.000670	300.0	1150.0	1350.0	3723.3	36.50	1.90
HH3603A	649.	124.	0.000100	900.0	1600.0	2200.0	6768.0	21.50	1.25
HH8808A	704.	83.	0.000250	20.0	200.0	380.0	0.0	0.0	0.50
HH8808A	704.	110.	0.000670	60.0	260.0	305.0	1252.7	26.50	1.00
HH8808A	704.	152.	0.010000	14.0	64.0	84.0	211.1	27.50	2.50
HH8735A	704.	90.	0.005000	0.0	800.0	850.0	2349.3	54.00	4.50
HH8735A	704.	55.	0.000103	160.0	0.0	0.0	0.0	0.72	0.0
HH7686A	704.	90.	0.000200	10.0	425.0	625.0	4529.9	20.50	0.40
HH7686A	704.	55.	0.000014	3100.0	5800.0	0.0	0.0	0.30	0.0
HH7686A	704.	69.	0.000125	100.0	4000.0	8000.0	21259.0	17.00	1.60
HH7686A	704.	41.	0.000020	1400.0	5000.0	0.0	0.0	0.20	0.0
HH8416A	704.	124.	0.008600	25.0	94.0	120.0	294.4	24.00	2.00
HH8416A	704.	103.	0.001000	30.0	230.0	320.0	1057.9	12.50	0.70
HH8416A	704.	79.	0.000170	0.0	1800.0	2700.0	9479.0	11.00	0.70

Table A4. (Continued)

Heat No.	Temp. (°C)	Stress (MPa)	$\dot{e}_m$	t_1	t_2	t_{ss}	t_r	e_t	e_{ss}
HH3603A	704.	124.	0.015000	25.0	160.0	175.0	570.9	43.00	4.10
HH3603A	704.	69.	0.000300	100.0	4000.0	5200.0	17828.0	27.50	2.20
HH8416A	732.	55.	0.000063	160.0	0.0	0.0	0.0	0.0	0.0
HH8808A	760.	55.	0.001300	5.0	180.0	370.0	0.0	6.40	0.80
HH8808A	760.	48.	0.000120	60.0	900.0	0.0	0.0	0.26	0.0
HH8808A	760.	69.	0.058800	0.0	30.0	45.0	536.4	58.00	3.00
HH8735A	760.	69.	0.030000	5.0	140.0	145.0	575.3	37.00	5.00
HH8735A	760.	90.	0.427000	3.5	18.0	0.0	83.2	72.60	0.0
HH8735A	760.	28.	0.000050	210.0	0.0	0.0	0.0	0.12	0.0
HH8735A	760.	55.	0.001070	0.0	360.0	400.0	3018.6	35.00	0.50
HH8735A	760.	41.	0.000875	0.0	4400.0	4600.0	11995.0	26.00	4.00
HH7686A	760.	55.	0.000400	0.0	1500.0	1825.0	7981.6	19.50	1.00
HH7686A	760.	62.	0.000640	0.0	500.0	925.0	3676.5	18.00	0.80
HH7686A	760.	34.	0.000002	3000.0	4750.0	0.0	0.0	0.0	0.0
HH7686A	760.	83.	0.074000	2.0	155.0	165.0	340.6	63.00	13.00
HH7686A	760.	48.	0.000300	50.0	1000.0	1625.0	7088.7	14.00	0.80
HH7686A	760.	69.	0.024300	0.0	85.0	95.0	585.6	35.00	2.50
HH8808A	760.	90.	0.081000	3.0	14.0	16.0	149.0	62.50	2.50
HH8808A	760.	90.	0.240000	4.0	11.0	14.0	91.4	58.00	4.40
HH8416A	760.	55.	0.000140	0.0	2100.0	3700.0	9814.0	13.50	0.70
HH8416A	760.	69.	0.004600	0.0	140.0	310.0	1144.9	18.00	1.60
HH8416A	760.	31.	0.000001	3800.0	0.0	0.0	0.0	0.10	0.0
HH3603A	760.	48.	0.000800	0.0	3800.0	4800.0	12001.0	25.00	4.10
HH3603A	760.	69.	0.009000	0.0	440.0	450.0	1522.3	39.00	4.50
HH3603A	760.	28.	0.000003	2850.0	0.0	0.0	0.0	0.20	0.0

Table A4. (Continued)

Heat No.	Temp. (°C)	Stress (MPa)	$\dot{e}_m$	t_1	t_2	t_{ss}	t_r	e_t	e_{ss}
HH7686A	816.	33.	0.000100	0.0	4500.0	5300.0	13471.0	23.50	0.50
HH7686A	816.	61.	0.144000	0.0	8.0	10.0	113.5	72.00	1.50
HH8808A	816.	61.	0.340000	13.0	41.0	42.0	80.7	84.00	19.00
HH8808A	816.	61.	0.400000	0.0	37.0	39.5	84.3	72.50	16.00
HH8416A	816.	61.	0.012800	5.0	65.0	85.0	382.0	26.00	1.40
HH8416A	816.	21.	0.000013	750.0	1700.0	0.0	0.0	0.0	0.0
HH8416A	816.	41.	0.000083	0.0	2400.0	6300.0	10730.0	10.50	0.90
HH8416A	816.	37.	0.000040	500.0	0.0	0.0	0.0	0.13	0.0
HH3603A	816.	61.	0.100000	0.0	55.0	56.0	234.7	72.00	6.50
HH3603A	816.	28.	0.000110	0.0	1500.0	4000.0	0.0	1.90	0.64
HH3603A	816.	21.	0.000023	1800.0	3000.0	0.0	0.0	0.50	0.0
HH8808A	871.	28.	0.000200	0.0	370.0	520.0	0.0	10.00	0.30
HH8808A	871.	34.	0.012000	0.0	30.0	40.0	446.8	41.00	0.70
HH8735A	871.	10.	0.000048	250.0	1400.0	0.0	0.0	0.29	0.0
HH8735A	871.	17.	0.000150	0.0	1900.0	2250.0	7204.7	33.50	0.40
HH8735A	871.	41.	0.110000	47.0	97.0	98.0	154.3	76.50	23.00
HH7686A	871.	28.	0.000075	0.0	1450.0	3050.0	4989.4	4.00	0.20
HH7686A	871.	24.	0.000039	475.0	1000.0	0.0	0.0	0.20	0.0
HH7686A	871.	41.	0.004000	0.0	140.0	150.0	513.1	31.00	0.50
HH7686A	871.	34.	0.000280	70.0	980.0	1420.0	2245.8	11.00	0.65
HH7686A	871.	34.	0.008500	5.0	110.0	180.0	864.9	31.00	1.90
HH8735A	871.	28.	0.009200	0.0	110.0	140.0	879.4	33.50	1.50
HH8808A	871.	41.	0.375000	0.0	57.0	62.0	131.4	86.50	24.00
HH8808A	871.	41.	0.125000	0.0	10.0	12.0	117.6	58.00	1.50
HH7534A	871.	28.	0.000250	0.0	900.0	1300.0	2476.1	20.00	0.80
HH8285A	871.	21.	0.000013	1500.0	3100.0	0.0	0.0	0.30	0.0

[a]A value of 0.0 implies that an accurate value could not be determined.

Table A5. Sandvik Sanicro 31 Creep Data

PRODUCT FORM	HEAT NUMBER	SPECIMEN NUMBER	TEMP (C)	STRESS (MPA)	RUPTURE LIFE (HR)	ELONG (%)	RED IN AREA (%)
135MMOD X 7MMWT TUBE	7.52438	3994	600.	208.2	446.0	51.00	51.00
	7.52438	3995	600.	177.2	1063.0	57.00	55.00
	7.52438	3996	600.	155.8	2763.0	35.00	38.00
	7.52438	3997	600.	135.1	8888.0	28.00	27.00
	7.52438	3998	600.	113.8	32422.0	31.00	19.00
	7.52438	4014	700.	104.1	158.0	90.00	78.00
	7.52438	4015	700.	93.1	248.0	91.00	80.00
	7.52438	4016	700.	84.8	574.0	81.00	75.00
	7.52438	4017	700.	73.8	1199.0	67.00	75.00
	7.52438	4018	700.	64.1	3667.0	67.00	65.00
16MM BAR	6.53436	13605	700.				48.00
197MMOD X 19MMWT TUBE	7.53353	4975	600.	208.2	1845.0	23.00	32.00
	7.53353	4976	600.	177.2	8629.0	23.00	27.00
	7.53353	4977	600.	155.8	16637.0	7.00	13.00
	7.53353	4978	600.	135.1	39694.0	12.00	17.00
	7.53353	4979	600.	113.8	68404.0	14.00	15.00
50MMOD X 7MMWT TUBE	4.98180	11076	700.	104.1	689.0	56.00	65.00
	4.98180	11078	700.	93.1	1353.0	45.00	49.00

Table A5. (Continued)

PRODUCT FORM	HEAT NUMBER	SPECIMEN NUMBER	TEMP (C)	STRESS (MPA)	RUPTURE LIFE (HR)	ELONG (%)	RED IN AREA (%)
50MMOD X 7MMWT TUBE	4.98180	11080	700.	84.8	2259.0	58.00	54.00
	4.98180	11082	700.	73.8	6065.0	35.00	19.00
	4.98180	11084	700.	64.1	11907.0	42.00	39.00
	4.98180	11458	700.	57.9	12473.0	37.00	38.00
	4.98180	11460	700.	53.1	23114.0	34.00	28.00
75MMOD X 14MMWT TUBE	7.53723	5877	700.	104.1	694.0	54.00	51.00
	7.53723	5879	700.	93.8	1275.0	51.00	42.00
	7.53723	5884	700.	84.8	2709.0	54.00	55.00
	7.53723	5886	700.	73.8	6148.0	36.00	37.00
	7.53723	5891	700.	57.9	17588.0	32.00	37.00

Table A5. (Continued)

ANN/0.17/1050/WQ

PRODUCT FORM	HEAT NUMBER	SPECIMEN NUMBER	TEMP (C)	STRESS (MPA)	RUPTURE LIFE (HR)	ELONG (%)	RED IN AREA (%)
16MM BAR	6.53438	13521	600.	219.9	144.0	88.00	72.00
	6.53438	13844	600.	219.9	131.0	89.00	60.00
	6.53438	13540	600.	184.8	364.0	93.00	68.00
	6.53438	13559	600.	160.0	760.0	77.00	62.00
	6.53438	13578	600.	140.0	1482.0	84.00	58.00
	6.53438	13597	600.	124.8	2351.0	50.00	49.00
	7.73207	13520	600.	219.9	308.0	61.00	55.00
	7.73207	13539	600.	184.8	863.0	58.00	49.00
	7.73207	13558	600.	160.0	2578.0	36.00	36.00
	7.73207	13577	600.	140.0	4207.0	33.00	31.00
	6.53438	13145	650.	150.3	137.0	83.00	75.00
	6.53438	13164	650.	124.8	304.0	88.00	73.00
	6.53438	13183	650.	104.8	602.0	86.00	70.00
	6.53438	13202	650.	90.3	963.0	68.00	61.00
	6.53438	13221	650.	80.0	2743.0	68.00	57.00
	7.73207	13144	650.	150.3	299.0	69.00	63.00
	7.73207	13163	650.	124.8	695.0	60.00	67.00
	7.73207	13182	650.	104.8	1172.0	52.00	51.00
	7.73207	13201	650.	90.3	3315.0	44.00	39.00
	7.73207	13220	650.	80.0	3567.0	45.00	36.00

Table A5. (Continued)

ANN/0.17/1100/WQ

PRODUCT FORM	HEAT NUMBER	SPECIMEN NUMBER	TEMP (C)	STRESS (MPA)	RUPTURE LIFE (HR)	ELONG (%)	RED IN AREA (%)
16MM BAR	6.53438	13519	600.	219.9	322.0	65.00	50.00
	6.53438	13843	600.	219.9	292.0	60.00	54.00
	6.53438	13538	600.	184.8	1079.0	57.00	51.00
	6.53438	13557	600.	160.0	2095.0	65.00	69.00
	6.53438	13576	600.	140.0	5545.0	40.00	38.00
	7.73207	13518	600.	219.9	630.0	37.00	40.00
	7.73207	13537	600.	184.8	2337.0	34.00	27.00
	7.73207	13556	600.	160.0	6565.0	23.00	23.00
	6.53438	13143	650.	150.3	368.0	81.00	66.00
	6.53438	13162	650.	124.8	742.0	75.00	60.00
	6.53438	13181	650.	104.8	1929.0	58.00	54.00
	6.53438	13200	650.	90.3	4520.0	47.00	46.00
	6.53438	13219	650.	80.0	6566.0	43.00	44.00
	7.73207	13142	650.	150.3	599.0	48.00	56.00
	7.73207	13161	650.	124.8	2035.0	45.00	42.00
	7.73207	13180	650.	104.8	4765.0	41.00	42.00
	4.98180	11464	700.	104.1	699.0	58.00	50.00
	4.98180	11465	700.	93.1	1217.0	60.00	58.00
	4.98180	11466	700.	84.8	1857.0	36.00	33.00

Table A5. (Continued)

ANN/0.17/1100/WQ
(CONTINUED)

PRODUCT FORM	HEAT NUMBER	SPECIMEN NUMBER	TEMP (C)	STRESS (MPA)	RUPTURE LIFE (HR)	ELONG (%)	RED IN AREA (%)
16MM BAR	4.98180	11467	700.	73.8	3945.0	58.00	54.00
	4.98180	11468	700.	64.1	9290.0	48.00	42.00
	4.98180	11469	700.	57.9	14035.0	38.00	35.00
	4.98180	11470	700.	53.1	26791.0	31.00	32.00

Table A5. (Continued)

ANN/0.17/1140/WQ

PRODUCT FORM	HEAT NUMBER	SPECIMEN NUMBER	TEMP (C)	STRESS (MPA)	RUPTURE LIFE (HR)	ELONG (%)	RED IN AREA (%)
16MM BAR	4.98180	10895	700.	111.7	639.0	40.00	41.00
	4.98180	10901	700.	93.8	2130.0	31.00	32.00
	4.98180	10907	700.	73.8	8380.0	28.00	37.00
	4.98180	10913	700.	64.1	19199.0	18.00	19.00
25MMOD X 5MMWT TUBE	5.67078	5060	600.	264.8	155.0	24.00	21.00
	5.67078	5063	600.	235.1	1017.0	14.00	16.00
	5.67078	5066	600.	208.9	2857.0	12.00	12.00
	5.67078	5069	600.	177.2	7604.0	9.00	9.00
	5.67078	5072	600.	135.1	29548.0	5.00	6.00
	5.67107	5061	600.	264.8	294.0	12.00	10.00
	5.67107	5064	600.	235.1	946.0	11.00	12.00
	5.67107	5067	600.	208.9	3187.0	7.00	7.00
	5.67107	5070	600.	177.2	8740.0	8.00	4.00
	5.67107	5073	600.	135.1	28673.0	6.00	4.00
	7.07711	5062	600.	264.8	174.0	14.00	13.00
	7.07711	5065	600.	235.1	421.0	11.00	16.00
	7.07711	5068	600.	208.9	1085.0	8.00	7.00
	7.07711	5071	600.	177.2	6004.0	6.00	6.00

Table A5. (Continued)

ANN/0.17/1140/WQ
(CONTINUED)

PRODUCT FORM	HEAT NUMBER	SPECIMEN NUMBER	TEMP (C)	STRESS (MPA)	RUPTURE LIFE (HR)	ELONG (%)	RED IN AREA (%)
25MMOD X 5MMWT TUBE	7.07711	5074	600.	135.1	29385.0	3.00	7.00
	5.67078	5243	650.	157.2	352.0	42.00	48.00
	5.67078	5246	650.	137.2	541.0	56.00	51.00
	5.67078	5249	650.	124.1	2294.0	22.00	23.00
	5.67107	5244	650.	157.2	283.0	43.00	44.00
	5.67107	5247	650.	137.2	3905.0	15.00	13.00
	5.67107	5250	650.	124.1	3405.0	24.00	21.00
	7.07711	5245	650.	157.2	2650.0	8.00	10.00
	7.07711	5248	650.	137.2	2714.0	30.00	29.00
	7.07711	5251	650.	124.1	3182.0	14.00	13.00
	5.67078	5075	700.	104.1	589.0	72.00	49.00
	5.67078	5876	700.	104.1	339.0	61.00	47.00
	5.67078	5078	700.	88.3	1112.0	43.00	47.00
	5.67078	5883	700.	84.8	1720.0	47.00	45.00
	5.67078	5850	700.	73.8	2996.0	37.00	34.00
	5.67078	5890	700.	68.9	10382.0	23.00	23.00
	5.67107	5076	700.	104.1	956.0	37.00	40.00
	5.67107	5079	700.	88.3	1441.0	27.00	33.00

Table A5. (Continued)

ANN/0.17/1140/WQ
(CONTINUED)

PRODUCT FORM	HEAT NUMBER	SPECIMEN NUMBER	TEMP (C)	STRESS (MPA)	RUPTURE LIFE (HR)	ELONG (%)	RED IN AREA (%)
25MMOD X 5MMWT TUBE	5.67107	5851	700.	73.8	4669.0	28.00	25.00
	7.07711	5077	700.	104.1	1432.0	30.00	25.00
	7.07711	5080	700.	88.3	2583.0	23.00	11.00
	7.07711	5852	700.	73.8	6315.0	18.00	23.00
	7.07766	5622	700.	106.9	516.0	33.00	29.00
	7.07766	5623	700.	106.9	613.0	34.00	29.00
	7.07766	5624	700.	106.9	1131.0	26.00	24.00
	7.07766	5628	700.	106.9	625.0	38.00	31.00
	7.07766	5844	700.	106.9	618.0	46.00	37.00
	7.07766	5845	700.	106.9	681.0	43.00	33.00
	7.07766	5846	700.	106.9	573.0	42.00	37.00
	7.07766	5625	700.	86.9	2650.0	16.00	16.00
	7.07766	5626	700.	86.9	1671.0	25.00	21.00
	7.07766	5627	700.	86.9	3751.0	14.00	12.00
	7.07766	5847	700.	86.9	2211.0	22.00	16.00
	7.07766	5848	700.	86.9	2089.0	21.00	19.00
	7.07766	5849	700.	86.9	2141.0	28.00	27.00
60MMOD X 10MMWT TUBE	7.53088	4470	600.	208.2	704.0	39.00	38.00

Table A5. (Continued)

ANN/0.17/1140/WQ
(CONTINUED)

PRODUCT FORM	HEAT NUMBER	SPECIMEN NUMBER	TEMP (C)	STRESS (MPA)	RUPTURE LIFE (HR)	ELONG (%)	RED IN AREA (%)
60MMOD X 10MMWT TUBE	7.53088	4471	600.	177.2	1906.0	41.00	32.00
	7.53088	4472	600.	155.8	7637.0	26.00	26.00
	7.53088	4473	600.	135.1	31062.0	21.00	44.00
	7.53088	4474	600.	124.8	30735.0	20.00	21.00

Table A5. (Continued)

ANN/0.17/1150/WQ

PRODUCT FORM	HEAT NUMBER	SPECIMEN NUMBER	TEMP (C)	STRESS (MPA)	RUPTURE LIFE (HR)	ELONG (%)	RED IN AREA (%)
16.0MM BAR	4.81837	13413	550.	299.9	3090.0	14.00	15.00
	6.53433	13412	550.	299.9	1665.0	14.00	13.00
	6.53433	13421	550.	270.3	2765.0	12.00	9.00
	6.53434	13417	550.	299.9	292.0	18.00	19.00
	6.53434	13426	550.	270.3	619.0	19.00	15.00
	6.53434	13435	550.	230.3	1845.0	24.00	17.00
	6.53434	13444	550.	199.9	4534.0	21.00	17.00
	6.53435	13418	550.	299.9	586.0	24.00	22.00
	6.53435	13427	550.	270.3	1051.0	20.00	17.00
	6.53435	13436	550.	230.3	2600.0	21.00	19.00
	6.53435	13445	550.	199.9	6053.0	19.00	9.00
	6.53436	13419	550.	299.9	862.0	31.00	26.00
	6.53436	13428	550.	270.3	1714.0	23.00	22.00
	6.53436	13437	550.	230.3	3916.0	22.00	16.00
	6.53438	12695	550.	299.9	1360.0	21.00	15.00
	6.53438	13420	550.	299.9	1651.0	20.00	15.00
	6.53438	13429	550.	270.3	4963.0	14.00	9.00
	7.73207	13414	550.	299.9	1355.0	16.00	13.00
	7.73207	13423	550.	270.3	3657.0	11.00	9.00

Table A5. (Continued)

ANN/0.17/1150/WQ
(CONTINUED)

PRODUCT FORM	HEAT NUMBER	SPECIMEN NUMBER	TEMP (C)	STRESS (MPA)	RUPTURE LIFE (HR)	ELONG (%)	RED IN AREA (%)
16.0MM BAR	7.74129	13415	550.	299.9	598.0	22.00	24.00
	7.74129	13424	550.	270.3	1231.0	21.00	19.00
	7.74129	13433	550.	230.3	4103.0	18.00	15.00
	7.76025	13416	550.	299.9	2198.0	13.00	15.00
	7.76025	13425	550.	270.3	4477.0	10.00	8.00
	7.74129	13544	600.	160.0	3020.0	31.00	26.00
	7.76025	13507	600.	219.9	3525.0	5.00	5.00
	4.81837	13504	600.	219.9	1111.0	22.00	28.00
	4.81837	13523	600.	184.8	4152.0	35.00	38.00
	6.53433	13503	600.	219.9	1870.0	7.00	8.00
	6.53433	13522	600.	184.8	5828.0	6.00	7.00
	6.53434	13508	600.	219.9	164.0	23.00	23.00
	6.53434	13527	600.	184.8	644.0	25.00	27.00
	6.53434	13546	600.	160.0	1313.0	35.00	33.00
	6.53434	13565	600.	140.0	3332.0	33.00	30.00
	6.53434	13584	600.	124.8	7077.0	33.00	30.00
	6.53435	13509	600.	219.9	326.0	27.00	26.00
	6.53435	13528	600.	184.8	1107.0	41.00	34.00
	6.53435	13547	600.	160.0	1638.0	32.00	30.00

Table A5. (Continued)

ANN/0.17/1150/WQ
(CONTINUED)

PRODUCT FORM	HEAT NUMBER	SPECIMEN NUMBER	TEMP (C)	STRESS (MPA)	RUPTURE LIFE (HR)	ELONG (%)	RED IN AREA (%)
16.0MM BAR	6.53435	13566	600.	140.0	4382.0	35.00	30.00
	6.53436	13510	600.	219.9	413.0	23.00	28.00
	6.53436	13529	600.	184.8	1285.0	30.00	31.00
	6.53436	13548	600.	160.0	2180.0	29.00	26.00
	6.53436	13567	600.	140.0	4855.0	30.00	28.00
	6.53438	13511	600.	219.9	456.0	29.00	28.00
	6.53438	13841	600.	219.9	414.0	40.00	36.00
	6.53438	13530	600.	184.8	1304.0	32.00	21.00
	6.53438	13886	600.	184.8	1016.0	66.00	37.00
	6.53438	13549	600.	160.0	2438.0	24.00	24.00
	6.53438	13887	600.	160.0	1472.0		
	6.53438	13568	600.	140.0	7801.0	18.00	17.00
	6.53438	13888	600.	140.0	1374.0		
	6.53438	13889	600.	124.8	1374.0		
	7.73207	13505	600.	219.9	484.0	25.00	27.00
	7.73207	13524	600.	184.8	2010.0	22.00	19.00
	7.73207	13543	600.	160.0	5065.0	17.00	22.00
	7.74129	13506	600.	219.9	368.0	28.00	25.00
	7.74129	13525	600.	184.8	1550.0	28.00	25.00

Table A5. (Continued)

ANN/0.17/1150/WQ
(CONTINUED)

PRODUCT FORM	HEAT NUMBER	SPECIMEN NUMBER	TEMP (C)	STRESS (MPA)	RUPTURE LIFE (HR)	ELONG (%)	RED IN AREA (%)
16.0MM BAR	4.81837	13128	650.	150.3	1326.0	35.00	40.00
	4.81837	13147	650.	124.8	3056.0	39.00	37.00
	4.81837	13166	650.	104.8	7660.0	26.00	29.00
	6.53433	13127	650.	150.3	4523.0	10.00	13.00
	6.53434	13132	650.	150.3	330.0	45.00	40.00
	6.53434	13151	650.	124.8	903.0	68.00	50.00
	6.53434	13170	650.	104.8	2463.0	56.00	42.00
	6.53434	13189	650.	90.3	7938.0	45.00	36.00
	6.53435	13133	650.	150.3	393.0	52.00	43.00
	6.53435	13152	650.	124.8	1228.0	55.00	45.00
	6.53435	13171	650.	104.8	3124.0	55.00	45.00
	6.53436	13134	650.	150.3	459.0	54.00	45.00
	6.53436	13153	650.	124.8	1285.0	51.00	44.00
	6.53436	13172	650.	104.8	3760.0	40.00	35.00
	6.53438	13135	650.	150.3	380.0	43.00	40.00
	6.53438	13154	650.	124.8	1267.0	41.00	30.00
	6.53438	13173	650.	104.8	3537.0	36.00	32.00
	7.73207	13129	650.	150.3	672.0	33.00	34.00
	7.73207	13148	650.	124.8	1766.0	36.00	33.00

Table A5. (Continued)

ANN/0.17/1150/WQ
(CONTINUED)

PRODUCT FORM	HEAT NUMBER	SPECIMEN NUMBER	TEMP (C)	STRESS (MPA)	RUPTURE LIFE (HR)	ELONG (%)	RED IN AREA (%)
16.0MM BAR	7.73207	13167	650.	104.8	4642.0	31.00	28.00
	7.74129	13130	650.	150.3	504.0	48.00	45.00
	7.74129	13168	650.	104.8	3601.0	33.00	29.00
16MM BAR	7.76025	13150	650.	124.8	5073.0	33.00	33.00
	7.74129	13149	650.	124.8	1580.0	48.00	42.00
	4.81837	13599	700.	100.0	1549.0	40.00	41.00
	4.81837	13608	700.	84.8	2413.0	36.00	39.00
	6.53433	13598	700.	100.0	2731.0	27.00	40.00
	6.53433	13607	700.	84.8	4688.0	45.00	36.00
	6.53434	13603	700.	100.0	545.0	82.00	70.00
	6.53434	13612	700.	84.8	1291.0	88.00	67.00
	6.53434	13621	700.	70.3	3255.0	71.00	76.00
	6.53435	13604	700.	100.0	812.0	58.00	42.00
	6.53435	13613	700.	84.8	1449.0	74.00	57.00
	6.53435	13622	700.	70.3	6107.0	38.00	37.00
	6.53436	13614	700.	84.8	1792.0	56.00	49.00
	6.53438	13606	700.	100.0	771.0	57.00	50.00
	6.53438	13615	700.	84.8	1606.0	47.00	42.00
	7.73207	13600	700.	100.0	1056.0	49.00	42.00

Table A5. (Continued)

ANN/0.17/1150/WQ
(CONTINUED)

PRODUCT FORM	HEAT NUMBER	SPECIMEN NUMBER	TEMP (C)	STRESS (MPA)	RUPTURE LIFE (HR)	ELONG (%)	RED IN AREA (%)
16MM BAR	7.73207	13609	700.	84.8	2618.0	45.00	39.00
	7.74129	13601	700.	100.0	679.0	68.00	53.00
	7.74129	13610	700.	84.8	2435.0	55.00	45.00
	7.74129	13619	700.	70.3	7517.0	34.00	29.00
	7.76025	13602	700.	100.0	1970.0	41.00	38.00
	7.76025	13611	700.	84.8	2859.0	33.00	36.00
33MMOD X 5MMWT TUBE	4.98180	12068	600.	208.2	2203.0	21.00	26.00
	4.98180	12071	600.	186.8	2796.0	21.00	25.00
	4.98180	12074	600.	161.3	7482.0	20.00	21.00
	4.98180	12077	600.	146.2	14884.0	21.00	28.00
	4.98180	12080	600.	135.1	23645.0	19.00	23.00
	4.98180	11086	700.	104.1	996.0	21.00	29.00
	4.98180	12449	700.	104.1	497.0	28.00	29.00
	4.98180	12450	700.	104.1	516.0	28.00	29.00
	4.98180	12083	700.	93.8	989.0	56.00	59.00
	4.98180	12451	700.	93.8	1019.0	25.00	28.00
	4.98180	12452	700.	93.8	896.0	29.00	28.00
	4.98180	11087	700.	93.1	1519.0	25.00	28.00

Table A5. (Continued)

ANN/0.17/1150/WQ
(CONTINUED)

PRODUCT FORM	HEAT NUMBER	SPECIMEN NUMBER	TEMP (C)	STRESS (MPA)	RUPTURE LIFE (HR)	ELONG (%)	RED IN AREA (%)
33MMOD X 5MMWT TUBE	4.98180	11088	700.	84.8	3974.0	21.00	30.00
	4.98180	12453	700.	84.8	2112.0	27.00	23.00
	4.98180	12454	700.	84.8	2016.0	29.00	28.00
	4.98180	11089	700.	73.8	7927.0	14.00	30.00
	4.98180	12455	700.	73.8	14472.0	12.00	13.00
	4.98180	12456	700.	73.8	8588.0	14.00	25.00
	4.98180	12086	700.	68.9	11497.0	35.00	32.00
	4.98180	11090	700.	64.1	17007.0	16.00	15.00
	4.98180	12458	700.	64.1	23216.0	17.00	12.00
	4.98180	12089	700.	57.9	23269.0	25.00	30.00
42MMOD X 5MMWT TUBE	4.98198	12067	600.	208.2	1333.0	22.00	22.00
	4.98198	12070	600.	186.8	1712.0	20.00	25.00
	4.98198	12073	600.	161.3	4021.0	21.00	18.00
	4.98198	12076	600.	146.2	4363.0	12.00	23.00
	4.98198	12079	600.	135.1	12276.0	14.00	21.00
	4.98198	12082	700.	93.1	663.0	27.00	35.00
	4.98198	12085	700.	68.9	11658.0	20.00	26.00

Table A5. (Continued)

ANN/0.17/1150/WQ
(CONTINUED)

PRODUCT FORM	HEAT NUMBER	SPECIMEN NUMBER	TEMP (C)	STRESS (MPA)	RUPTURE LIFE (HR)	ELONG (%)	RED IN AREA (%)
42MMOD X 9MMWT TUBE	4.98195	11276	600.	208.2	3313.0	15.00	18.00
	4.98195	12066	600.	208.2	2031.0	18.00	23.00
	4.98195	11279	600.	186.8	9290.0	15.00	18.00
	4.98195	12069	600.	186.8	2374.0	23.00	18.00
	4.98195	11282	600.	161.3	18513.0	6.00	14.00
	4.98195	12072	600.	161.3	5515.0	16.00	16.00
	4.98195	11285	600.	146.2	23233.0	1.00	7.00
	4.98195	12075	600.	146.2	11873.0	12.00	25.00
	4.98195	11288	600.	135.1	26349.0	8.00	10.00
	4.98195	12078	600.	135.1	17303.0	10.00	12.00
	4.98195	11291	700.	93.1	1476.0	40.00	35.00
	4.98195	12081	700.	93.1	1295.0	28.00	26.00
	4.98195	11294	700.	80.0	5949.0	30.00	30.00
	4.98195	11297	700.	68.9	13057.0	27.00	24.00
	4.98195	12084	700.	68.9	13291.0	21.00	30.00
	4.98195	11300	700.	64.1	22215.0	14.00	14.00
	4.98195	12087	700.	57.9	25667.0	25.00	21.00
43MMOD X 6MMWT TUBE	7.05801	3970	700.	104.1	940.0	53.00	42.00

Table A5. (Continued)

ANN/0.17/1150/WQ
(CONTINUED)

PRODUCT FORM	HEAT NUMBER	SPECIMEN NUMBER	TEMP (C)	STRESS (MPA)	RUPTURE LIFE (HR)	ELONG (%)	RED IN AREA (%)
43MMOD X 6MMWT TUBE	7.05801	3972	700.	84.8	3050.0	32.00	36.00
	7.05801	3974	700.	73.8	5552.0	31.00	40.00
	7.05801	3976	700.	64.1	14990.0		
	7.76411	13890	700.	90.3	4409.0	29.00	28.00
50MMOD X 7MMWT TUBE	4.98180	11077	700.	104.1	1017.0	33.00	33.00
	4.98180	11079	700.	93.1	1357.0	63.00	55.00
	4.98180	11081	700.	84.8	2524.0	42.00	49.00
	4.98180	11083	700.	73.8	7073.0	34.00	32.00
	4.98180	11085	700.	64.1	15801.0	28.00	28.00
	4.98180	11459	700.	57.9	14221.0	31.00	38.00
60MMOD X 10MMWT TUBE	7.53088	4490	700.	111.7	260.0	74.00	54.00
	7.53088	5875	700.	104.1	386.0	41.00	54.00
	7.53088	4491	700.	93.1	777.0	60.00	53.00
	7.53088	4492	700.	84.8	1610.0	57.00	51.00
	7.53088	5882	700.	84.8	1652.0	73.00	50.00
	7.53088	4493	700.	73.8	3520.0	51.00	46.00
	7.53088	5889	700.	68.9	6283.0	38.00	34.00

Table A5. (Continued)

ANN/0.17/1150/WQ
(CONTINUED)

PRODUCT FORM	HEAT NUMBER	SPECIMEN NUMBER	TEMP (C)	STRESS (MPA)	RUPTURE LIFE (HR)	ELONG (%)	RED IN AREA (%)
60MMOD X 10MMWT TUBE	7.53088	4494	700.	64.1	9678.0	40.00	34.00
64MMOD X 6MMWT TUBE	7.72471	11275	600.	208.2	2290.0	23.00	20.00
	7.72471	11278	600.	186.8	4604.0	21.00	26.00
	7.72471	11281	600.	161.3	6922.0	17.00	26.00
	7.72471	11284	600.	146.2	9310.0	18.00	19.00
	7.72471	11287	600.	135.1	16520.0	16.00	18.00
	7.72471	11290	700.	93.1	1148.0	53.00	49.00
	7.72471	11293	700.	80.0	5930.0	31.00	43.00
	7.72471	11296	700.	68.9	11199.0	33.00	32.00
	7.72471	11299	700.	64.1	33629.0	24.00	14.00

Table A5. (Continued)

ANN/0.17/1170/WQ

PRODUCT FORM	HEAT NUMBER	SPECIMEN NUMBER	TEMP (C)	STRESS (MPA)	RUPTURE LIFE (HR)	ELONG (%)	RED IN AREA (%)
16MM BAR	4.98180	10896	700.	111.7	654.0	44.00	43.00
	4.98180	10902	700.	93.8	1956.0	37.00	42.00
	4.98180	10908	700.	73.8	7765.0	31.00	40.00
	4.98180	10914	700.	64.1	26509.0	22.00	15.00

ANN/0.17/980/WQ

16.0MM BAR	6.53442	13502	600.	104.8	5360.0	66.00	51.00

Table A5. (Continued)

ANN/0.25/1150/#Q

PRODUCT FORM	HEAT NUMBER	SPECIMEN NUMBER	TEMP (C)	STRESS (MPA)	RUPTURE LIFE (HR)	ELONG (%)	RED IN AREA (%)
16.0MM BAR	7.54214	7194	600.	235.1	265.0	22.00	67.00
	7.54214	7195	600.	213.7	449.0	26.00	32.00
	7.54214	7196	600.	197.9	874.0	24.00	29.00
	7.54214	7197	600.	177.2	1708.0	22.00	23.00
	7.54214	7198	600.	155.8	4597.0	24.00	25.00
16MM BAR	7.54214	7382	700.	111.7	187.0	59.00	64.00
	7.54214	7383	700.	93.1	788.0	60.00	58.00
	7.54214	7384	700.	84.8	1655.0	59.00	52.00
	7.54214	11022	700.	84.8	1527.0	31.00	59.00
	7.54214	7385	700.	73.8	4255.0	45.00	47.00
	7.54214	11023	700.	70.3	10152.0	38.00	42.00
	7.54214	7386	700.	64.1	14070.0	37.00	39.00
	7.54214	11024	700.	64.1	12888.0	34.00	47.00
20.0MM BAR	7.06745	4239	600.	208.2	10377.0	7.00	12.00
	7.06745	4240	600.	177.2	27653.0	5.00	6.00
	7.06745	4241	600.	155.8	56073.0	4.00	4.00
	7.06745	4242	600.	135.1	83030.0	4.00	2.00
	7.06745	4243	600.	124.8	83030.0		
20MM BAR	7.06745	5862	700.	122.0	386.0	56.00	51.00

Table A5. (Continued)

ANN/0.25/1150/WQ
(CONTINUED)

PRODUCT FORM	HEAT NUMBER	SPECIMEN NUMBER	TEMP (C)	STRESS (MPA)	RUPTURE LIFE (HR)	ELONG (%)	RED IN AREA (%)
20MM BAR	7.06745	4244	700.	104.1	3800.0	11.00	18.00
	7.06745	5864	700.	104.1	682.0	61.00	47.00
	7.06745	4247	700.	84.8	10715.0	7.00	7.00
	7.06745	5866	700.	84.8	3243.0	44.00	43.00
	7.06745	4250	700.	73.8	10578.0	31.00	32.00
	7.06745	5868	700.	73.8	8242.0	34.00	33.00
	7.06745	5870	700.	64.1	15937.0	32.00	32.00
	7.06863	4245	700.	104.1	1145.0	47.00	47.00
	7.06863	5872	700.	93.8	2254.0	40.00	42.00
	7.06863	4248	700.	84.8	4682.0	31.00	38.00
	7.06863	4251	700.	73.8	8713.0	34.00	40.00
	7.06863	5873	700.	64.1	22027.0	29.00	32.00
	7.52399	5863	700.	122.0	255.0	76.00	55.00
	7.52399	4246	700.	104.1	496.0	87.00	52.00
	7.52399	5865	700.	104.1	338.0	68.00	56.00
	7.52399	4249	700.	84.8	6437.0	28.00	32.00
	7.52399	5867	700.	84.8	2163.0	66.00	53.00
	7.52399	4252	700.	73.8	4378.0	52.00	44.00
	7.52399	5869	700.	73.8	5509.0	32.00	25.00

Table A5. (Continued)

ANN/0.25/1150/WQ
(CONTINUED)

PRODUCT FORM	HEAT NUMBER	SPECIMEN NUMBER	TEMP (C)	STRESS (MPA)	RUPTURE LIFE (HR)	ELONG (%)	RED IN AREA (%)
20MM BAR	7.52399	4255	700.	64.1	12953.0		
	7.52399	5871	700.	64.1	11938.0	36.00	32.00
25.0MM BAR	5.67078	5037	600.	306.1	67.0	22.00	18.00
	5.67078	5040	600.	275.8	143.0	23.00	22.00
	5.67078	5043	600.	244.8	255.0	19.00	19.00
	5.67078	4766	600.	213.7	1351.0	13.00	13.00
	5.67078	4768	600.	186.8	3804.0	13.00	10.00
	5.67078	4772	600.	155.8	12976.0	11.00	13.00
	5.67078	4775	600.	124.8	50684.0	6.00	6.00
	5.67107	5036	600.	306.1	87.0	23.00	27.00
	5.67107	5039	600.	275.8	396.0	13.00	19.00
	5.67107	5042	600.	244.8	720.0	13.00	13.00
	5.67107	4767	600.	213.7	3215.0	10.00	13.00
	5.67107	4770	600.	186.8	8268.0	8.00	10.00
	5.67107	4773	600.	155.8	28769.0	5.00	9.00
	5.67107	4776	600.	124.8	47383.0	4.00	7.00
	7.07711	5038	600.	306.1	105.0	21.00	19.00
	7.07711	5041	600.	275.8	146.0	18.00	14.00
	7.07711	5044	600.	244.8	442.0	12.00	11.00

Table A5. (Continued)

ANN/0.25/1150/WQ
(CONTINUED)

PRODUCT FORM	HEAT NUMBER	SPECIMEN NUMBER	TEMP (C)	STRESS (MPA)	RUPTURE LIFE (HR)	ELONG (%)	RED IN AREA (%)
25.0MM BAR	7.07711	4765	600.	213.7	2613.0	9.00	11.00
	7.07711	4768	600.	186.8	7097.0	6.00	8.00
	7.07711	4771	600.	155.8	29133.0	5.00	5.00
25MM BAR	5.67078	4778	700.	111.7	273.0	72.00	52.00
	5.67078	4781	700.	93.1	606.0	61.00	52.00
	5.67078	4784	700.	80.0	2275.0	50.00	41.00
	5.67078	4787	700.	64.1	6467.0	29.00	30.00
	5.67107	4779	700.	111.7	495.0	57.00	41.00
	5.67107	4782	700.	93.1	1124.0	46.00	46.00
	5.67107	4785	700.	80.0	4877.0	31.00	30.00
	5.67107	5853	700.	64.1	11959.0	32.00	26.00
	6.26273	11039	700.	104.1	711.0	57.00	65.00
	6.26273	11043	700.	93.8	1624.0	52.00	53.00
	6.26273	11047	700.	84.8	3856.0	33.00	40.00
	6.26273	11051	700.	73.8	9624.0	28.00	28.00
	6.26273	11055	700.	64.1	33197.0	29.00	20.00
	6.27271	11037	700.	104.1	1396.0	40.00	45.00
	6.27271	11041	700.	93.8	3496.0	37.00	34.00
	6.27271	11045	700.	84.8	6174.0	29.00	33.00

Table A5. (Continued)

ANN/0.25/1150/WQ
(CONTINUED)

PRODUCT FORM	HEAT NUMBER	SPECIMEN NUMBER	TEMP (C)	STRESS (MPA)	RUPTURE LIFE (HR)	ELONG (%)	RED IN AREA (%)
25MM BAR	6.27271	11049	700.	73.8	10292.0	23.00	28.00
	6.27272	11038	700.	104.1	798.0	39.00	50.00
	6.27272	11042	700.	93.8	1643.0	34.00	42.00
	6.27272	11046	700.	84.8	3193.0	40.00	40.00
	6.27272	11050	700.	73.8	7350.0	28.00	26.00
	6.27272	11054	700.	64.1	17121.0	18.00	20.00
	7.07711	4777	700.	111.7	336.0	55.00	41.00
	7.07711	4780	700.	93.1	990.0	37.00	36.00
	7.07711	4783	700.	80.0	3375.0	33.00	31.00
	7.07711	4786	700.	64.1	7629.0	27.00	28.00
75MMOD X 14MMWT TUBE	7.53723	5874	700.	104.1	737.0	56.00	53.00
	7.53723	5881	700.	84.8	2727.0	72.00	53.00
	7.53723	5888	700.	68.9	10924.0	40.00	34.00

Table A5. (Continued)

ANN/0.5/1000/WQ

PRODUCT FORM	HEAT NUMBER	SPECIMEN NUMBER	TEMP (C)	STRESS (MPA)	RUPTURE LIFE (HR)	ELONG (%)	RED IN AREA (%)
16.0MM BAR	5.67942	8008	550.	319.2	261.0	35.00	36.00
	5.67942	8012	550.	277.9	727.0	22.00	21.00
	5.67942	8016	550.	246.8	3101.0	12.00	15.00
	5.67942	8020	550.	215.8	10889.0	11.00	11.00
	5.67943	8009	550.	319.2	315.0	25.00	32.00
	5.67943	8013	550.	277.9	1019.0	20.00	23.00
	5.67943	8017	550.	246.8	3156.0	14.00	16.00
	5.67943	8021	550.	215.8	11087.0	10.00	13.00
	5.70037	8011	550.	319.2	400.0	44.00	45.00
	5.70037	8015	550.	277.9	2927.0	20.00	21.00
	5.70037	8019	550.	246.8	8805.0	18.00	5.00
	5.70037	8023	550.	215.8	26941.0	12.00	13.00
	7.07765	8010	550.	319.2	226.0	48.00	49.00
	7.07765	8014	550.	277.9	648.0	29.00	29.00
	7.07765	8018	550.	246.8	1606.0	19.00	20.00
	7.07765	8022	550.	215.8	8207.0	13.00	13.00
	7.07765	8026	550.	184.8	38585.0	9.00	9.00
	5.67942	8028	600.	235.1	234.0	45.00	45.00
	5.67942	8032	600.	213.7	435.0	41.00	41.00

Table A5. (Continued)

ANN/0.5/1000/WQ
(CONTINUED)

PRODUCT FORM	HEAT NUMBER	SPECIMEN NUMBER	TEMP (C)	STRESS (MPA)	RUPTURE LIFE (HR)	ELONG (%)	RED IN AREA (%)
16.0MM BAR	5.67942	8036	600.	197.9	521.0	46.00	45.00
	5.67942	8040	600.	182.0	806.0	40.00	41.00
	5.67942	8044	600.	166.2	2073.0	28.00	29.00
	5.67943	8029	600.	235.1	237.0	50.00	48.00
	5.67943	8033	600.	213.7	455.0	42.00	42.00
	5.67943	8037	600.	197.9	666.0	42.00	41.00
	5.67943	8041	600.	182.0	969.0	40.00	42.00
	5.67943	8045	600.	166.2	1669.0	34.00	36.00
	5.70037	8031	600.	235.1	283.0	63.00	60.00
	5.70037	8035	600.	213.7	680.0	56.00	53.00
	5.70037	8039	600.	197.9	956.0	54.00	51.00
	5.70037	8043	600.	182.0	1271.0	50.00	48.00
	5.70037	8047	600.	166.2	3676.0	29.00	37.00
	7.07765	8030	600.	235.1	147.0	49.00	45.00
	7.07765	8034	600.	213.7	369.0	44.00	47.00
	7.07765	8038	600.	197.9	475.0	44.00	41.00
	7.07765	8042	600.	182.0	595.0	44.00	43.00
	7.07765	8046	600.	166.2	1185.0	41.00	40.00

Table A5. (Continued)

ANN/0.5/1140/WQ

PRODUCT FORM	HEAT NUMBER	SPECIMEN NUMBER	TEMP (C)	STRESS (MPA)	RUPTURE LIFE (HR)	ELONG (%)	RED IN AREA (%)
16MM BAR	4.98180	10897	700.	111.7	590.0	46.00	41.00
	4.98180	10903	700.	93.8	2068.0	37.00	37.00
	4.98180	10909	700.	73.8	8424.0	28.00	33.00
	4.98180	10915	700.	64.1	26840.0	21.00	17.00

Table A5. (Continued)

ANN/0.5/1150/WQ

PRODUCT FORM	HEAT NUMBER	SPECIMEN NUMBER	TEMP (C)	STRESS (MPA)	RUPTURE LIFE (HR)	ELONG (%)	RED IN AREA (%)
16MM BAR	6.53438	13141	650.	150.3	439.0	40.00	36.00
	6.53438	13160	650.	124.8	1374.0	40.00	33.00
	6.53438	13179	650.	104.8	3430.0	33.00	29.00
	7.73207	13140	650.	150.3	532.0	40.00	40.00
	7.73207	13159	650.	124.8	1795.0	39.00	33.00
	7.73207	13178	650.	104.8	5165.0	30.00	30.00
	7.73697	12166	700.	93.8	1716.0	27.00	32.00
	7.73697	12167	700.	80.0	4606.0	22.00	23.00
	7.73697	12168	700.	68.9	8502.0	16.00	10.00
	7.73697	12196	700.	64.1	14986.0	12.00	11.00
20MM BAR	6.26772	9390	700.	122.0	432.0	47.00	51.00
	6.26772	9394	700.	104.1	1421.0	44.00	43.00
	6.26772	9398	700.	84.8	5852.0	22.00	30.00
	6.26772	9402	700.	73.8	11130.0	10.00	29.00
	6.26772	9406	700.	64.1	34411.0	21.00	17.00
25MM BAR	6.27461	11914	700.	122.0	595.0	52.00	48.00
	6.27461	11917	700.	104.1	1934.0	33.00	47.00
	6.27461	11920	700.	84.8	9013.0	15.00	21.00
	6.27461	11923	700.	73.8	19723.0	16.00	11.00

Table A5. (Continued)

ANN/0.5/1170/WQ

PRODUCT FORM	HEAT NUMBER	SPECIMEN NUMBER	TEMP (C)	STRESS (MPA)	RUPTURE LIFE (HR)	ELONG (%)	RED IN AREA (%)
16MM BAR	4.98180	12754	700.	128.3	184.0	53.00	51.00
	4.98180	10898	700.	111.7	614.0	39.00	45.00
	4.98180	12757	700.	108.9	543.0	57.00	55.00
	4.98180	12760	700.	97.9	1123.0	41.00	39.00
	4.98180	10904	700.	93.8	2293.0	36.00	28.00
	4.98180	12763	700.	88.3	2529.0	44.00	39.00
	4.98180	12766	700.	79.3	5378.0	33.00	29.00
	4.98180	10910	700.	73.8	7025.0	30.00	37.00
	4.98180	10916	700.	64.1	19467.0	18.00	17.00
	7.76211	13893	700.	90.3	3655.0	36.00	39.00
	7.76411	13891	700.	90.3	1815.0	24.00	25.00
	7.76411	13896	700.	80.0	3936.0	17.00	13.00

Table A5. (Continued)

ANN/0.50/1150/WQ

PRODUCT FORM	HEAT NUMBER	SPECIMEN NUMBER	TEMP (C)	STRESS (MPA)	RUPTURE LIFE (HR)	ELONG (%)	RED IN AREA (%)
16.0MM BAR	6.53438	13517	600.	219.9	777.0	19.00	26.00
	6.53438	13842	600.	219.9	485.0	41.00	36.00
	6.53438	13536	600.	184.8	1166.0	30.00	25.00
	6.53438	13555	600.	160.0	3101.0	20.00	19.00
	6.53438	13574	600.	140.0	7795.0	16.00	11.00
	7.73207	13516	600.	219.9	730.0	21.00	26.00
	7.73207	13535	600.	184.8	1601.0	21.00	23.00
	7.73207	13554	600.	160.0	5392.0	16.00	19.00
	7.73697	12151	600.	208.2	4650.0	11.00	12.00
	7.73697	12152	600.	186.8	10419.0	8.00	10.00

Table A5. (Continued)

ANN/0.67/1090/AC

PRODUCT FORM	HEAT NUMBER	SPECIMEN NUMBER	TEMP (C)	STRESS (MPA)	RUPTURE LIFE (HR)	ELONG (%)	RED IN AREA (%)
38MMOD X 6MMWT TUBE	7.54802	7871	700.	111.7	251.0	58.00	58.00
	7.54802	7872	700.	93.1	739.0	50.00	52.00
	7.54802	7873	700.	84.8	1081.0	56.00	52.00
	7.54802	7874	700.	73.8	2610.0	36.00	40.00
	7.54802	7875	700.	64.1	6622.0	19.00	28.00

Table A5. (Continued)

ANN/2.0/1140/WQ

PRODUCT FORM	HEAT NUMBER	SPECIMEN NUMBER	TEMP (C)	STRESS (MPA)	RUPTURE LIFE (HR)	ELONG (%)	RED IN AREA (%)
16MM BAR	4.98180	10899	700.	111.7	608.0	50.00	48.00
	4.98180	10905	700.	93.8	2087.0	34.00	39.00
	4.98180	10911	700.	73.8	8784.0	24.00	30.00
	4.98180	10917	700.	64.1	26859.0	20.00	21.00

ANN/2.0/1170/WQ

16MM BAR	4.98180	10900	700.	111.7	523.0	46.00	48.00
	4.98180	10906	700.	93.8	1816.0	37.00	36.00
	4.98180	10912	700.	73.8	7283.0	31.00	30.00
	4.98180	10918	700.	64.1	14013.0	18.00	21.00

APPENDIX B

APPENDIX B

The points in the following plots represent available experimental creep data. The solid lines were predicted by the present equation; the dashed lines were predicted by the Sterling equation.

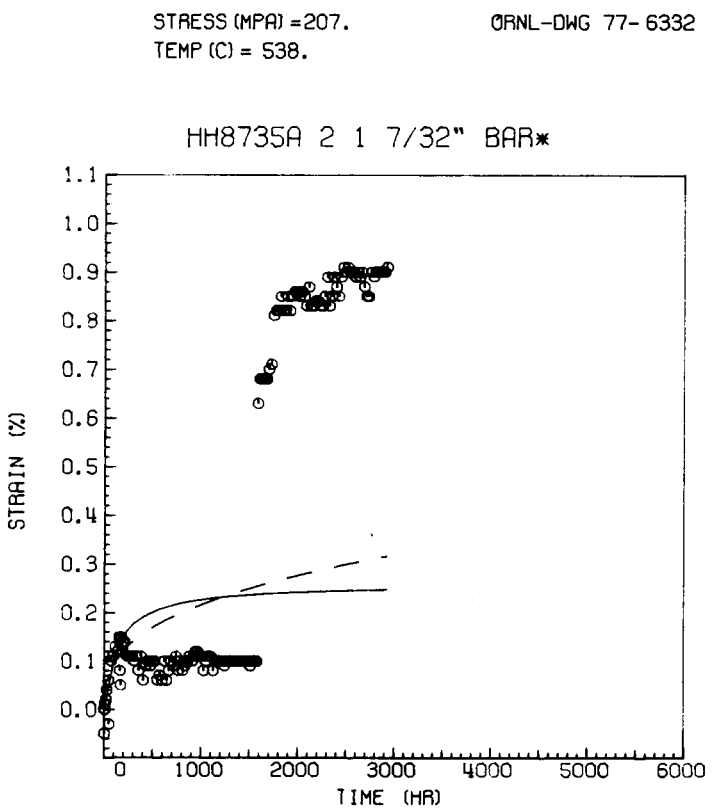

STRESS (MPA) = 138.
TEMP (C) = 649.

ORNL-DWG 77-6327

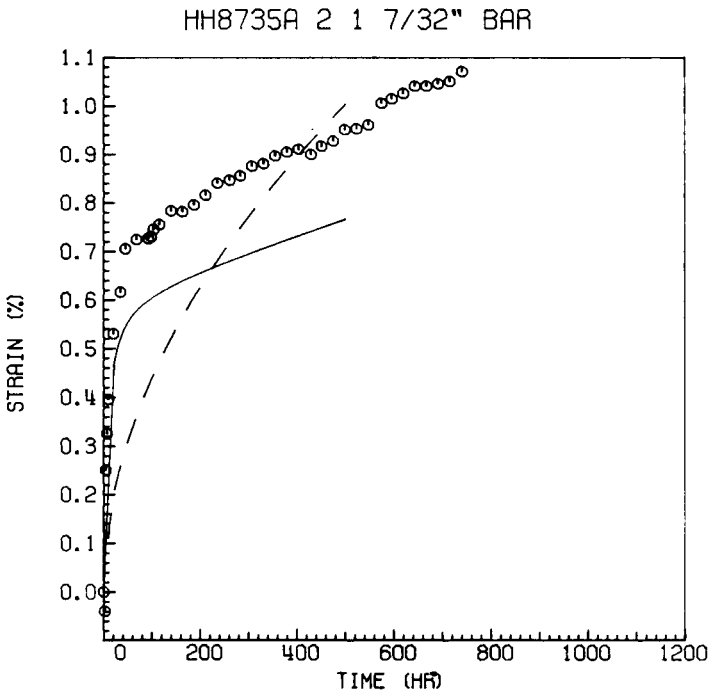

STRESS (MPA) = 55.
TEMP (C) = 704.

ORNL-DWG 77-6331

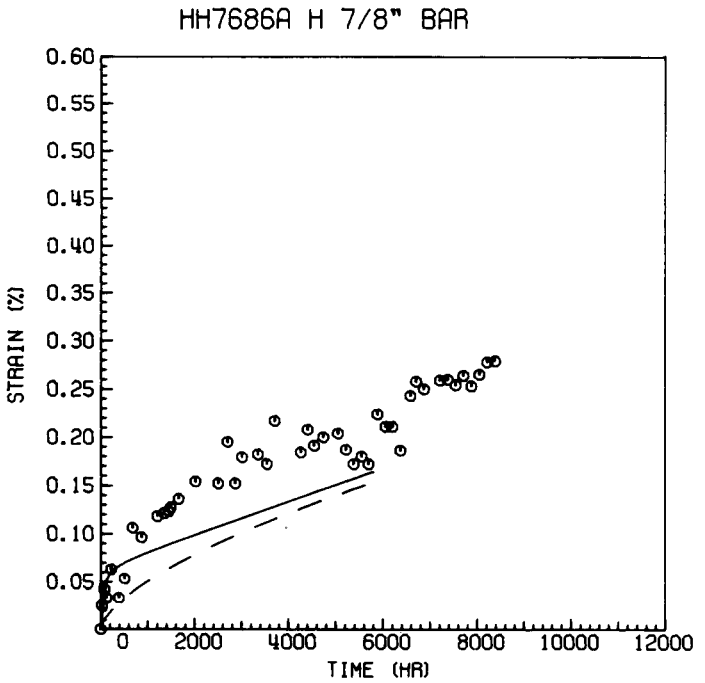

STRESS (MPA) = 41.
TEMP (C) = 704.

ORNL-DWG 77-6330

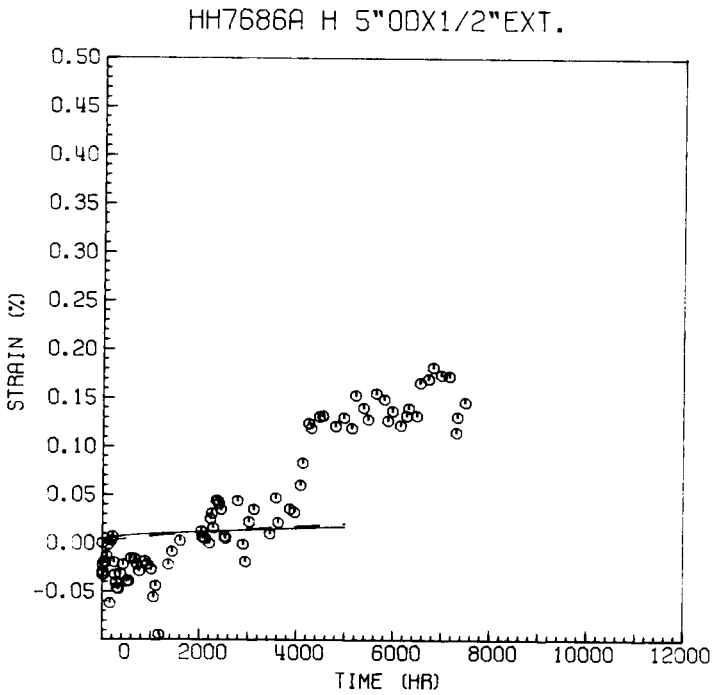

STRESS (MPA) =207.
TEMP (C) = 649.

ORNL-DWG 77-6328

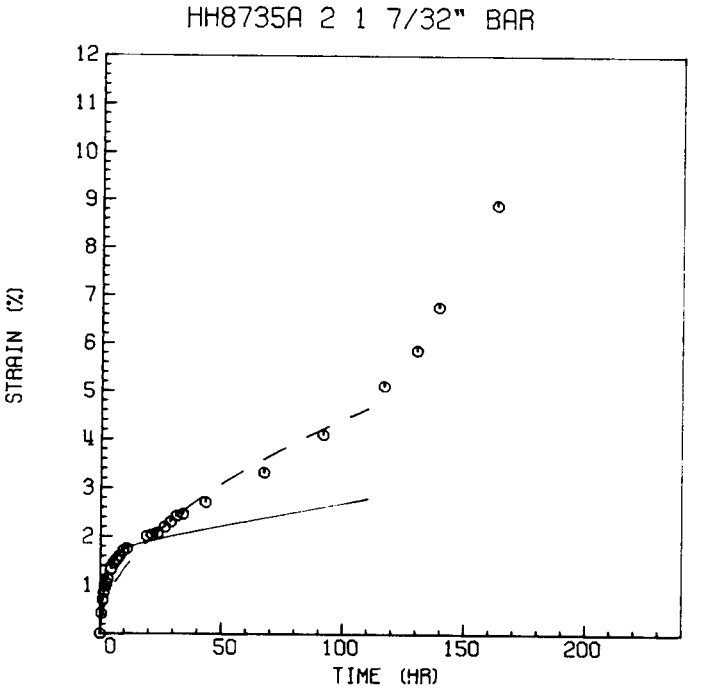

STRESS (MPA) = 103.
TEMP (C) = 649.

ORNL-DWG 77-6329

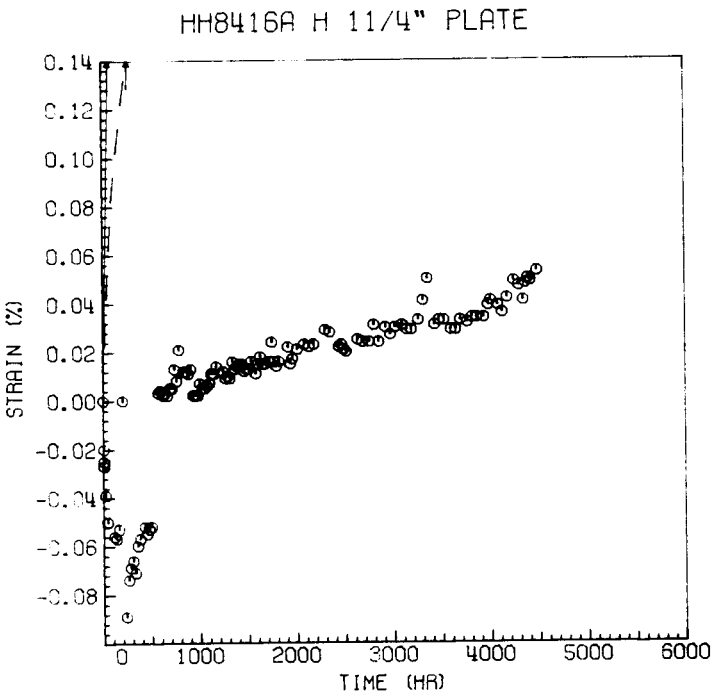

STRESS (MPA) = 241.
TEMP (C) = 593.

ORNL-DWG 77-6324

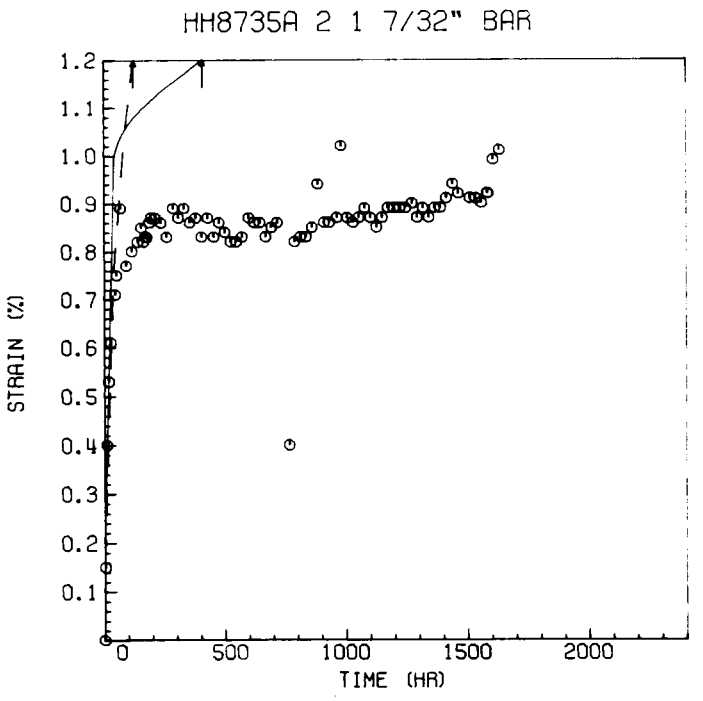

STRESS (MPA) =207.
TEMP (C) = 593.

ORNL-DWG 77-6323

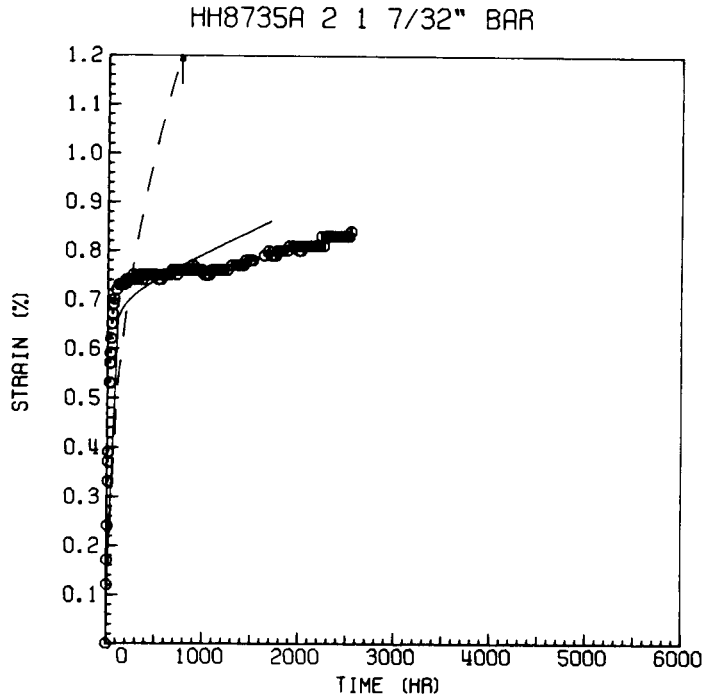

STRESS (MPA) =241.
TEMP (C) = 649.

ORNL-DWG 77-6325

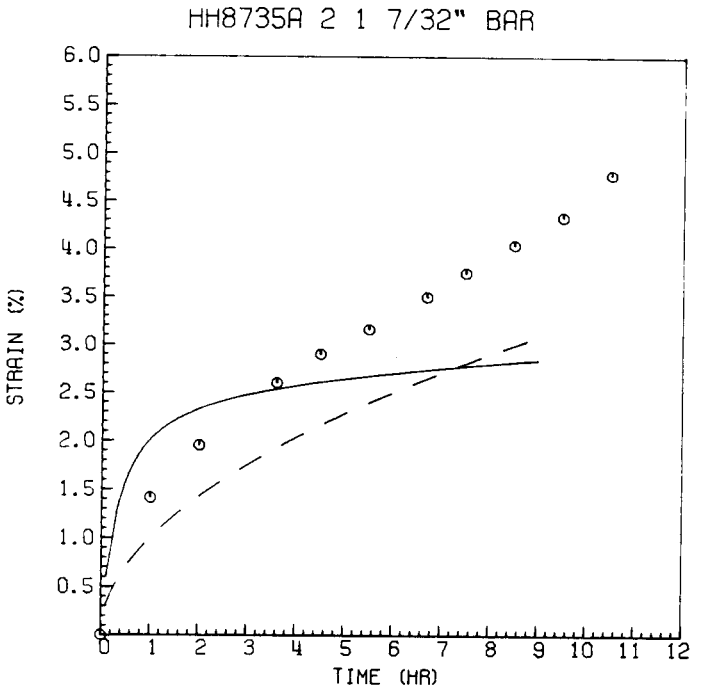

STRESS (MPA) = 172.
TEMP (C) = 649.

ORNL-DWG 77-6326

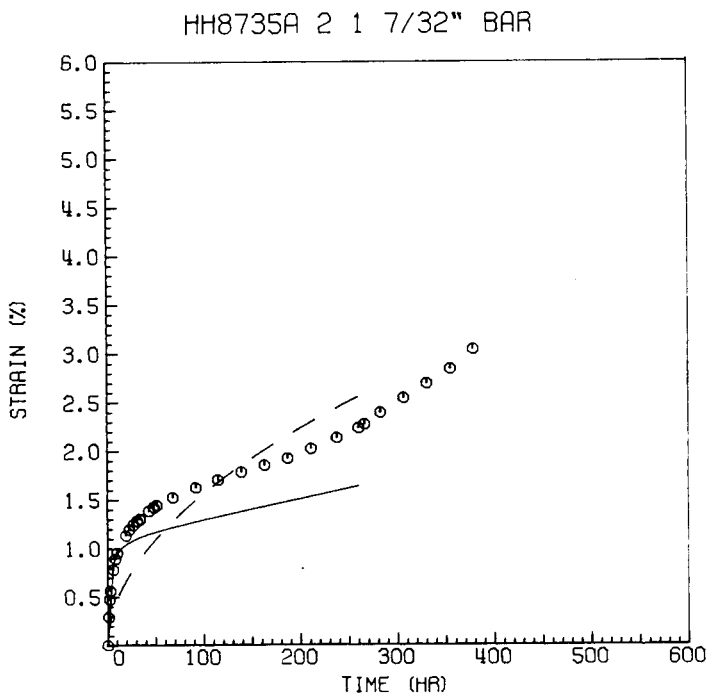

STRESS (MPA) = 345.
TEMP (C) = 538.

ORNL-DWG 77-6321

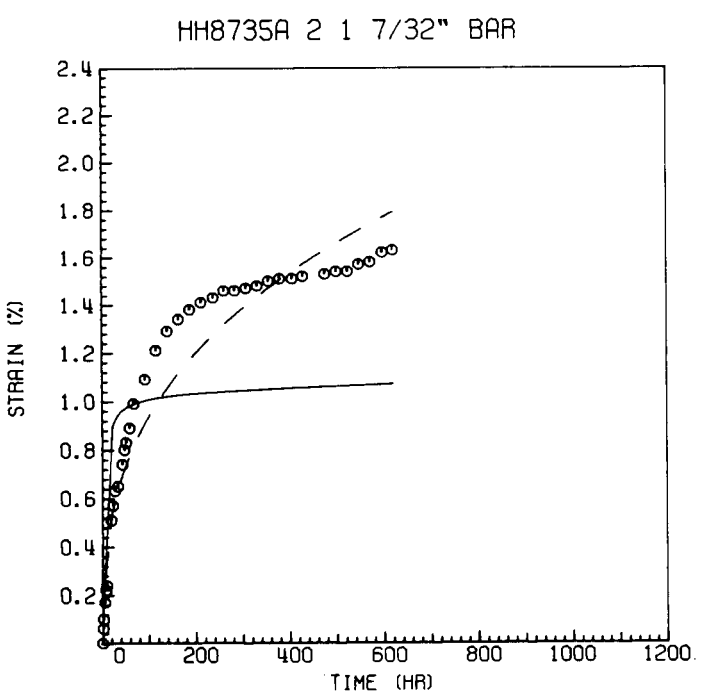

STRESS (MPA) =310. ORNL-DWG 77- 6322
TEMP (C) = 593.

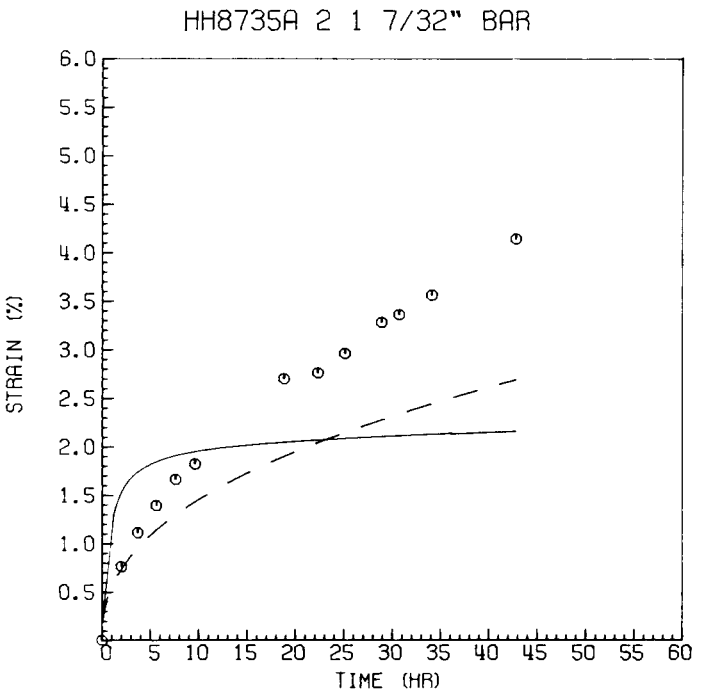

STRESS (MPA) = 83. ORNL-DWG 77- 6319
TEMP (C) = 760.

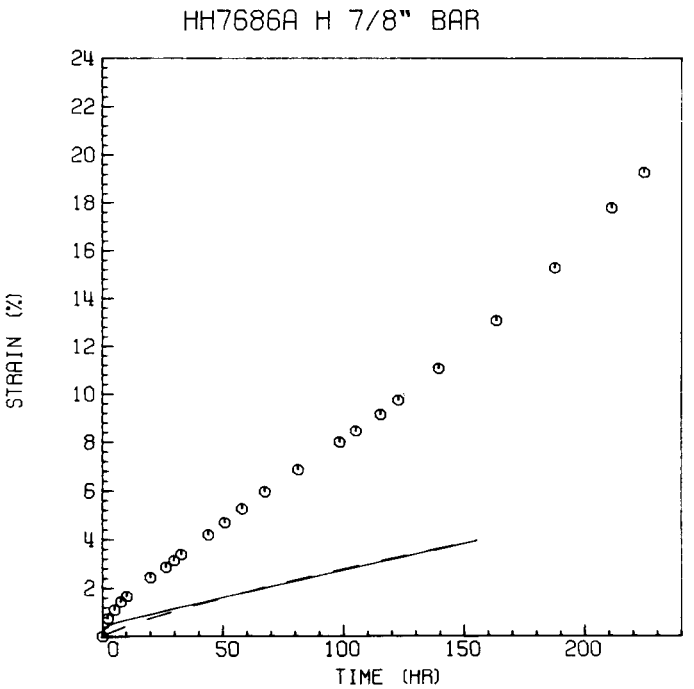

STRESS (MPA) = 34.
TEMP (C) = 760.

ORNL-DWG 77-6318

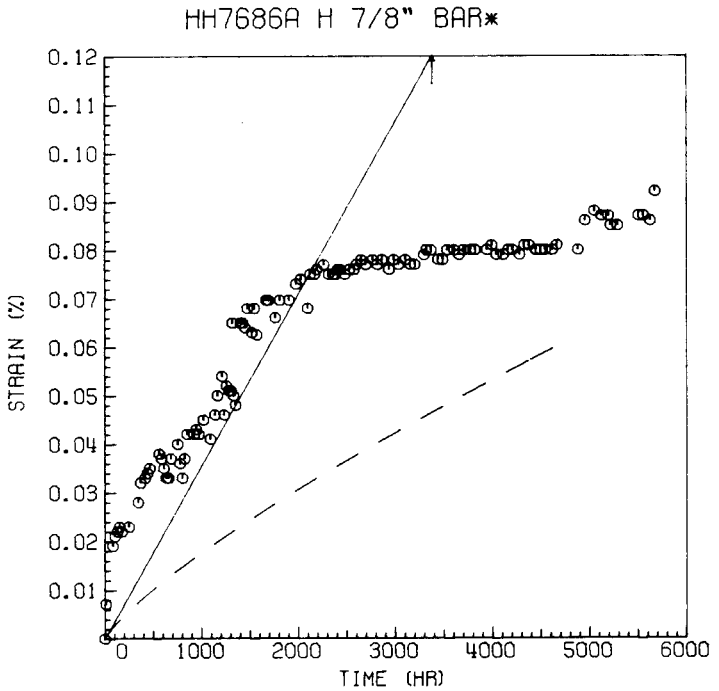

STRESS (MPA) = 62.
TEMP (C) = 760.

ORNL-DWG 77-6317

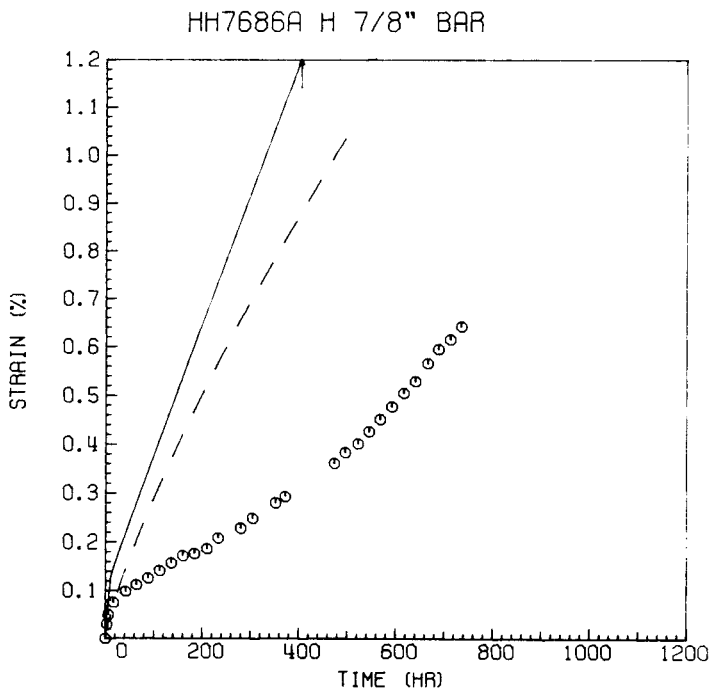

STRESS (MPA) =310.
TEMP (C) = 538.

ORNL-DWG 77- 6320

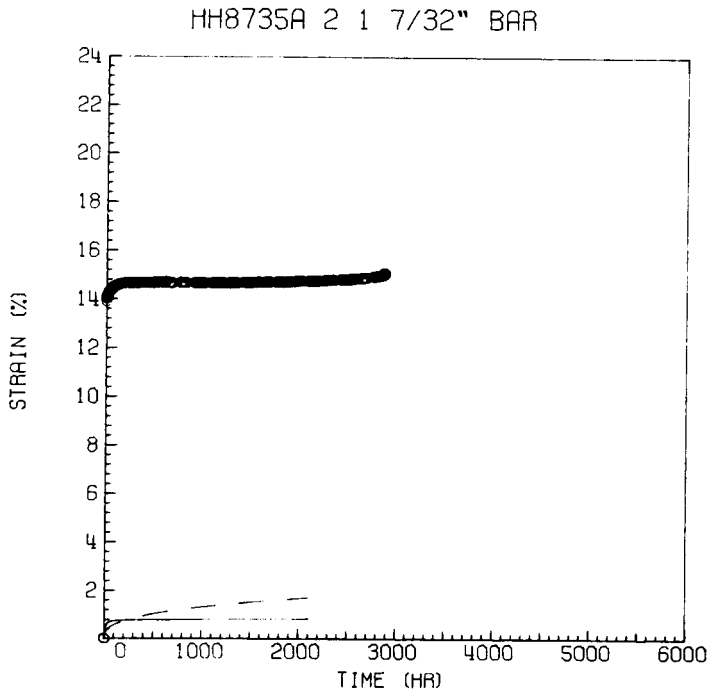

STRESS (MPA) = 55.
TEMP (C) = 760.

ORNL-DWG 77- 6316

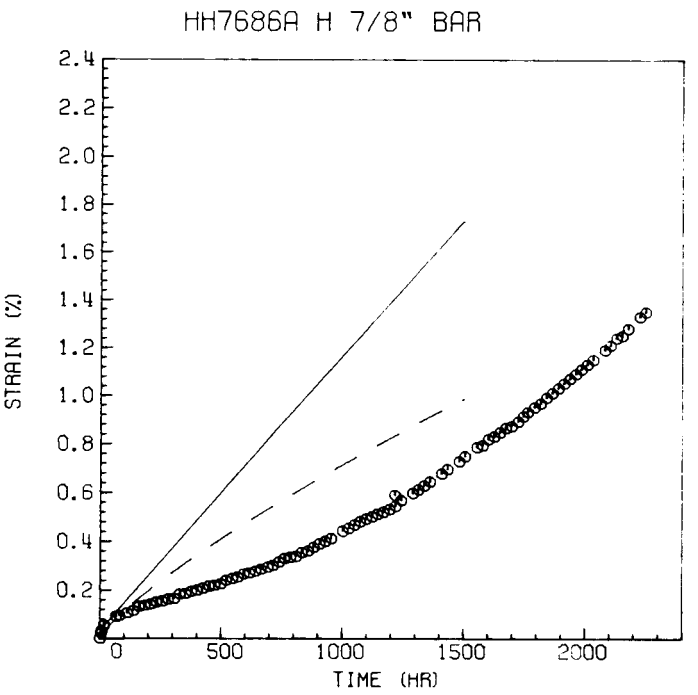

STRESS (MPA) = 90.
TEMP (C) = 704.

ORNL-DWG 77-6315

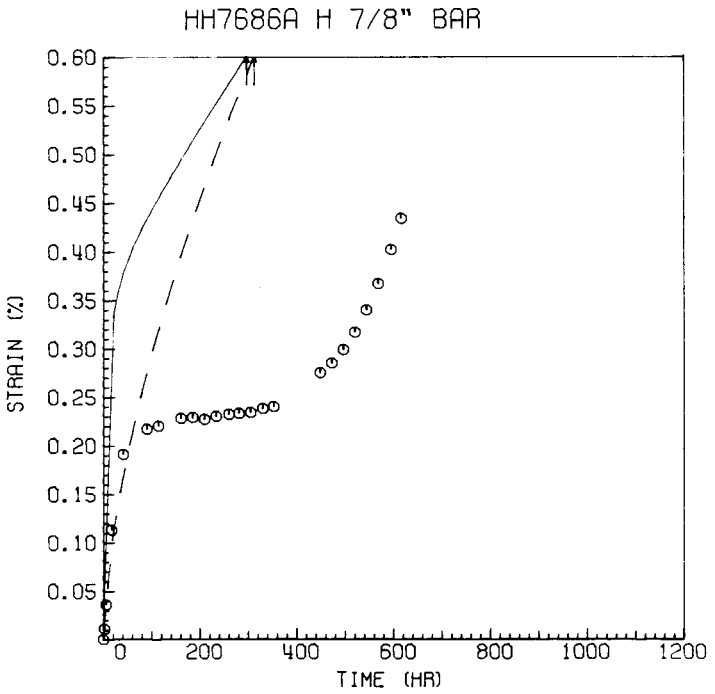

STRESS (MPA) =207.
TEMP (C) = 649.

ORNL-DWG 77-6314

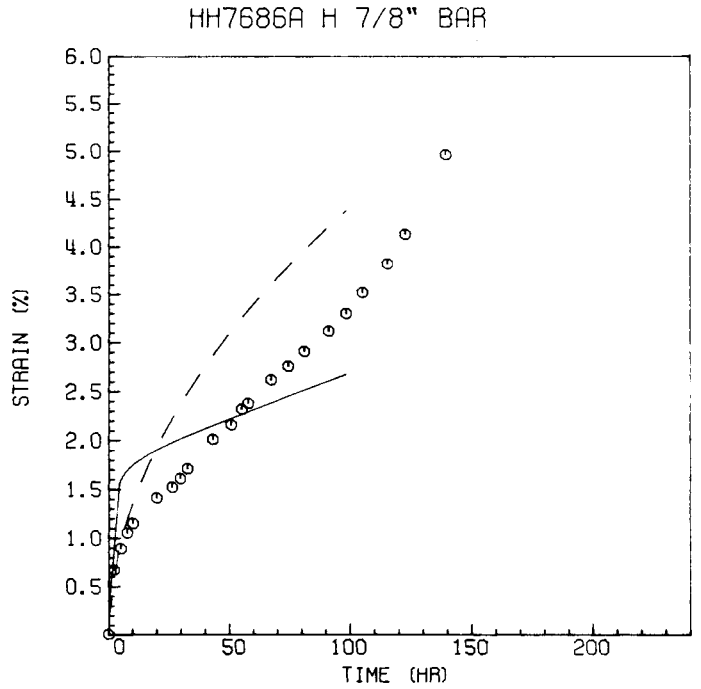

ORNL-DWG 77-6351

STRESS (MPA) = 103.
TEMP (C) = 649.

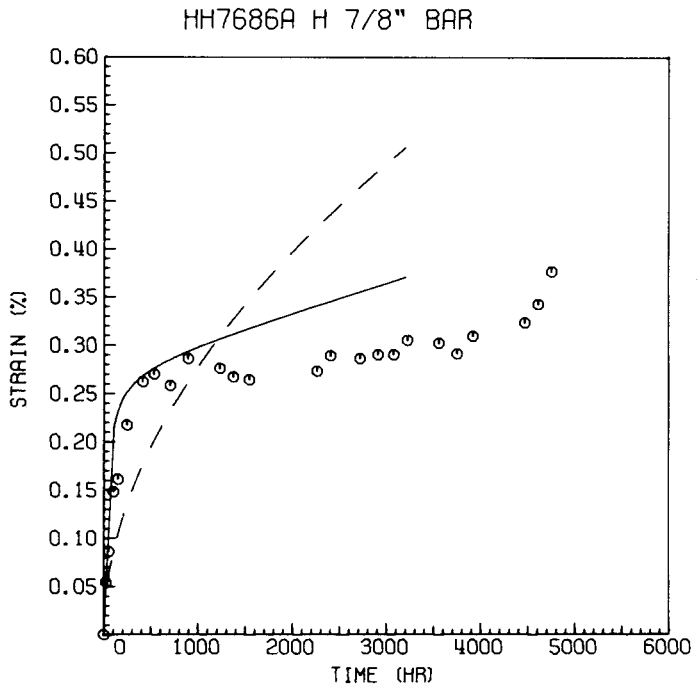

ORNL-DWG 77-6350

STRESS (MPA) = 145.
TEMP (C) = 649.

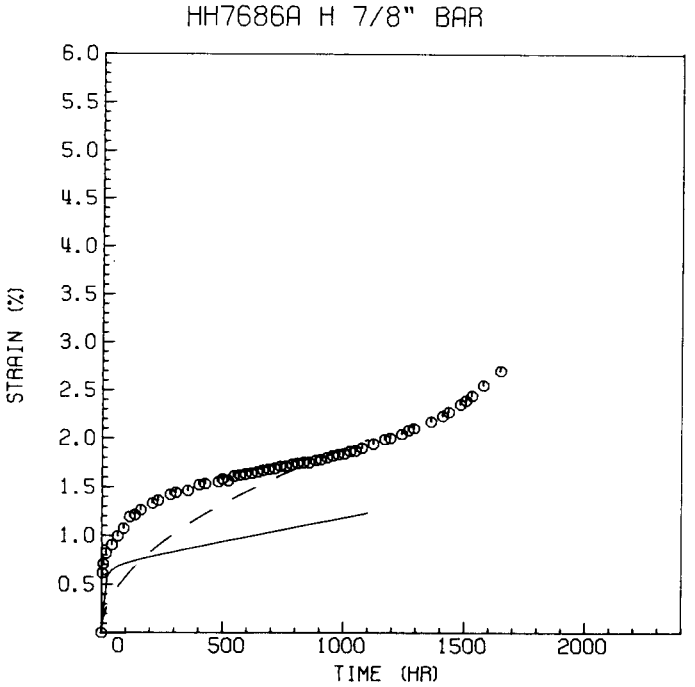

ORNL-DWG 77-6349

STRESS (MPA) = 124.
TEMP (C) = 649.

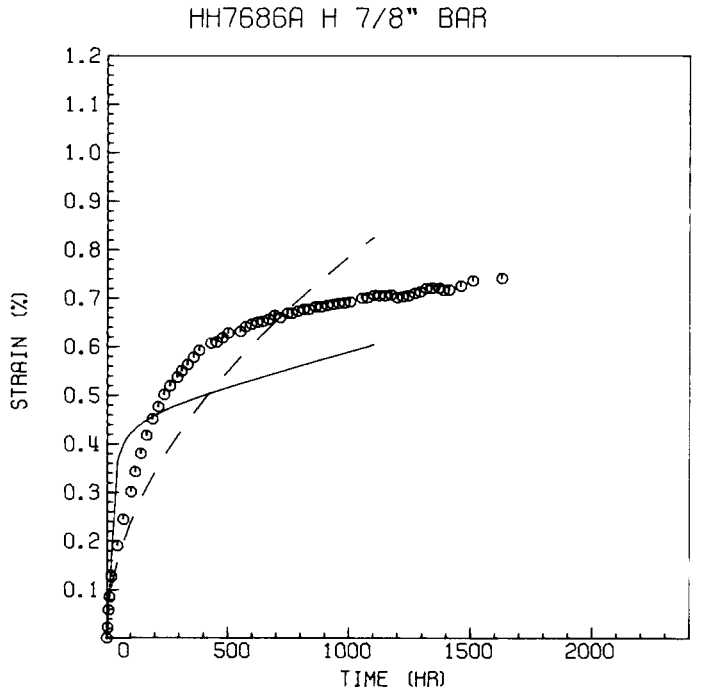

ORNL-DWG 77-6348

STRESS (MPA) = 55.
TEMP (C) = 760.

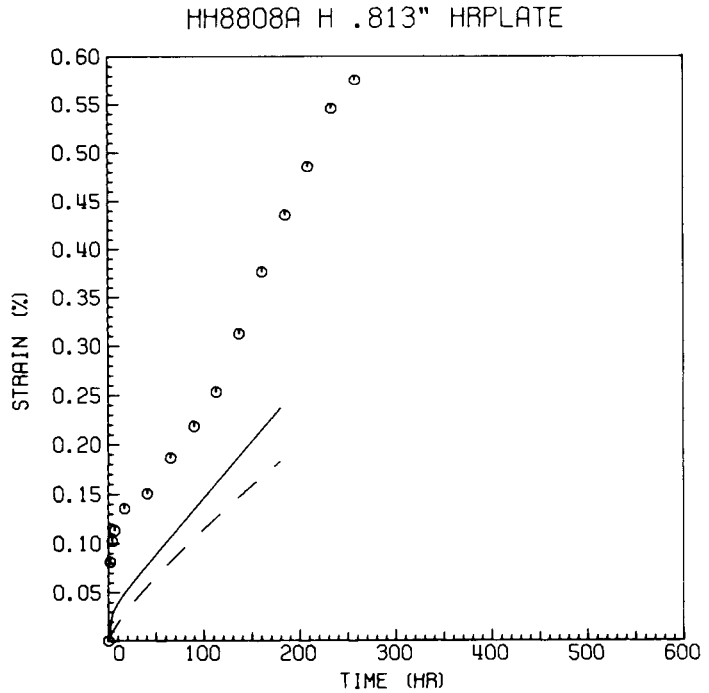

ORNL-DWG 77-6347

STRESS (MPA) = 48.
TEMP (C) = 760.

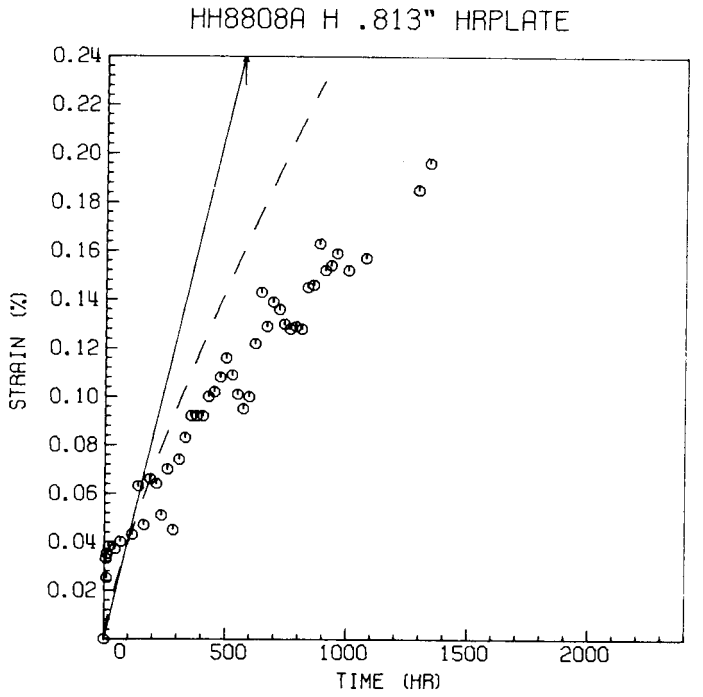

ORNL-DWG 77-6346

STRESS (MPA) = 69.
TEMP (C) = 760.

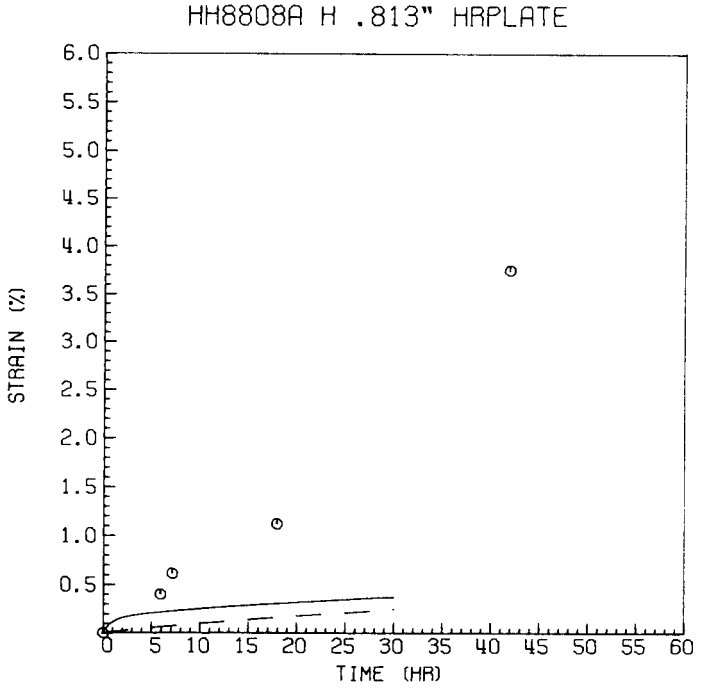

ORNL-DWG 77-6345

STRESS (MPA) = 83.
TEMP (C) = 704.

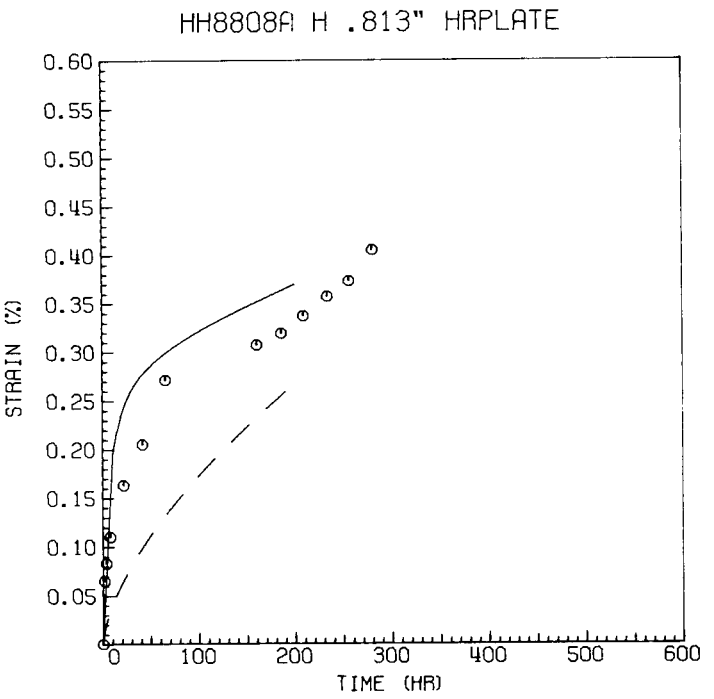

ORNL-DWG 77-6344

STRESS (MPA) = 110.
TEMP (C) = 704.

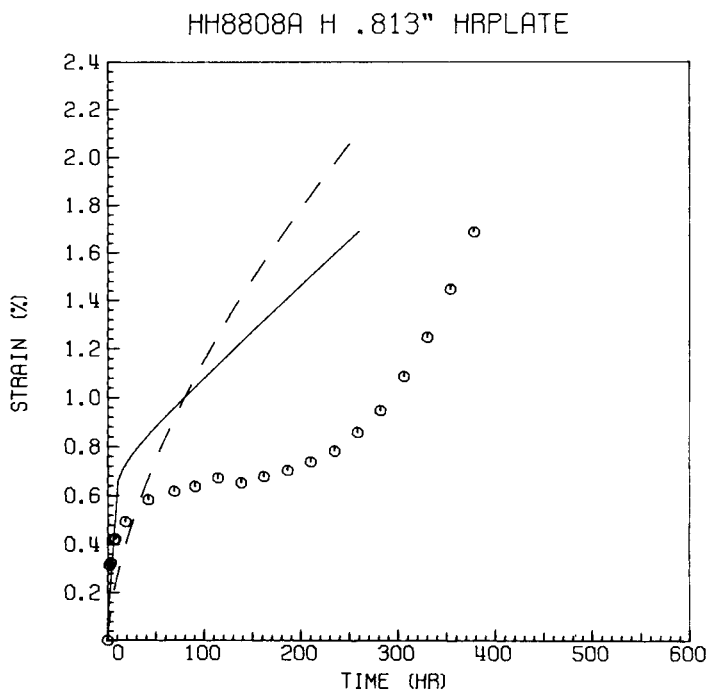

ORNL-DWG 77-6343

STRESS (MPA) = 152.
TEMP (C) = 704.

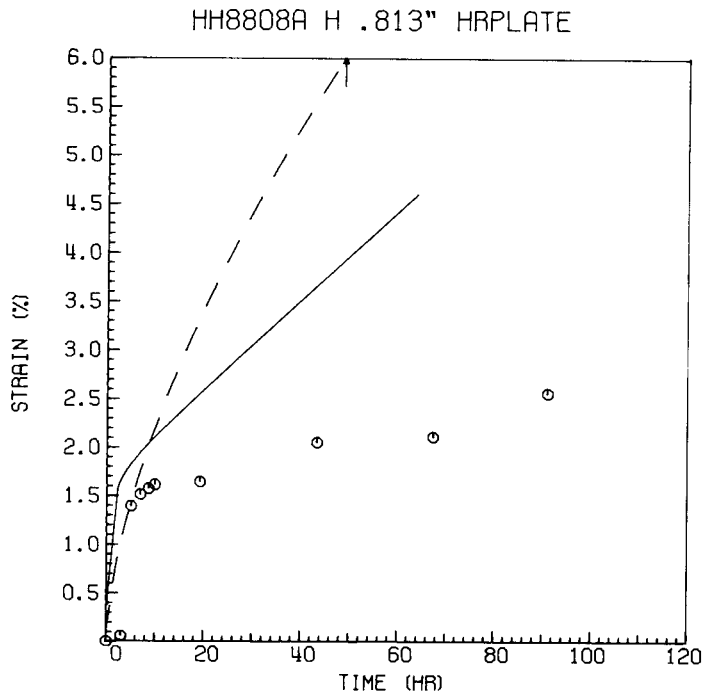

ORNL-DWG 77-6342

STRESS (MPA) = 165.
TEMP (C) = 649.

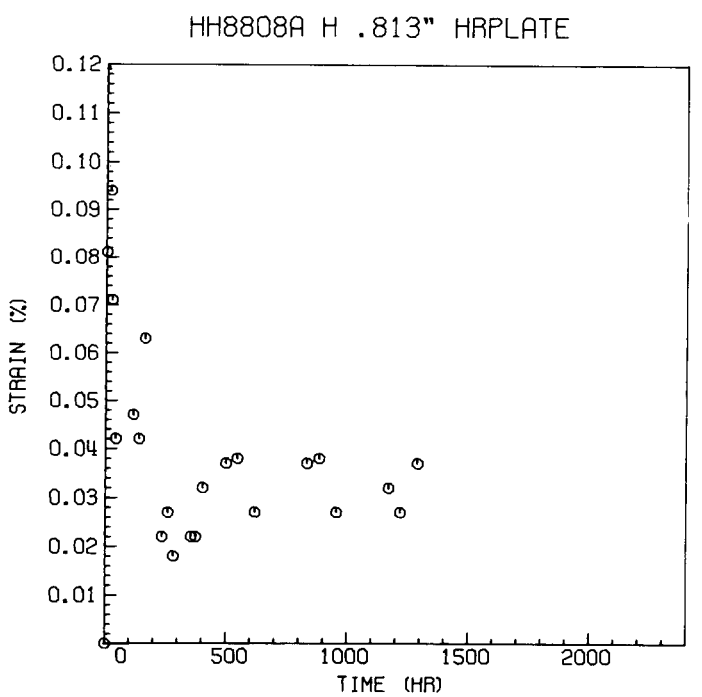

ORNL-DWG 77-6341

STRESS (MPA) = 69.
TEMP (C) = 760.

HH8735A 2 1 7/32" BAR

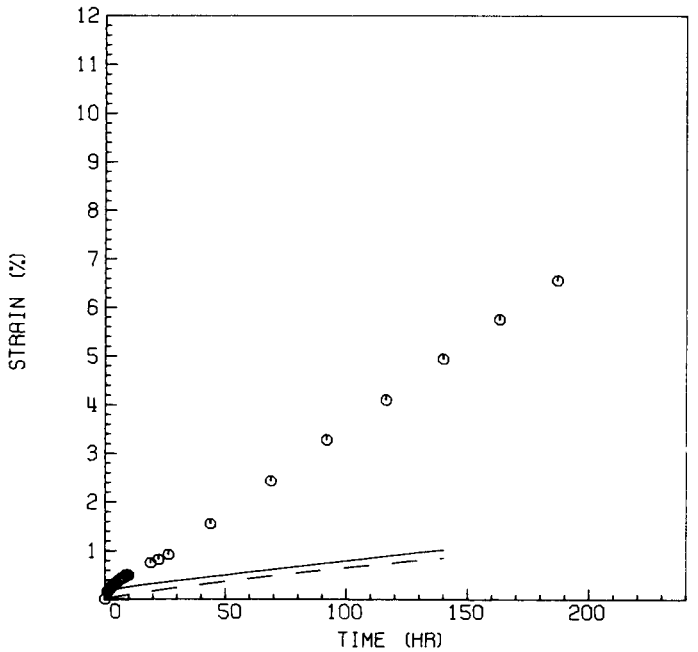

ORNL-DWG 77-6340

STRESS (MPA) = 90.
TEMP (C) = 760.

HH8735A 2 1 7/32" BAR

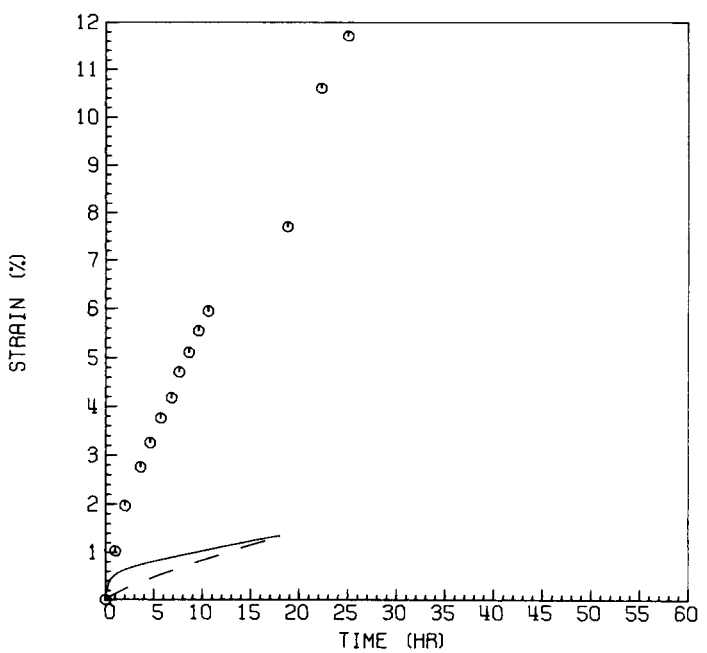

ORNL-DWG 77-6339

STRESS (MPA) = 28.
TEMP (C) = 760.

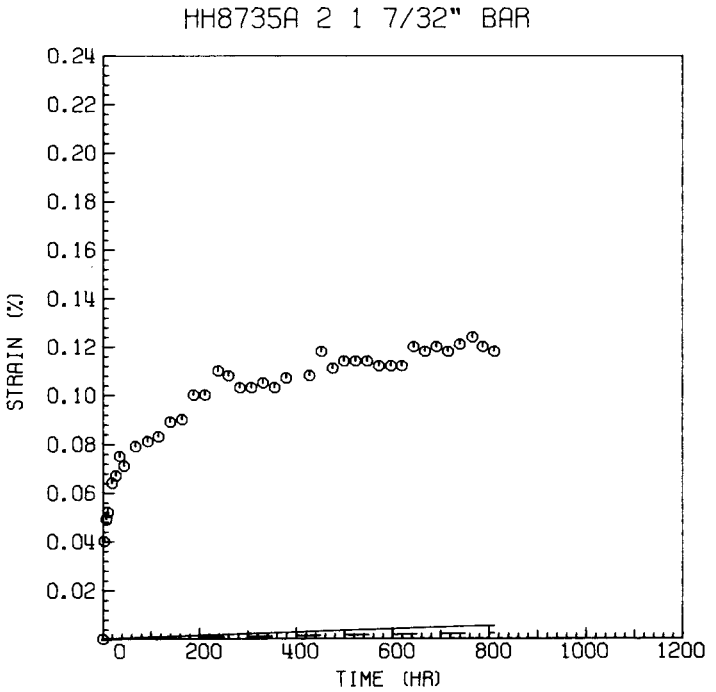

ORNL-DWG 77-6338

STRESS (MPA) = 55.
TEMP (C) = 760.

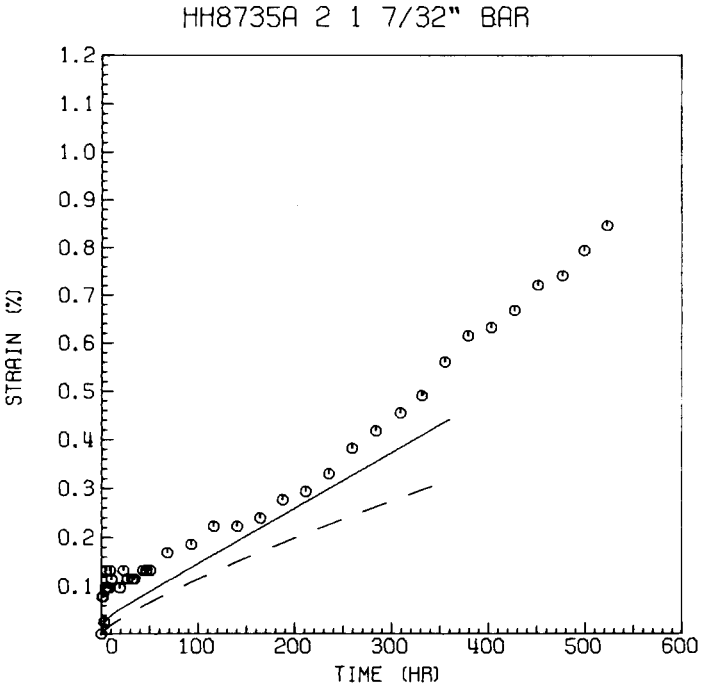

ORNL-DWG 77-6337

STRESS (MPA) = 41.
TEMP (C) = 760.

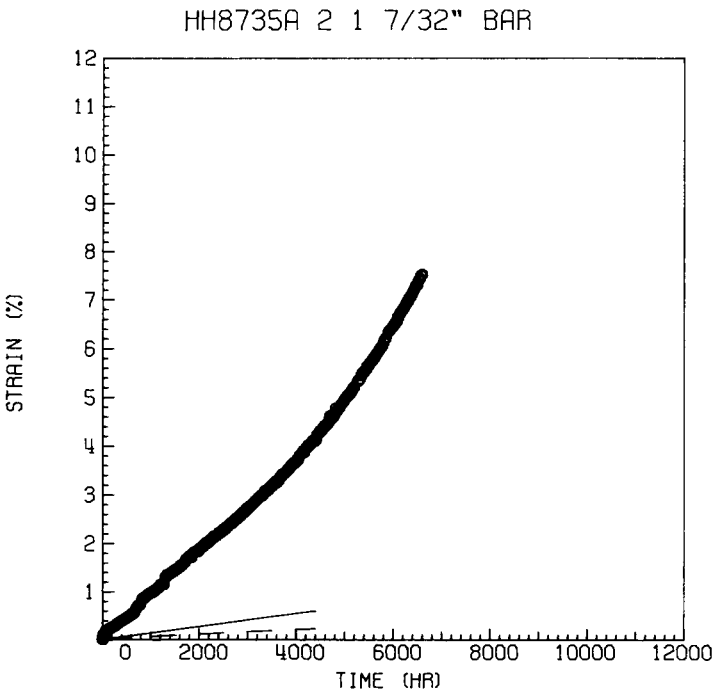

ORNL-DWG 77-6336

STRESS (MPA) = 90.
TEMP (C) = 704.

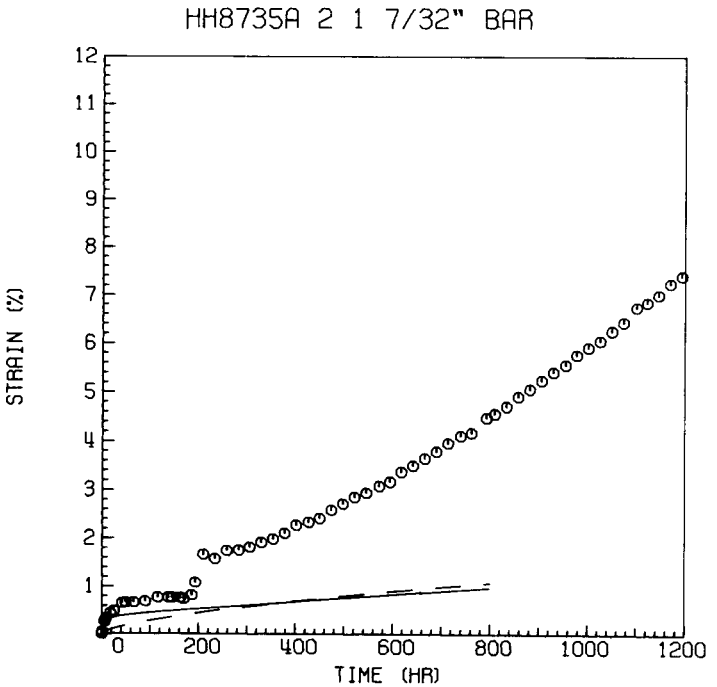

ORNL-DWG 77-6335

STRESS (MPA) = 55.
TEMP (C) = 704.

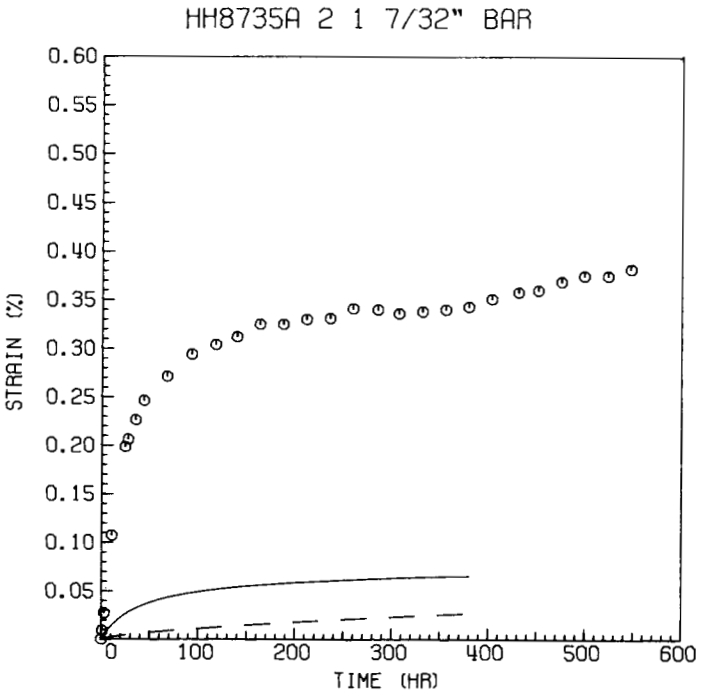

ORNL-DWG 77-6334

STRESS (MPA) = 69.
TEMP (C) = 649.

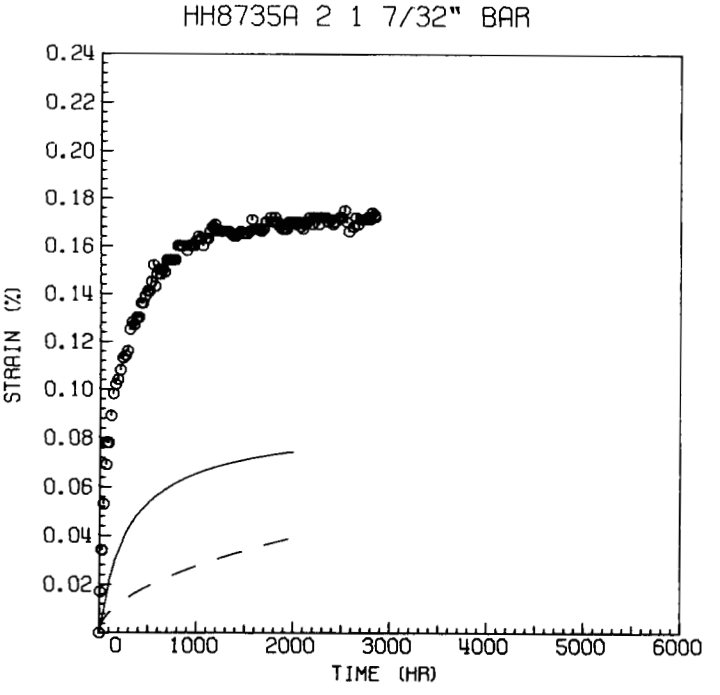

ORNL-DWG 77-6333

STRESS (MPA) = 117.
TEMP (C) = 649.

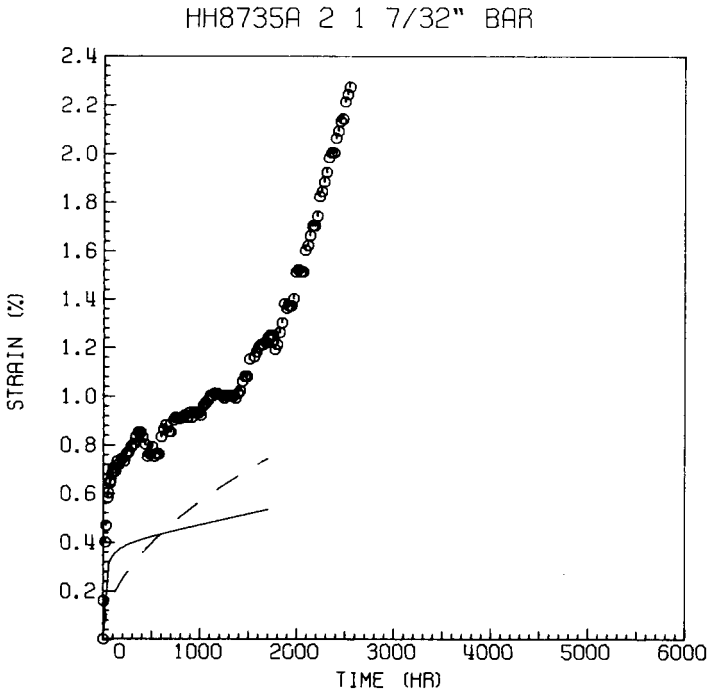

ORNL-DWG 77-6352

STRESS (MPA) = 179.
TEMP (C) = 649.

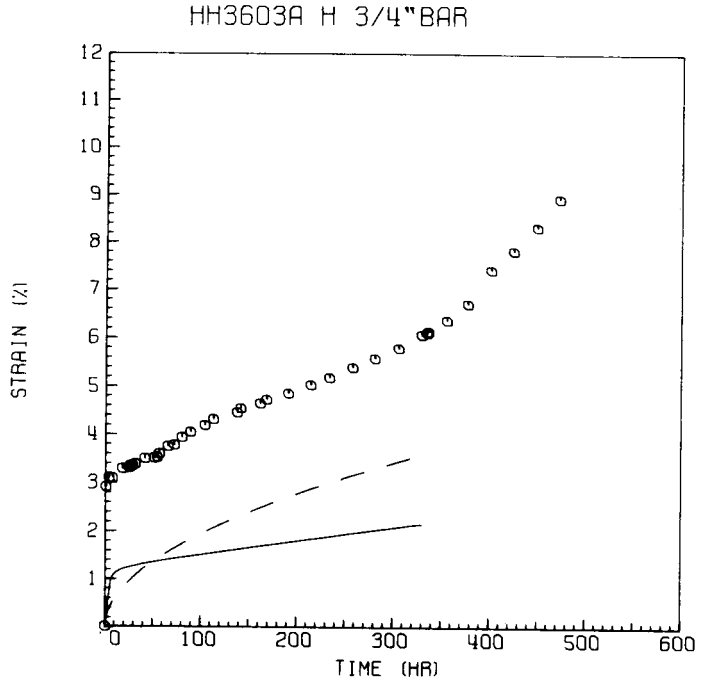

ORNL-DWG 77-6353

STRESS (MPA) = 138.
TEMP (C) = 649.

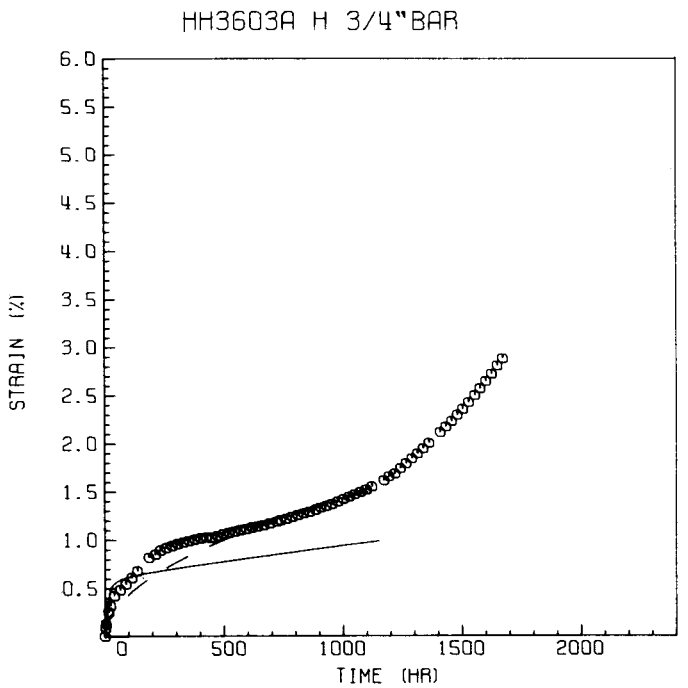

ORNL-DWG 77-6354

STRESS (MPA) = 124.
TEMP (C) = 649.

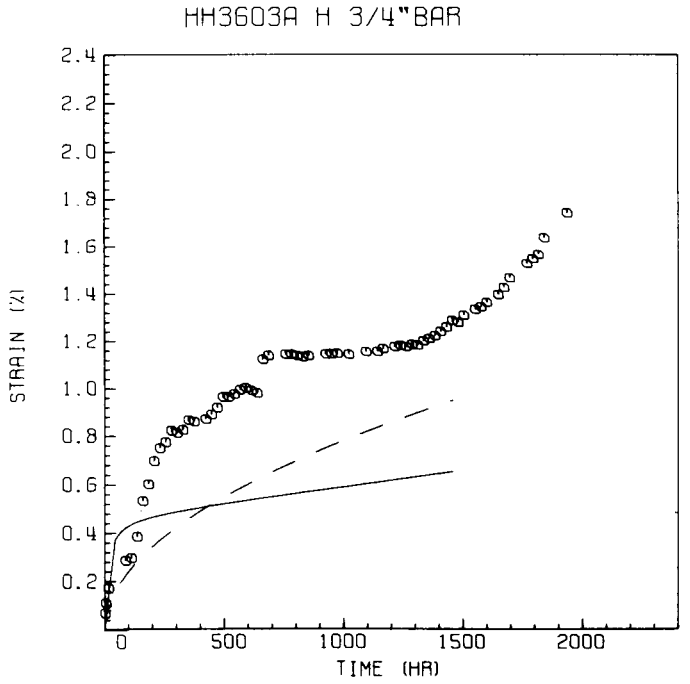

ORNL-DWG 77-6355

STRESS (MPA) = 124.
TEMP (C) = 649.

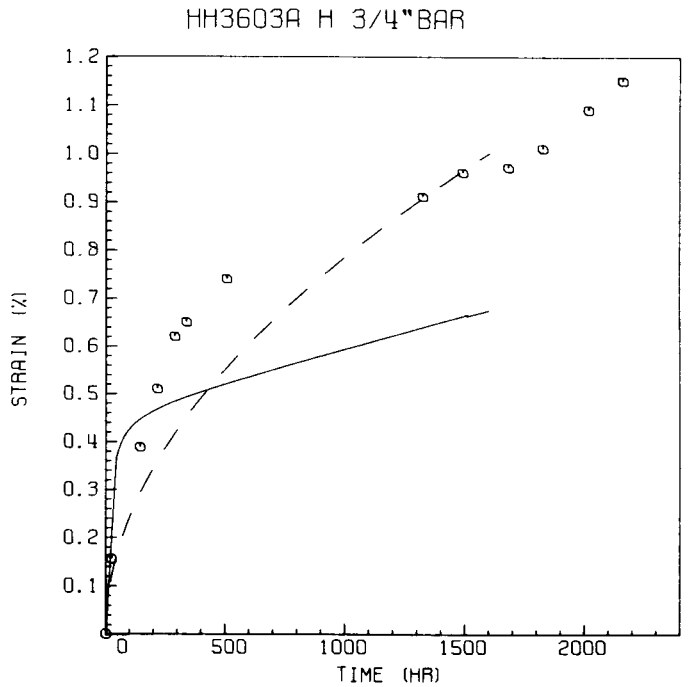

ORNL-DWG 77-6356

STRESS (MPA) = 83.
TEMP (C) = 649.

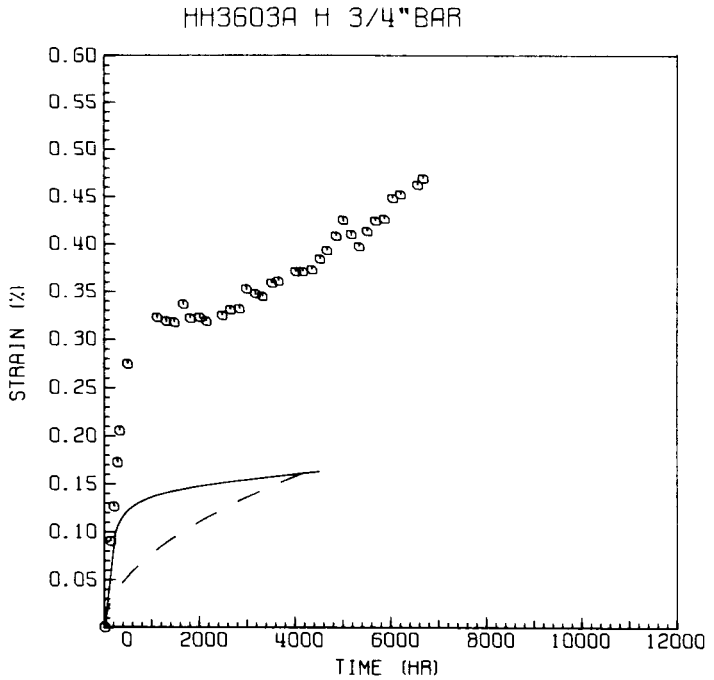

ORNL-DWG 77-6357

STRESS (MPA) = 124.
TEMP (C) = 704

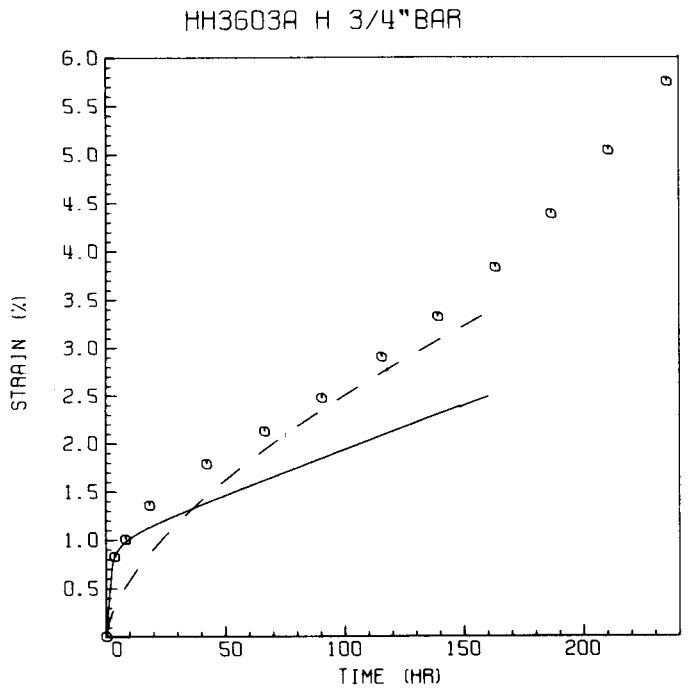

ORNL-DWG 77-6358

STRESS (MPA) = 69.
TEMP (C) = 704.

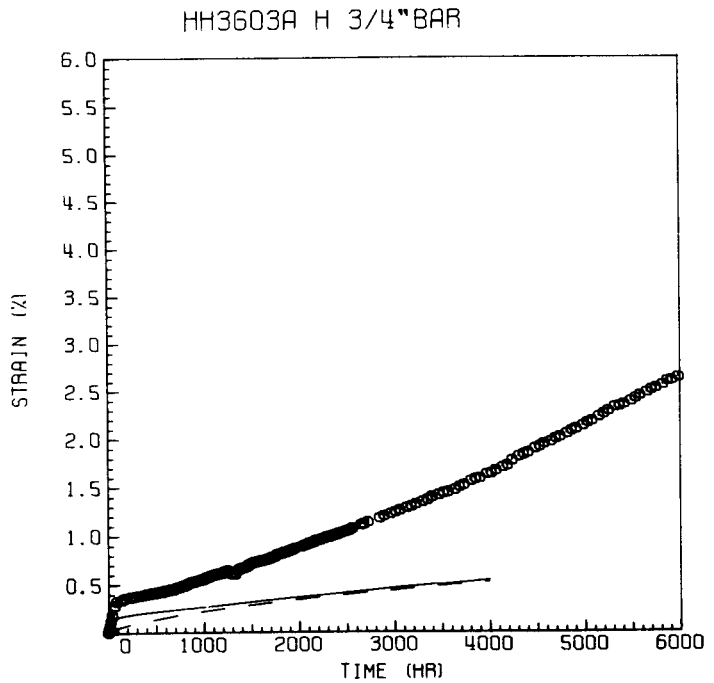

ORNL-DWG 77-6359

STRESS (MPA) = 48.
TEMP (C) = 760.

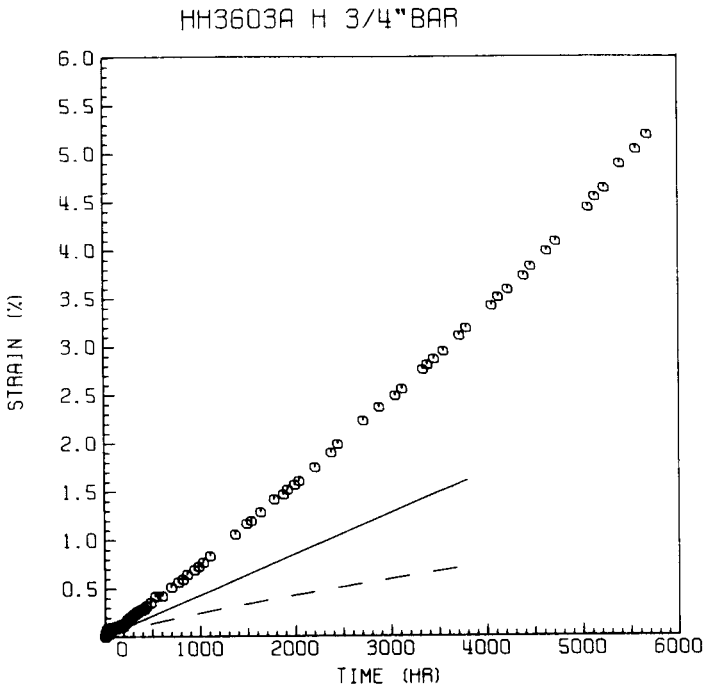

ORNL-DWG 77-6360

STRESS (MPA) = 69.
TEMP (C) = 760.

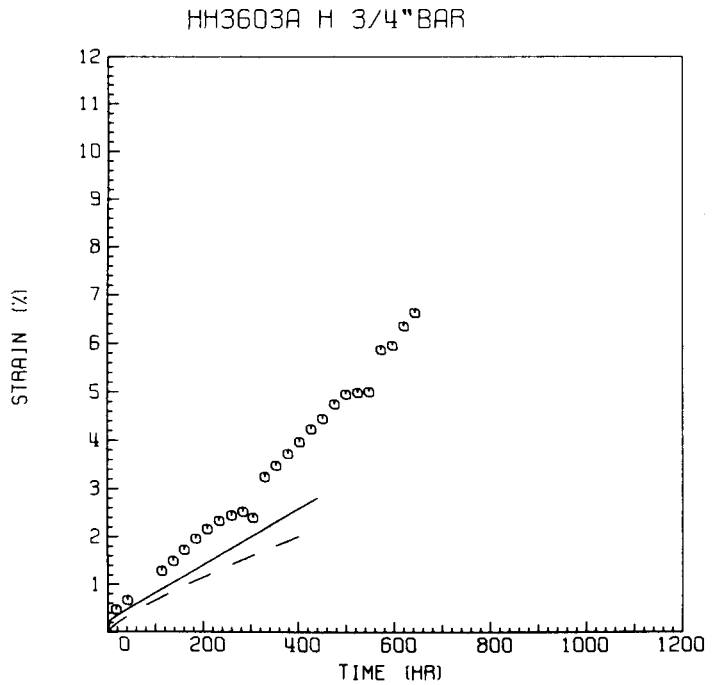

ORNL-DWG 77-6361

STRESS (MPA) = 28.
TEMP (C) = 760.

HH3603A H 3/4"BAR

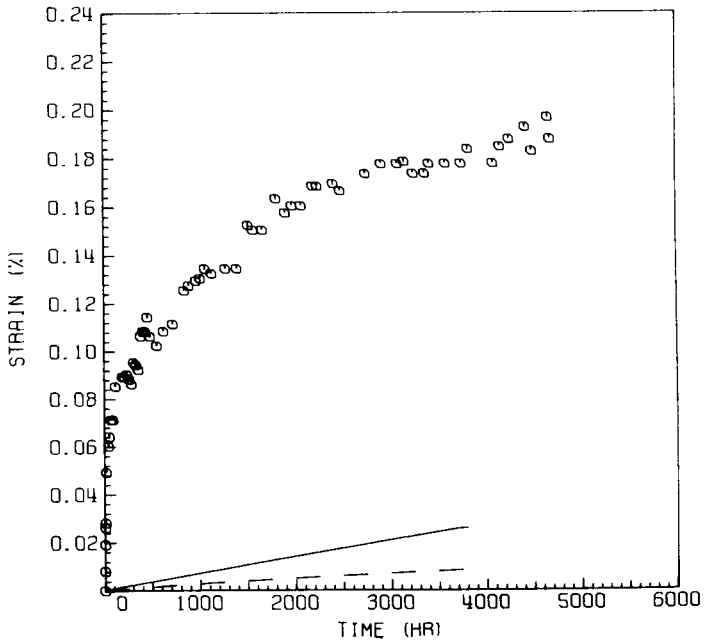

ORNL-DWG 77-6362

STRESS (MPA) = 310.
TEMP (C) = 593.

HH8808A H .813" HRPLATE

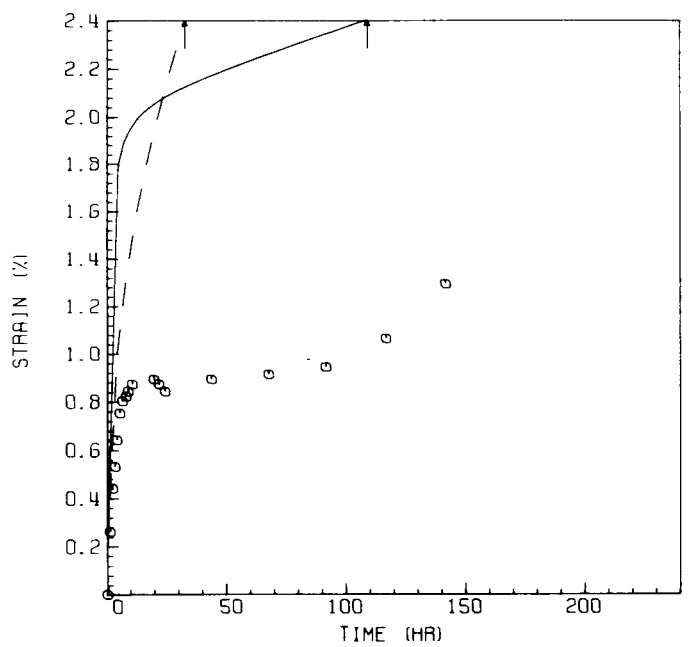

ORNL-DWG 77-6363

STRESS (MPA) = 310.
TEMP (C) = 593.

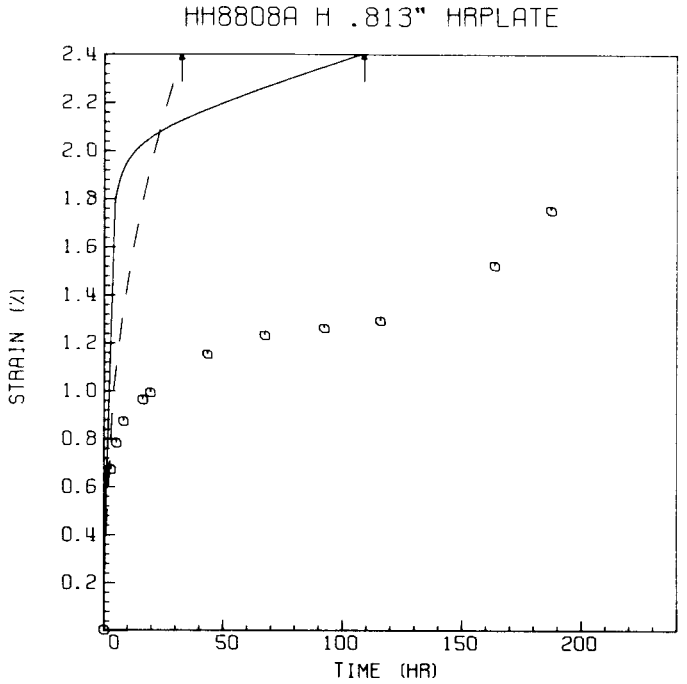

ORNL-DWG 77-6364

STRESS (MPA) = 179.
TEMP (C) = 649.

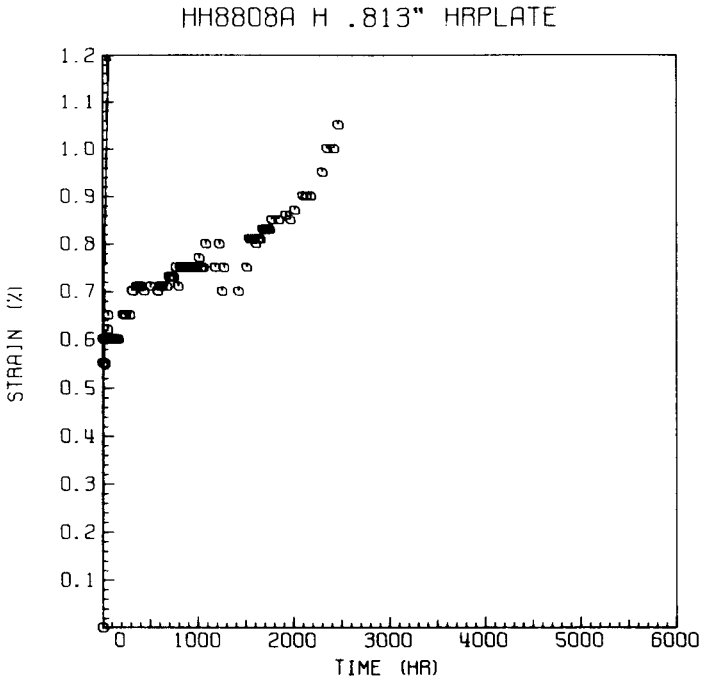

ORNL-DWG 77-6365

STRESS (MPA) = 207.
TEMP (C) = 649.

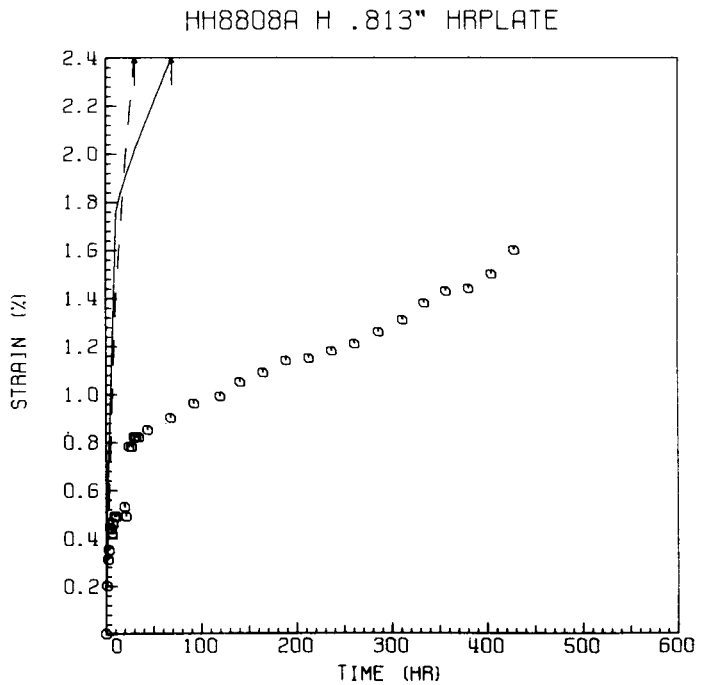

ORNL-DWG 77-6366

STRESS (MPA) = 207.
TEMP (C) = 649.

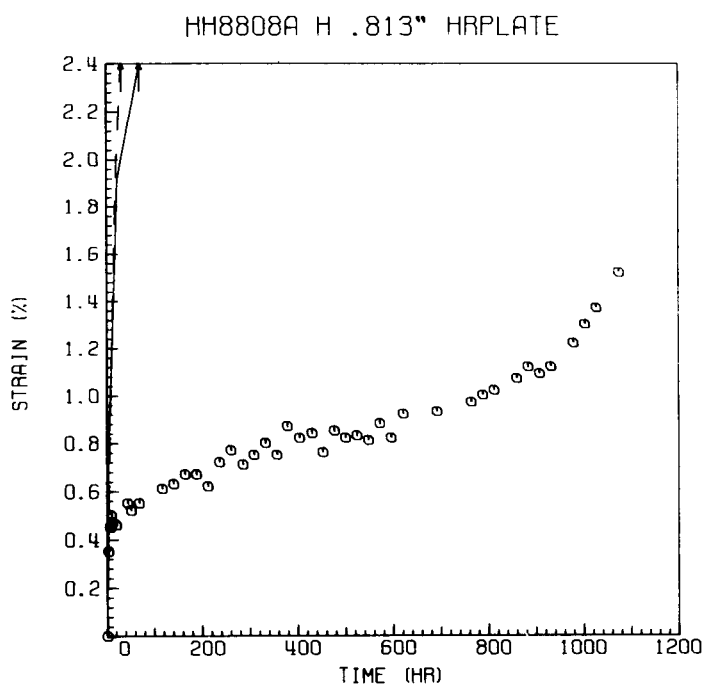

ORNL-DWG 77-6367

STRESS (MPA) = 90.
TEMP (C) = 760.

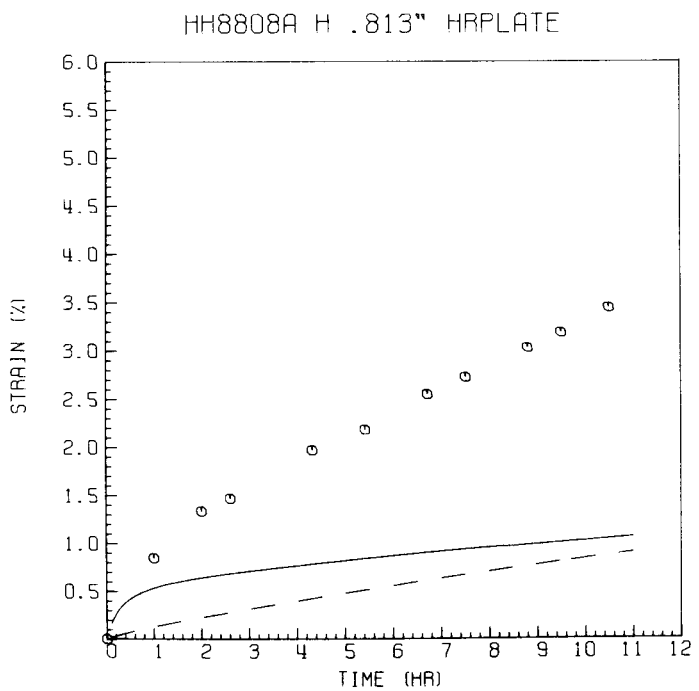

ORNL-DWG 77-6368

STRESS (MPA) = 90.
TEMP (C) = 760.

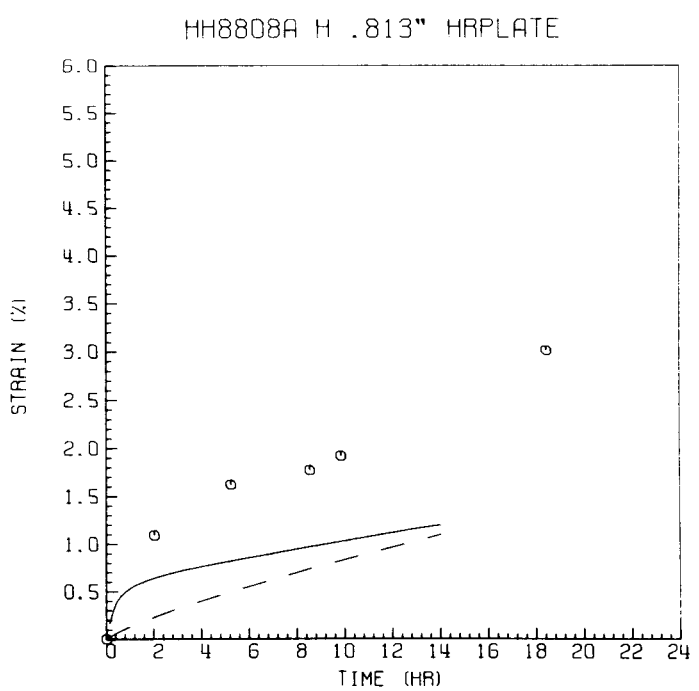

ORNL-DWG 77-6369

STRESS (MPA) = 241.
TEMP (C) = 649.

HH7686A H 5"ODX1/2"EXT.

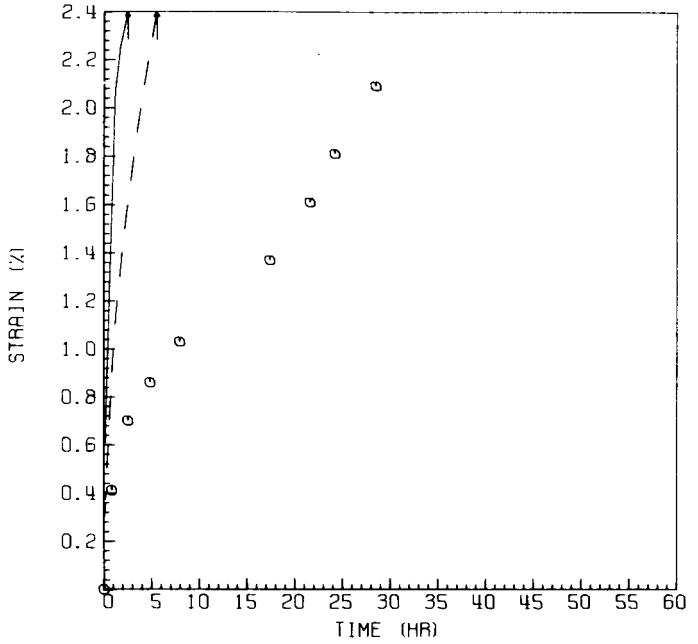

ORNL-DWG 77-6370

STRESS (MPA) = 179.
TEMP (C) = 649.

HH7686A H 5"ODX1/2"EXT.

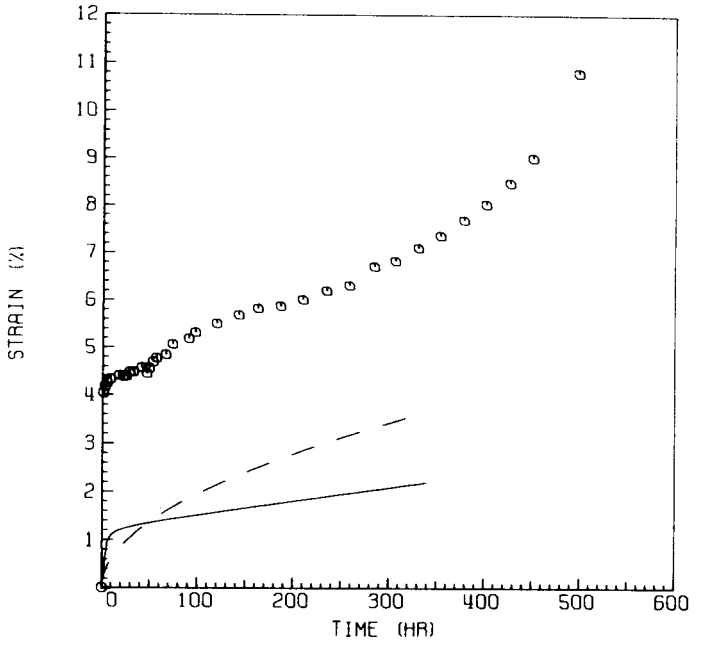

ORNL-DWG 77-6371

STRESS (MPA) = 138.
TEMP (C) = 649.

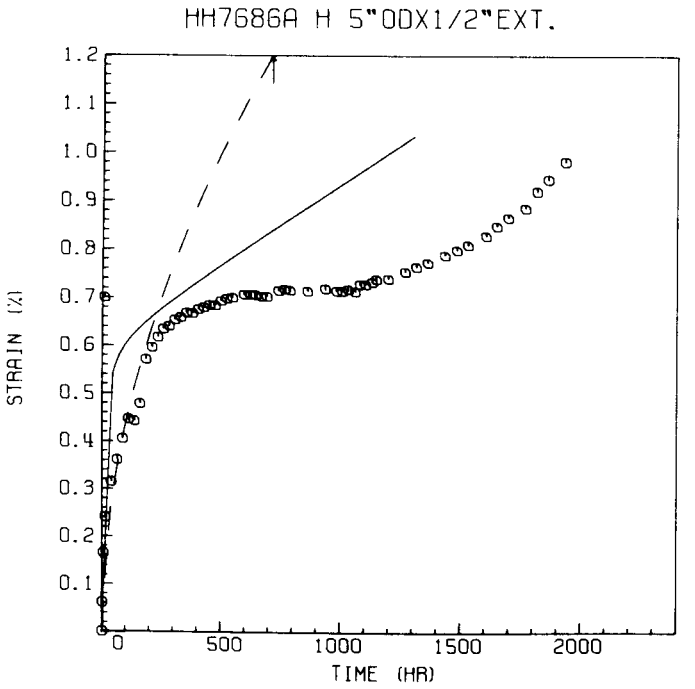

ORNL-DWG 77-6372

STRESS (MPA) = 124.
TEMP (C) = 649.

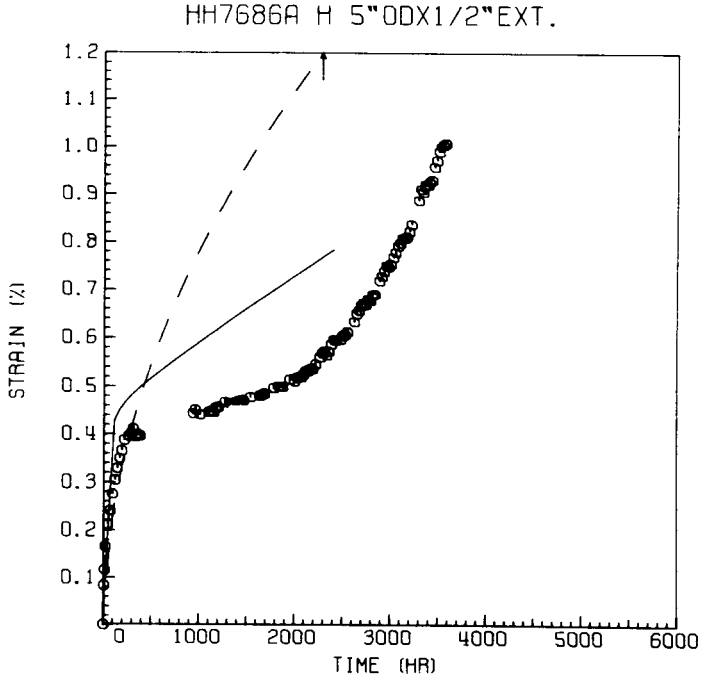

ORNL-DWG 77-6373

STRESS (MPA) = 83.
TEMP (C) = 649.

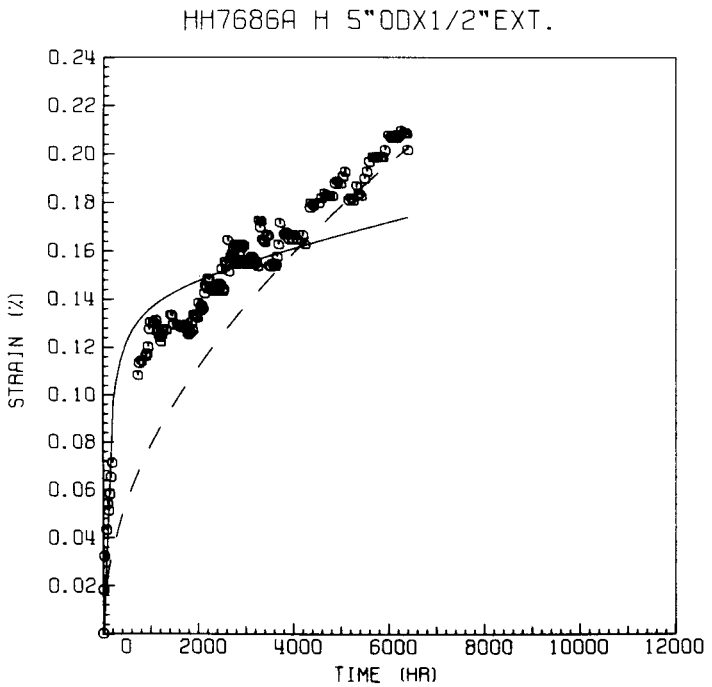

ORNL-DWG 77-6374

STRESS (MPA) = 69.
TEMP (C) = 704.

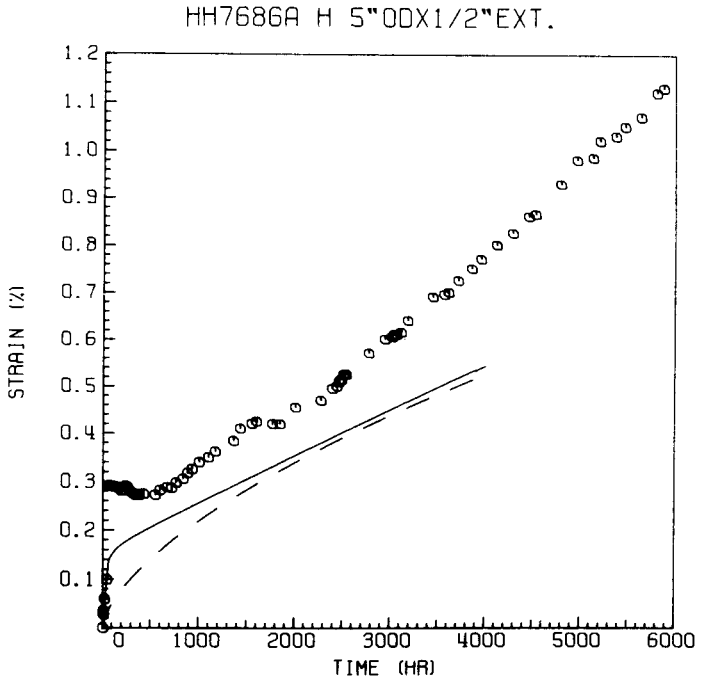

ØRNL-DWG 77-6375

STRESS (MPA) = 69.
TEMP (C) = 760.

HH7686A H 5"ODX1/2"EXT.

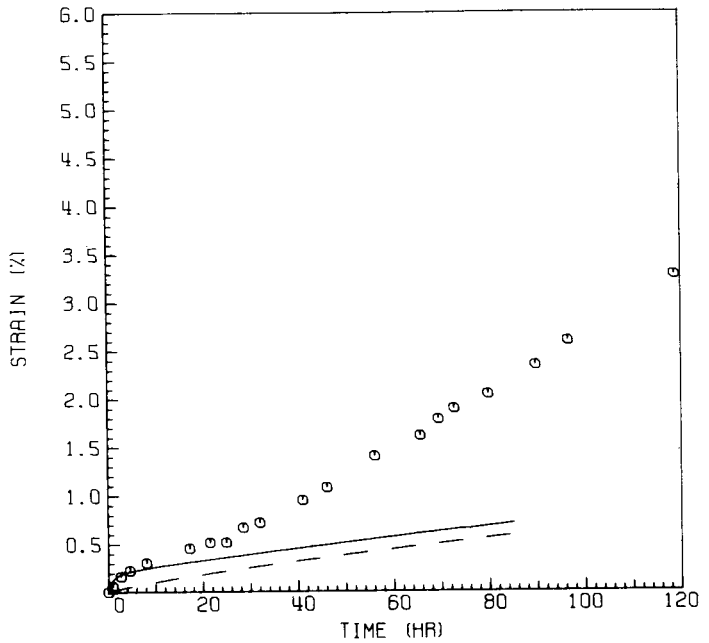

ØRNL-DWG 77-6376

STRESS (MPA) = 48.
TEMP (C) = 760.

HH7686A H 5"ODX1/2"EXT.

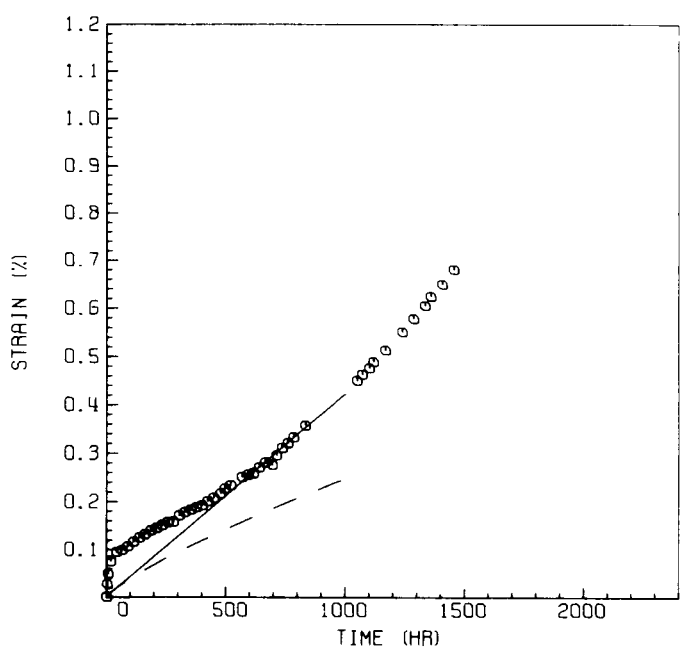

ORNL-DWG 77-6377

STRESS (MPA) = 241.
TEMP (C) = 649.

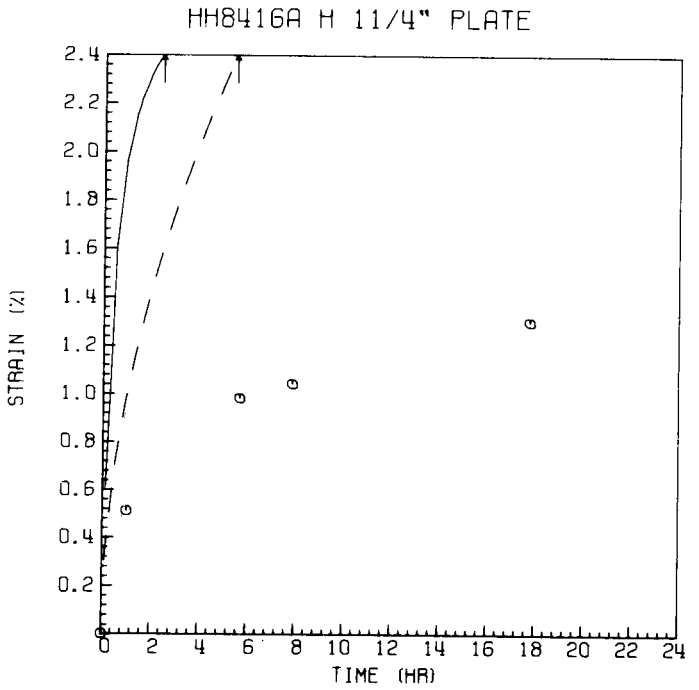

ORNL-DWG 77-6378

STRESS (MPA) = 179.
TEMP (C) = 649.

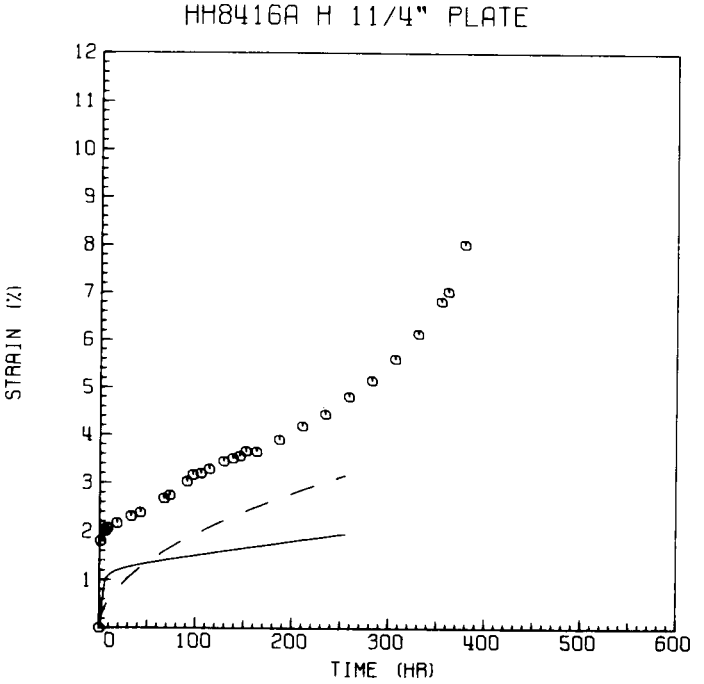

ORNL-DWG 77-6379

STRESS (MPA) = 117.
TEMP (C) = 649.

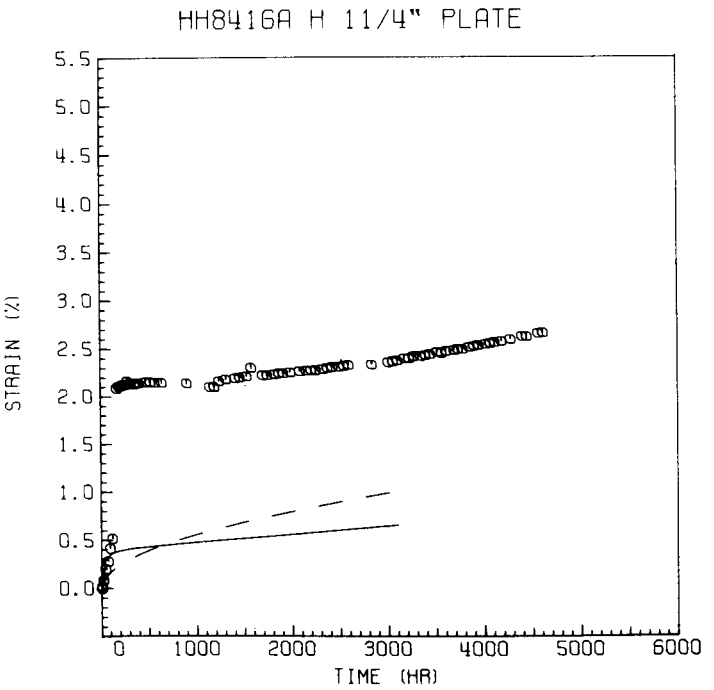

ORNL-DWG 77-6380

STRESS (MPA) = 138.
TEMP (C) = 649.

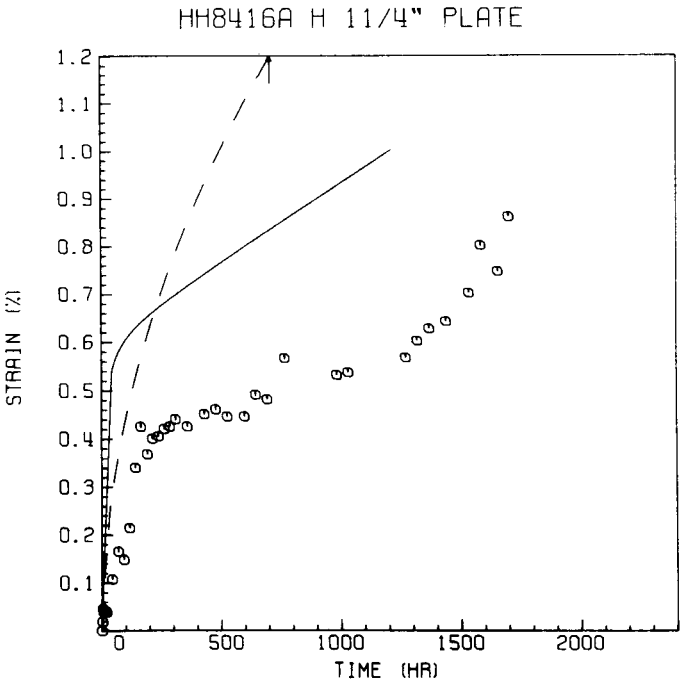

ORNL-DWG 77-6381

STRESS (MPA) = 124.
TEMP (C) = 704.

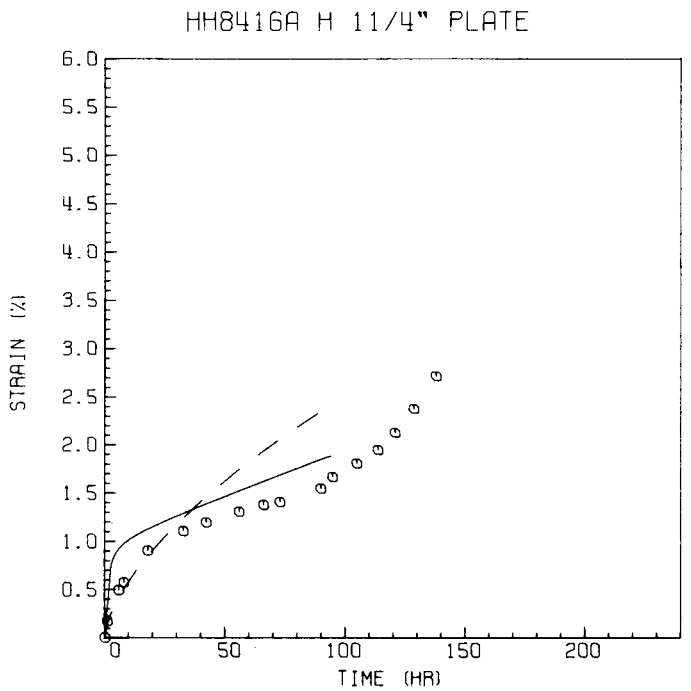

ORNL-DWG 77-6382

STRESS (MPA) = 103.
TEMP (C) = 704.

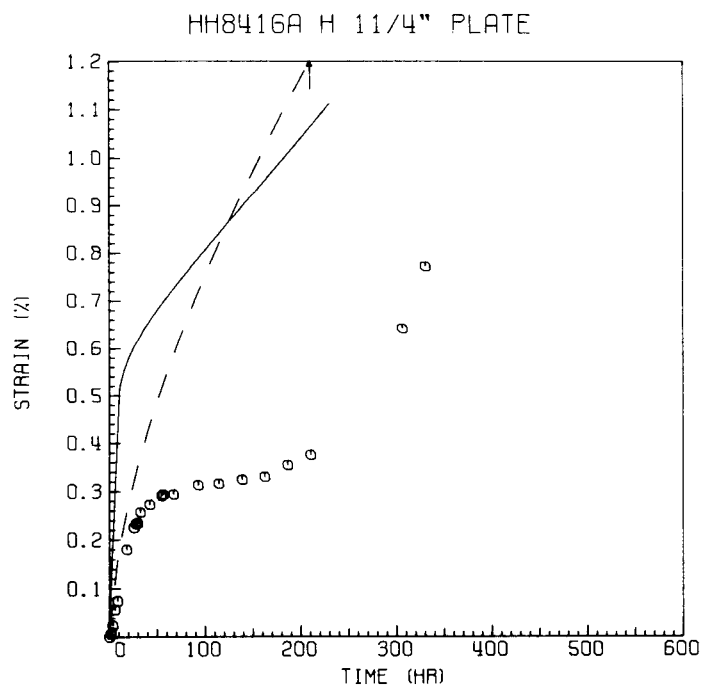

ORNL-DWG 77-6383

STRESS (MPA) = 79.
TEMP (C) = 704.

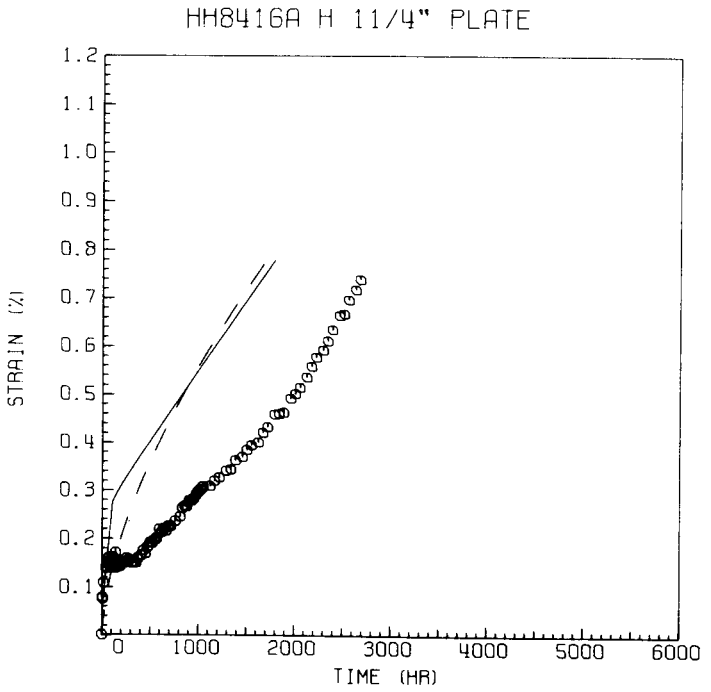

ORNL-DWG 77-6384

STRESS (MPA) = 55.
TEMP (C) = 732.

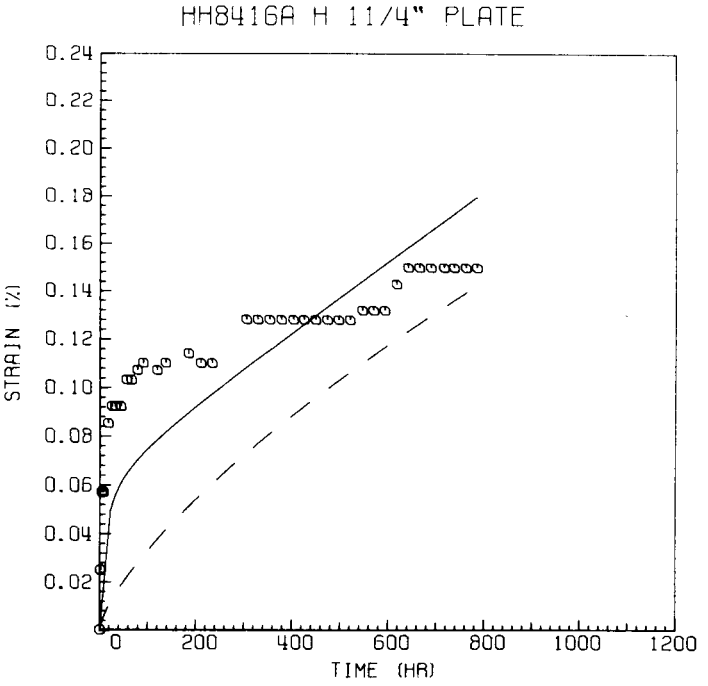

ORNL-DWG 77-6385

STRESS (MPA) = 55.
TEMP (C) = 760.

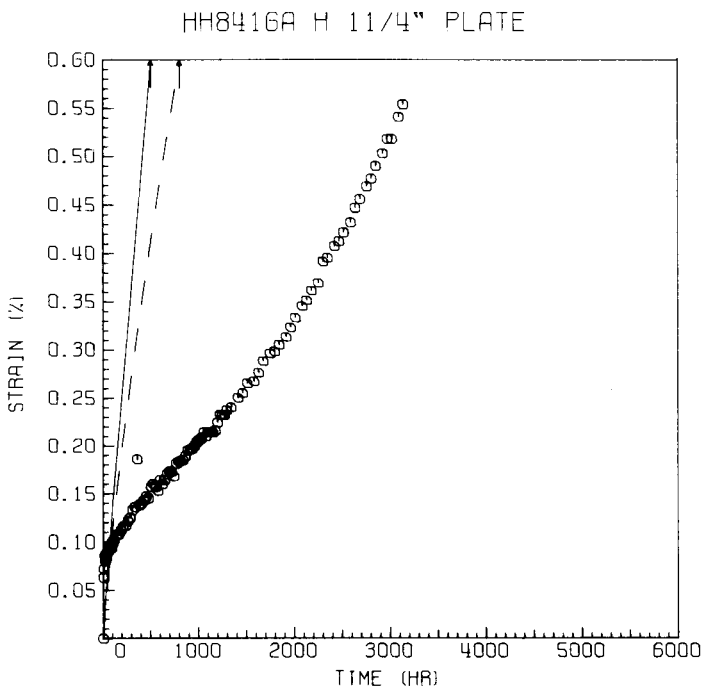

ORNL-DWG 77-6387

STRESS (MPA) = 31.
TEMP (C) = 760.

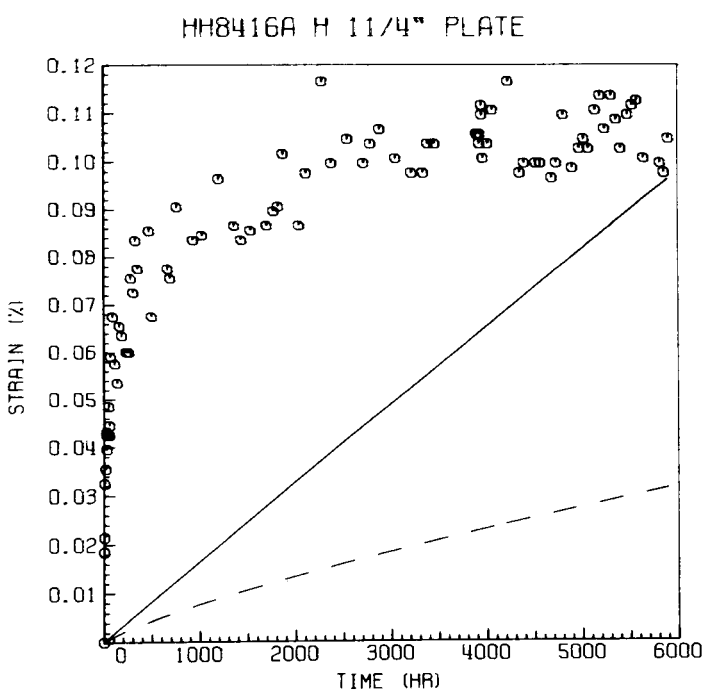

ORNL-DWG 77-6386

STRESS (MPA) = 69.
TEMP (C) = 760.

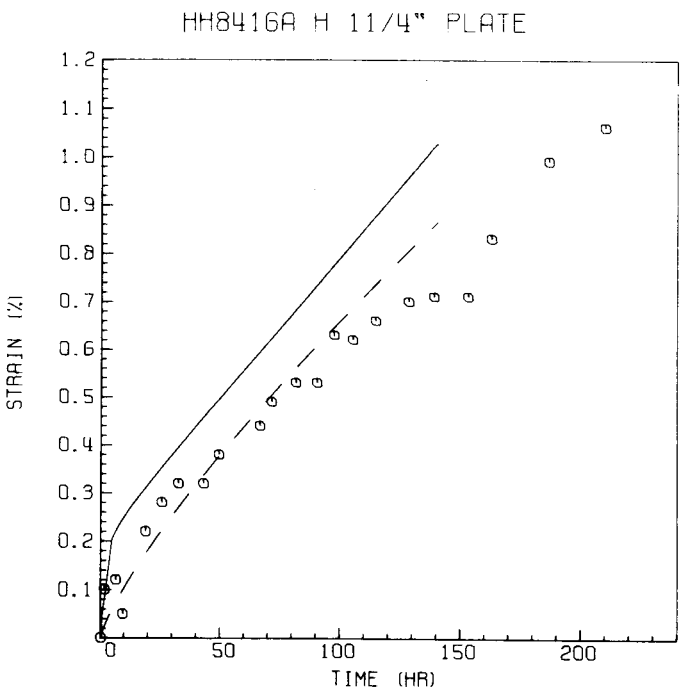

ORNL/TM-6029
Distribution
Category
UC-79b, -h, -k

INTERNAL DISTRIBUTION

1–3. Central Research Library
4. Document Reference Section
5–14. Laboratory Records Department
15. Laboratory Records, ORNL RC
16. ORNL Patent Office
17. G. M. Adamson
18–19. V. B. Baylor
20–21. B.L.P. Booker
22–31. M. K. Booker
32. C. R. Brinkman
33. D. A. Canonico
34. J. M. Corum
35. W. R. Corwin
36. J. E. Cunningham
37. J. H. DeVan
38. J. R. DiStefano
39. D. P. Edmonds
40. W. R. Gall
41. G. M. Goodwin
42. W. L. Greenstreet
43. W. O. Harms
44. R. F. Hibbs
45–47. M. R. Hill
48. J. P. Hammond
49. D. O. Hobson
50. P. R. Kasten
51. J. F. King
52. R. T. King
53. R. L. Klueh
54. A. L. Lotts
55. K. C. Liu
56. H. E. McCoy, Jr.
57. C. J. McHargue
58. A. J. Moorhead
59. P. Patriarca
60. H. Postma
61. C. E. Pugh
62. T. K. Roche
63. V. K. Sikka
64. G. M. Slaughter
65. J. O. Stiegler
66. J. P. Strizak
67. R. W. Swindeman
68. D. B. Trauger
69. W. E. Unger
70. J. R. Weir, Jr.
71. G. D. Whitman
72. R. W. Balluffi (consultant)
73. P. M. Brister (consultant)
74. W. R. Hibbard, Jr. (consultant)
75. N. E. Promisel (consultant)

EXTERNAL DISTRIBUTION

76–77. DOE DIVISION OF REACTOR DEVELOPMENT AND DEMONSTRATION,
Washington, DC 20545

Director

78–80. DOE DIVISION OF WASTE MANAGEMENT, PRODUCTION AND REPROCESSING,
Washington, DC 20545

Chief, Industrial Programs Branch
Chief, Projects Branch
Chief, Technology Branch

EXTERNAL DISTRIBUTION (Continued)

81–82. DOE OAK RIDGE OPERATIONS OFFICE, P.O. Box E, Oak Ridge, TN 37830

Director, Reactor Division
Director, Research and Technical Support Division

83–346. DOE TECHNICAL INFORMATION CENTER, Office of Information Services, P.O. Box 62, Oak Ridge, TN 37830

For distribution as shown in TID-4500 Distribution Category, UC-79b (Fuels and Materials Engineering Development); UC-79h (Structural Materials Design Engineering); and UC-79k (Components).

☆ U.S. GOVERNMENT PRINTING OFFICE: 1977-748-189/361